SYNTHESIS AND CHARACTERIZATION
OF
A NEW SELENOPHENE BASED ELECTROCHROMIC POLYMER

A THESIS SUBMITTED TO

THE GRADUATE SCHOOL OF NATURAL AND APPLIED SCIENCES

OF

ATILIM UNIVERSITY

BY

BARIŞ KARABAY

IN PARTIAL FULFILLMENT OF THE REQUIREMENTS FOR THE DEGREE OF

MASTER OF SCIENCE

IN

APPLIED CHEMISTRY

AT

THE DEPARTMENT OF CHEMICAL ENGINEERING AND APPLIED CHEMISTRY

DECEMBER 2014

Approval of the Graduate School of Natural and Applied Sciences, Atılım University.

_____

(Prof. Dr. İbrahim K. Akman)

Director

I certify that this thesis satisfies all the requirements as a thesis for the degree of Master of Science.

_____

Prof. Dr. Atilla Cihaner

Head of Department

This is to certify that we have read the thesis "Synthesis and Characterization of a New Selenophene Based Electrochromic Polymer" submitted by "Barış KARABAY" and that in our opinion it is fully adequate, in scope and quality, as a thesis for the degree of Master of Science.

_____

Prof. Dr. Atilla Cihaner

Supervisor

Examining Committee Members

Prof. Dr. Ahmet Önal _____

Prof. Dr. Atilla Cihaner _____

Asst. Prof. Dr. Belgin S. İşgör _____

Asst. Prof. Dr. Murat Kaya _____

Asst. Prof. Dr. Hakan Kayı _____

Date: 26.12.2014

I declare and guarantee that all data, knowledge and information in this document has been obtained, processed and presented in accordance with academic rules and ethical conduct. Based on these rules and conduct, I have fully cited and referenced all material and results that are not original to this work.

Name, Last name: Barış Karabay

Signature:

ABSTRACT

SYNTHESIS AND CHARACTERIZATION OF A NEW SELENOPHENE BASED ELECTROCHROMIC POLYMER

Karabay, Barış

M.S., Chemical Engineering and Applied Chemistry

Supervisor: Prof. Dr. Atilla Cihaner

December 2014, 87 pages

A new derivative of 3,4-propylenedioxyselenophene bearing naphtyl appendages on the bridge, called 3,4-dihydro-3,3-bis ((naphthalen-1-yl)methyl)-2H-selenopheno[3,4-b][1,4]dioxepine (ProDOS-Np_2), was synthesized and polymerized via potentiostatic and potentiodynamic methods. Electrochemically obtained polymer film (PProDOS-Np_2) is pure blue at the neutral state and highly transparent at the oxidized state. An increase in the size of the substituents on the bridge resulted in an increase in the optical contrast ratio. Upon moving from naked bridge to benzyl and to naphtyl substituents on the bridge center, the optical contrast changed from 51% to 65% and finally to 84%. When compared to polythiophene analogue, the PProDOS-Np_2 has lower oxidation potential and band gap, higher optical contrast ratio, coloration efficiency, robustness and stability. The polymer film preserved its properties even after thousands of cycles under ambient conditions.

Keywords: Electropolymerization, Electrochromism, ProDOS, Selenophene, Alkylenedioxyselenophene.

ÖZ

SELENOFEN TABANLI YENİ BİR ELEKTROKROMİK POLİMERİN SENTEZİ VE KARAKTERİZASYONU

Karabay, Barış

Yüksek Lisans, Kimya Mühendisliği ve Uygulamalı Kimya Bölümü

Tez Yöneticisi: Prof. Dr. Atilla Cihaner

Aralık 2014, 87 sayfa

Naftalin grubu içeren yeni bir 3,4-propilendioksiselenofen türevi; 3,4-dihidro-3,3-bis ((naftalin-1-il)methil)-2H-selenofeno[3,4-b][1,4]dioksefin (ProDOS-Np_2 sentezlenip potensiostatik ve potensiodinamik yöntemlerle polimerleştirilmiştir. Elektrokimyasal olarak elde edilen film ((PProDOS-Np_2) indirgenmiş halinde saf mavi ve yükseltgenmiş halinde ise oldukça şeffaf geçirgen bir renge sahiptir. Köprü üzerine bağlı olan eklerin büyüklüğünün artması optiksel geçirgenliğin artmasına neden olmuştur. Sırasıyla tek başına köprü ve bu köprünün merkezine bağlanan benzil ve naftalin gruplarıyla birlikte, optiksel geçirgenlik %51, %65 ve son olarak %84 olarak değişmiştir. Başka bir politiyofen tabanlı benzeri ile karşılaştırıldığında, PProDOS-Np_2' nin daha düşük yükseltgenme potansiyeli ve band aralığına, daha yüksek optiksel geçirgenlik oranına, dayanıklılığa ve kararlılığa sahip olduğu gözlenmiştir. Açık hava ortamında binlerce defa anahtarlanma sonrasında dahi polimer filmi özelliklerini korumuştur.

Anahtar Kelimeler: Elektropolimerizasyon, Elektrokromizm, ProDOS, Selenofen, Alkilendioksiselenofen.

To my lovely darling…
For your endless support and love

ACKNOWLEDGEMENTS

I would like to thanks to everyone who helped me during my all studies and the preparation of this thesis:

I would like to express my deepest appreciation to my supervisor, Prof. Dr. Atilla Cihaner, for his support, guidance, encouragement and patience during my research. He was not only my supervisor but also one of my friends in my life. I owe great thanks to him.

I wish to my endless thanks to Prof. Dr. Ahmet M. Önal for his answering my questions in any time and technical supports.

I also want to thanks Assoc. Prof. Dr Fatih Algı for improving my skills and for encouraging me during my organic synthesis.

I wish to express my thanks to all academic staffs in Department of Chemical Engineering and Applied Chemistry at Atilim University for their efforts and helps.

I would also wish to thank Esra Eroğlu, Emre Güner, Memduh Bilmez and Recep Taşpınar for their friendships, patience and motivation throughout this work
I also want to thanks to Fikret Pekel and Yasemin Pekel for priceless advices and supports.

I would like to thank to TÜBİTAK (Grant No: 111T976) for supplying financial supports during my studies.

Finally, I give my endless appreciation and thanks to Lütfiye Canan Pekel for her endless love. She is the source of my life and my inspiration.

TABLE OF CONTENTS

LIST OF FIGURES

LIST OF TABLES

LIST OF SCHEMES

LIST OF ABBREVIATIONS

CE	-	Coloration efficiency
CIE	-	Commission Internationale de I'Eclairage
DCM	-	Dichloromethane
DMS	-	3,4-dimethoxyselenophene
DMT	-	3,4-dimethoxythiophene
EDOS	-	3,4-ethylenedioxyselenophene
EDOT	-	3,4-propylenedioxythiophene
E_g	-	Band Gap Energy
eV	-	Electron-volt
HOMO	-	Highest Occupied Molecular Orbital
ITO	-	Indium Coated Tin Oxide
LUMO	-	Lowest Unoccupied Molecular Orbital
NIR	-	Near Infrared
OD	-	Optical Density
OFETs	-	Organic Field Effect Transistors
OLEDs	-	Organic Light-Emitting Diodes
PEDOS	-	Poly(3,4-ethylenedioxyselenophene)
PEDOT	-	Poly(3,4-propylenedioxythiophene)
ProDOS	-	3,4-propylenedioxyselenophenes
ProDOT	-	3,4-propylenedioxythiophene
PSS	-	Poly(styrene sulfonic acid)
PTSA	-	p-toluenesulfonic acid
Q_a	-	Amount of Charge
Q_c	-	Amount of Discharge

Q_d	-	Injected/Ejected Charge
RE	-	Reference Electrode
SCE	-	Saturated Calomel Electrode
TBAH	-	Tetrabutylammonium Hexafluorophosphate
THF	-	Tetrahydrofuran
WE	-	Working Electrode
Δ%Y	-	Relative Luminance Measurement

CHAPTER 1

INTRODUCTION

1.1 Conjugation and Mechanism

A conducting (conjugated, conductive) polymer may be defined as alternating single and double bonds via continuous overlapping p-orbitals. Any polymer that exhibits this property would become intrinsically conducting polymer. In order that any polymer may conduct the electricity, it should have not only charge carriers but also an orbital system that enables the charge carriers to move through a continuous π-orbitals overlapping in the polymer backbone [1].

1.1.1 Band Gap

The ability of any materials to conduct electricity can be defined by the determination of band gap energy (E_g), which is the energy of one electron to need to pass through from the highest occupied molecular orbital (HOMO) to the lowest unoccupied molecular orbital (LUMO). This gap between the HOMO and LUMO levels plays an important role on determining whether a material is conductor, semiconductor or insulator (**Figure 1.1**).

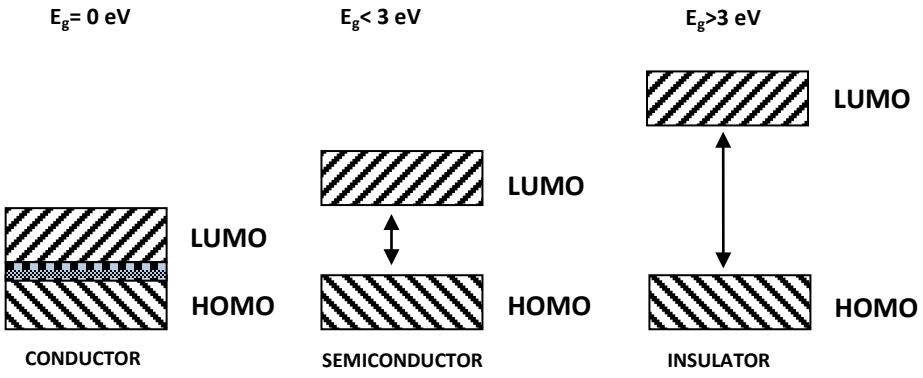

Figure 1.1 Illustration for band structures and band gap energies (E_g).

Depending on the width of the forbidden band (band gap), a gap is observed for semiconductors and insulators, whereas there is no gap for conductors between their valence (HOMO) and conduction (LUMO) bands. This difference is labelled as electron-volt (eV).

1.1.2 Doping-Dedoping Process

Conjugated polymers cannot conduct the electricity in their neutral states. Owing to this property, the conjugated polymers do not have intrinsic charge carriers. In order to obtain a conducting polymer, it should be doped or dedoped via chemical or electrochemical process. Moreover, in order to import charge carriers, conjugated polymers can be doped by two different ways: p-type doping (oxidation) and n-type doping (reduction) (**Figure 1.2**).

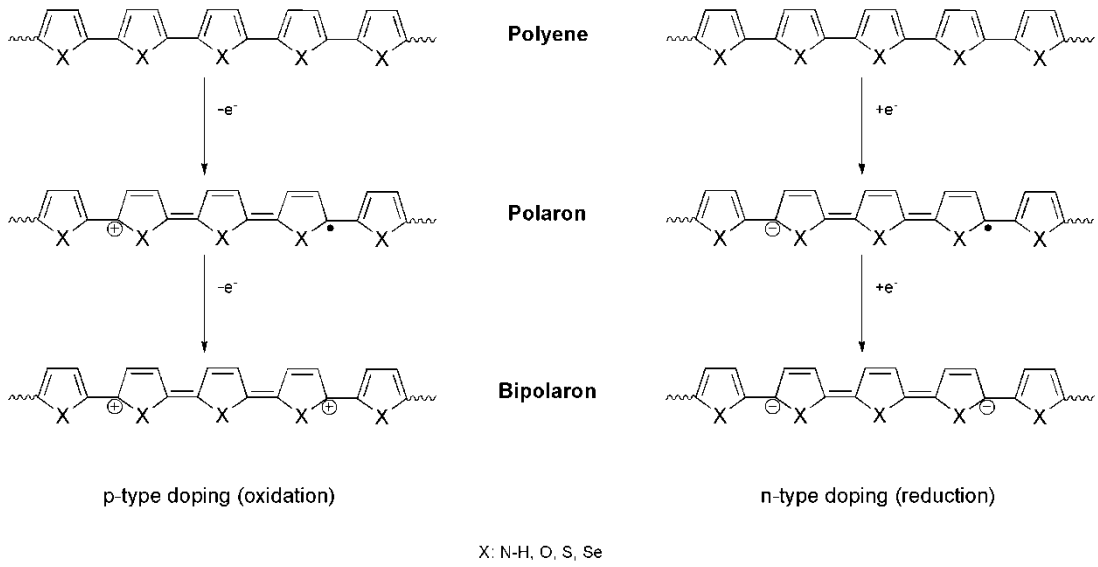

Figure 1.2 Schematic description of the formation of polaron and bipolaron charge carriers for any polyene.

1.2 Synthesis of Conducting Polymers

Although there are many ways to synthesize conducting polymers like photochemical, solid-state synthesis, biocatalayzed, etc., the widely used and most popular methods are chemical and electrochemical polymerization techniques [2].

1.2.1 Chemical Polymerization

Chemical polymerization is the most widely used method to get conducting polymers because the used chemical reagents are commercially available and quite cheap. Chemical polymerization can be performed by exposing the related monomers by using strong chemical oxidants such as ammonium peroxydisulfate, potassium permanganate, hydrogen peroxide, iron(III) chloride, etc. $FeCl_3$ is the most widely used chemical oxidant for the oxidative polymerization of five-membered heterocyclic compounds (**Scheme 1.1**).

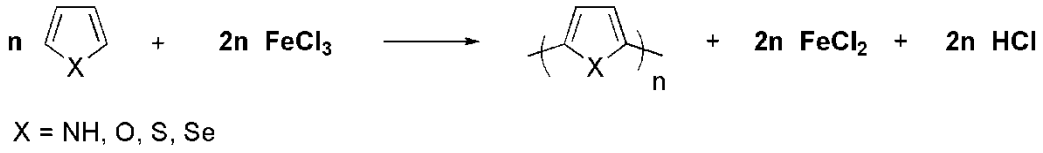

Scheme 1.1 A synthetic pathway for polymerization of any five-membered heterocyclic compound by using of $FeCl_3$ oxidant.

Unfortunately the chemical polymerization has some limitations like poor quality and overoxidation of the obtained polymers [3, 4].

1.2.2 Electrochemical Polymerization

Electrochemical polymerization is an easy and fast technique since the electroactive monomer is performed in order to get the related polymer on an electrode surface in a proper medium. In electrochemical polymerization, oxidation potential of a monomer is determined via cyclic voltammetry. When the determined oxidation potential was applied via potentiodynamic or potentiostatic method, reactive radical cations (or anions) are formed in the monomer structure and then

polymerization proceeds. In **Scheme 1.2**, the polymerization mechanism of thiophene has been illustrated. Firstly, a radical cation on thiophene is created by the removal of an electron from the ring by applying the determined oxidation potential. At this point, there are two possible ways, which are a radical-monomer coupling or a radical-radical coupling to get a dimer, the latter one generally has been accepted in literature [6]. After getting dimer units, the obtained dimers will create their own radical cation at lower potential than the monomer since dimers have more electron-rich nature. Finally, the continuous coupling will result in a polymer chain.

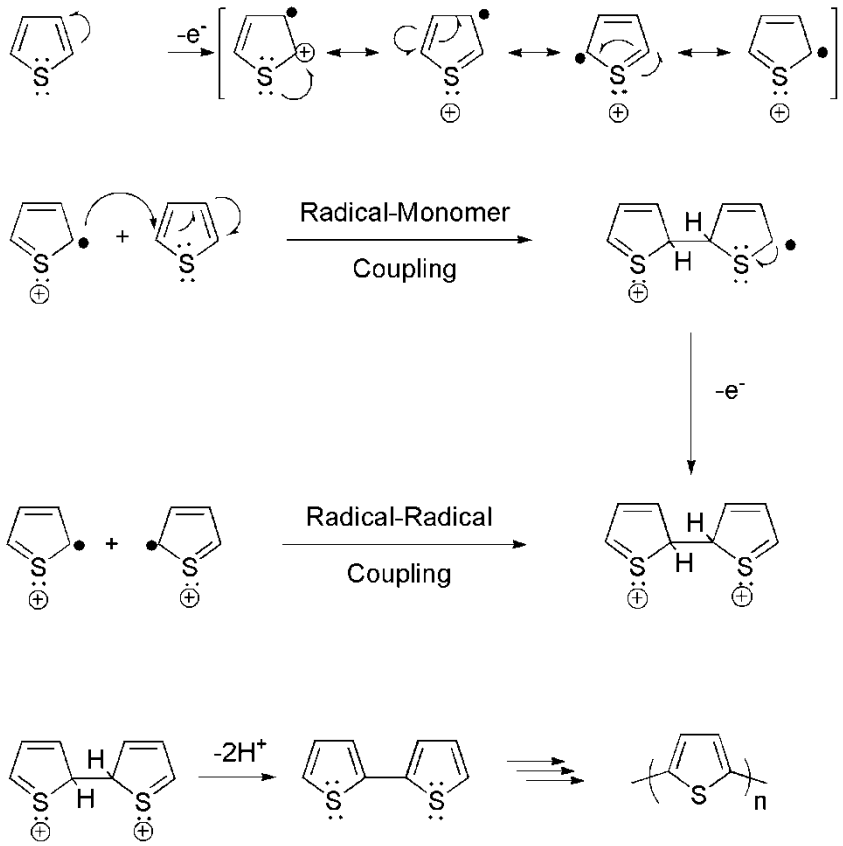

Scheme 1.2 A mechanism for the electrochemical polymerization of thiophene.

1.3 Definitions for Electroanalytical Methods

Cyclic voltammetry, differential pulse voltammetry and chronopotential coulometry are the widely used techniques for the characterization of the electroactive monomers and their corresponding polymers. The obtained data from these techniques give information about the oxidation-reduction potential, band gap

(electrochemical) and electrochemical stability of the related monomers and polymers. Furthermore, the electrochemical polymerization depends on some conditions like solvent medium, supporting electrolyte, electrode, temperature and working potential range.

1.3.1 Solvent Medium

The solvent should be proper in working range of the monomer and/or the polymer [5]. At first glance, ionic conductivity and electrochemical stability values may give an idea about whether the solvent is appropriate or not for electrochemical studies. For example, acetonitrile and dichloromethane are the most frequently used solvents because of their dielectric constants (37 and 9, respectively) and electrochemical stabilities. Moreover, acetonitrile works between -3.0 V and +3.0 V against the saturated calomel electrode (SCE). Also, like acetonitrile, it is well known that dichloromethane is highly stable up to 3.0 V under ambient conditions [6]. In additon to these common organic solvents, dimethylformamide and dimethylsulfoxide are the other solvents, which are not suitable for the potential larger than 1.0 V because they are easily decomposed at these potentials. Moreover, when focused on the dielectric constant, water is one of the good alternatives for the electrochemical studies. However, although the dielectric value of H_2O is 80 and it is a relieble solvent for the electrochemical studies; unfortunately, many electroactive compounds are not soluble in water [7, 8].

1.3.2 Supporting Electrolyte

All ionizable salts and/or compounds in any solvent may be defined as supporting electrode. Like solvent, the related electrolyte should be electroinactive in the applied potential range. Also, the supporting electrolyte should be soluble in used solvent system. Tetraalkylamonium salts are the widely used electrolytes owing to their high solubilities and working potential range in organic solvents. Also, perchlorate anions (ClO_4^-) are very useful up to +1.6 V vs. SCE. Moreover, tetrafluoroborate (BF_4^-) and hexafluorophosphate (PF_6^-) anions work up to +3.0 V vs. SCE [9].

1.3.3 Electrodes

Voltammetric characterizations are fulfilled by using an electrochemical cell including two or three electrodes immersed in a suitable electrolyte solution containing an electroactive compound.

1.3.3.1 Working Electrode

Working electrode is the electrode where an oxidation/reduction process occurs under the external potential. While platinium, palladium, gold, silver, glassy carbon or nickel are the most popular electrodes, coated indium tin oxide (ITO) electrode is widely used electrode for spectroelectrochemical characterizations because of its transparency.

1.3.3.2 Reference Electrode

Reference electrode has a well-defined electrode potential. In other words, when any potential is applied to the system, the potential should not change in time. Therefore, the potential difference between working and reference electrodes must be constant. Saturated calomel electrode (SCE), standard hydrogen electrode, silver (wire) electrode (Ag) and silver/silver chloride electrode (Ag/AgCl) are commonly used electrodes in the electrochemical cells. Depending on conditions, such as temperature, moisture etc., electroanalytical results can change and it can create some deviations in related studies. In order to eliminate these deviations, an internal standard reference is used to compare and check the applied potential. For example, ferrocene, which is the most widely used internal reference, can be oxidized reversibly to the ferrocenium ion at a half wave potential of 0.48 V vs Ag/Ag^{+} in acetonitrile solution [6].

1.3.3.3 Counter Electrode

Counter electrode is made of electrochemically inactive materials, such as platinum or graphite. This electrode conducts the electricity from the source of signal to the other electrodes in the electrolyte solution. Moreover, the surface area of

counter electrode should be larger than that of working electrode because some deviations may occur due to the additional resistance coming from counter electrode.

1.4 Intrinsic Properties of Conducting Polymer and Their Characterizations

After getting the conducting polymer, its intrinsic properties like band gap energy and electrochromic features should be determined clearly. In general, various band gap values can be calculated for each conducting polymer and each one can have different colors in their various oxidized states. Therefore, some electroanalytical methods are used in order to get related outcomes.

1.4.1 Band Gap

The band gap is the key for determining the intrinsic properties of any material because it plays an important role on the color of the absorbed and emited light. In literature, there are two different ways to determine the band gap value of the related polymer via electroanalytical and spectrochemical methods.

1.4.1.1 Electroanalytical Methods

Cyclic voltammetry, differential pulse voltammetry and chronopotential coulometry are the main techniques for the determination of electrochemical properties of any monomer or polymer because of their simplicity and versatility. Cyclic voltammetry is an electrochemical method that measures the current under the potential cycling. In other words, it measures the change in the current at the working electrode surface during the potential scanning. Cyclic voltammetry consists of three electodes containing reference, working and counter electrodes. The obtained graph from cyclic voltammetry is called as cyclic voltammogram (**Figure 1.3**).

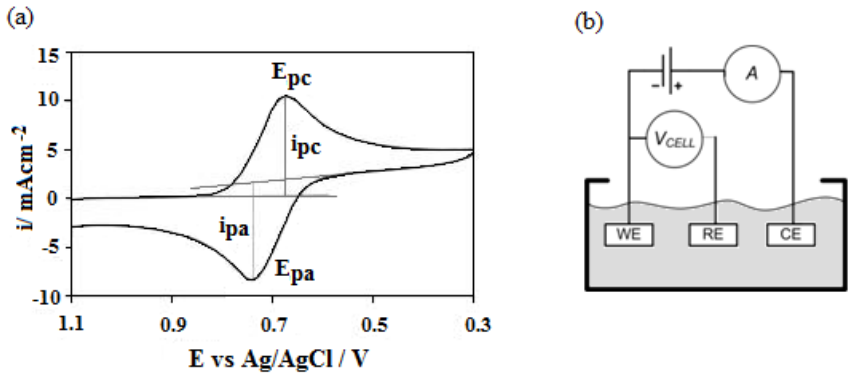

Figure 1.3 (a) An illustration of any cyclic voltammogram for any conducting polymer and (b) a three-electrode electrochemical cell, where RE: reference electrode, WE: working electrode and CE: counter electrode.

1.4.1.2 Spectroelectrochemical Methods

Spectroelectrochemical analysis gives information about not only band gap but also the electrochromic properties of related conductive polymer. By extrapolating the onset of π-π* transition, the band gap can be calculated easily (**Figure 1.3**). For band gap, the mathematically derived equation has been shown in Equation1.1, where λ is wavelength obtained by extrapolating onset of the longest wavelength of the π-π* transition band. The calculated band gap (E_g) value has a unit of *eV*.

$$E_g = \frac{1240}{\lambda} \qquad \text{Equation 1.1}$$

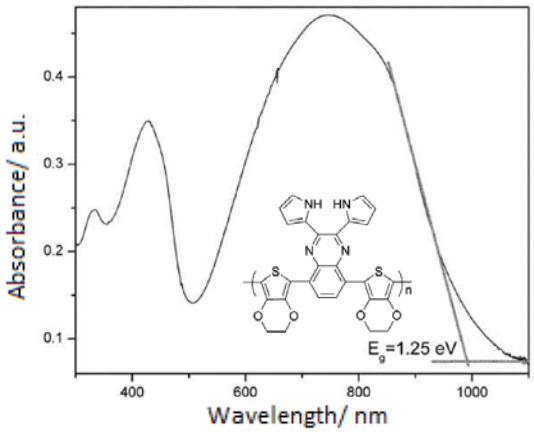

Figure 1.3 Absorption spectrum of a polymer on ITO at its neutral state in acetonitrile [10].

1.4.2 Electrochromic Properties

Electrochromism is the reversible color change of any materials under the external potential. The color may change from an observer to another one because of relativity. For this reason, these colors are evaluated by a standard color scale. In order to define the colors of the materials, a colorimetry method to quantify and to describe the human color perception is used. In the colorimetry, three components play an important role on the describing hue (chromatic color), saturation (purity, or intensity) and brightness (lightness, or luminance). In 1976, the CIE (Commission Internationale de l'Eclairage) has developed the CIELUV and CIELAB color spaces; L*a*b*, in order to define color changes in electrochromic properties during their redox states. L* defines the lightness of polymer (color) between 0 (black) and 100 (diffuse white), while a* indicates the red-green balance, b* is for yellow-blue balance (**Figure 1.4**).

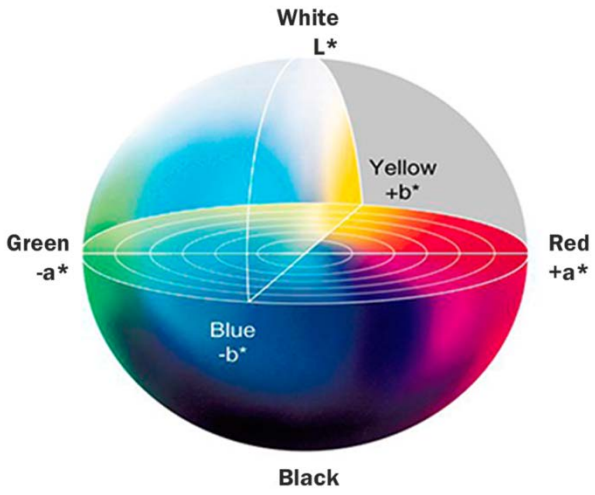

Figure 1.4 An example for color chart with L, a, b values [11].

Among many electrochromic materials; such as metal oxides, molecular dyes, conducting polymers, etc., only one of them called conducting polymers (electrochromic polymers) is superior than the others because of low processing cost, durability, stability, high coloration efficiency, fast switching and ease of modification (**Figure 1.5**). In all electrochromic polymers, each polymer will be compared in terms of its intrinsic properties like optical contrast, switching time and coloration efficiency [12].

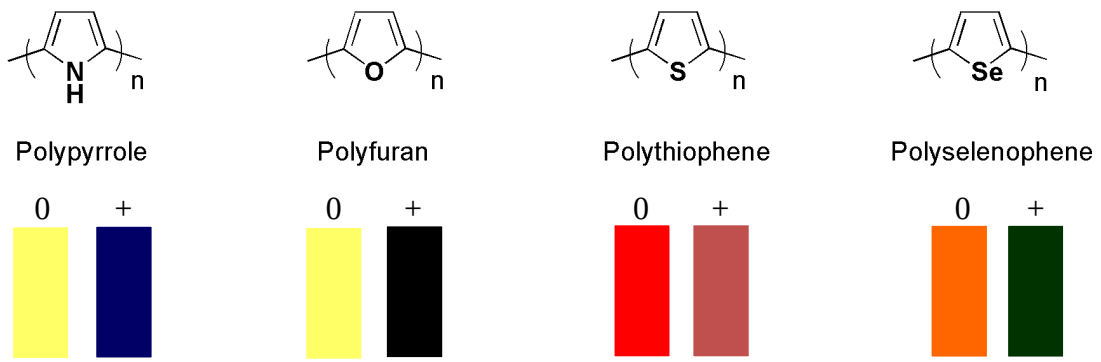

Figure 1.5 Some examples for electrochromic materials and their colors in their various redox state, 0: Neutral state and +: oxidized state.

1.4.2.1 Optical Contrast

In general, optical contrast can be defined as a percent transmittance change, Δ %T, at a given wavelength. When a electroactive polymer film coated on ITO is placed in front of the beam of the spectrophotometer, electrochromic transparency can be monitored by using a square-wave potential method between the neutral and oxidized states (**Figure 1.6**) [13].

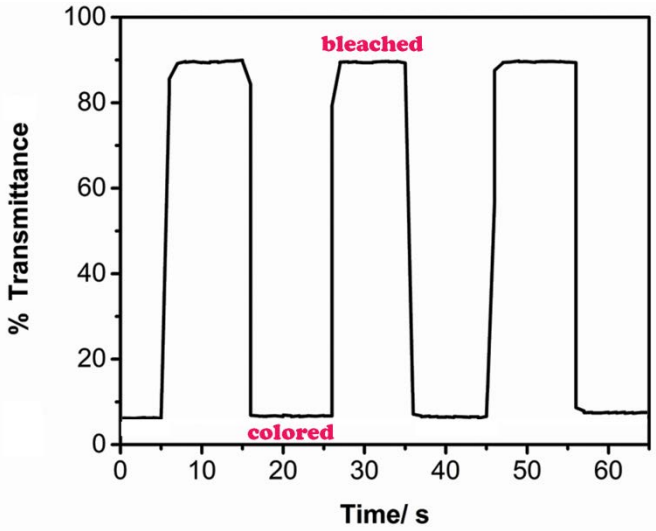

Figure 1.6 An illustration for the percent transmittance change of an electrochromic polymer via a square-wave potential method between its neutral and oxidized states in the electrolyte solution.

While the electrochromic polymer film is switched between its reduced (neutral) and oxidized states by means of electroanalytical methods, the chronoabsorptometry outputs are monitored *in-situ*. According to these results, optical contrast can be calculated by using Equation 1.2;

$$\Delta\%T = \%T_{bleached} - \%T_{colored} \qquad \text{Equation 1.2}$$

1.4.2.2 Switching Time

Switching time can be defined as the elapsed time to switch from the neutral state to the oxidized state and vice versa. The factors affecting the switching rate are the movement ability of counterions, the ease of diffusion of the ionic species across polymer backbone, and the surface morphology of the obtained polymer film. 95% of the full contrast is regarded as the switching time because human eye could be able to perceive this percentage.

1.4.2.3 Coloration Efficiency

Coloration efficiency (CE, η) is defined as the change in optical density (ΔOD) per density of injected/ejected charge (Q_d) for an electrochromic polymer during its oxidation/reduction states. Like the measurement of optical contrast, all parameters that has been placed in Equation 1.3 are obtained by chronoabsorptometry experiments.

$$\eta = \Delta OD / Q_d = (T_{bleached} / T_{colored}) / Q_d \qquad \text{Equation 1.3}$$

1.5 Conducting Polymers

It was believed that all of the polymers had been insulators until an "failure" in the calculation of the amount of a catalyst used in a chemical reaction. In fact, a visiting scientist added the necessary amount of the catalyst into the reaction flask as *mole* rather than *mmole* to synthesize the polyacetylene [14]. After the adition of excess amount of the catalyst, a "silvery shining layer" on the surface of the liquid in the reaction flask was observed. The formed film made a real question asked: "If the

plastic film shines like a metal, can it conduct the electricity, too?". Three scientists, Alan MacDiarmid, Hideki Shirakawa and Alan Heeger, showed that polyacetylene could be able to conduct the electricity when it was doped by iodine vapor [14]. This class of polymers called conducting (conjugated, conductive) polymers opened up a new door to material science and applications.

The development of conducting polymers had taken great attention since 1977 and this novel study had brought Nobel Prize in Chemistry toward Alan MacDiarmid, Hideki Shirakawa and Alan Heeger in 2000 [14]. In fact, conducting polymers attract considerable attention owing to their applications such as photovoltaic cells [15, 16], organic light-emitting diodes [17, 18] organic field effect transistors [19], electrochromic devices [20, 21], smart windows [22, 23], sensors [24], artificial muscles [25], and so forth.

After the pioneering study of Shirikawa in 1977, the field of conducting polymers started to get great importance on research and development studies in academic and industrial areas. Because of insolubility, infusibility and unstability problems of polyacetylene, many scientists have focused on the construction of new type monomers and their polymers. By means of the synthesis of second generation conducting polymers such as polypyrroles, polyfurans, polythiophenes, polyphenylenes, polyanilines, poly(phenylene vinylene)s, polycarbazoles and so forth (**Scheme 1.3**), researchers were able to overcome these problems that have been mentioned above [26]. Nevertheless, these compounds would not be enough to find solution for these limitations. Thus, the studies on conducting polymers have gained speed to overcome all these problems.

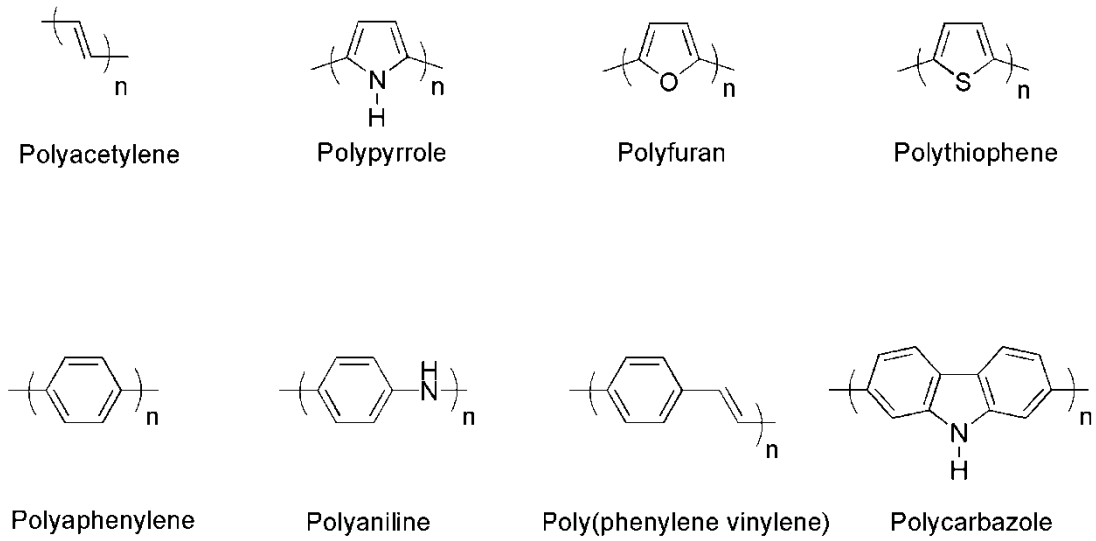

Scheme 1.3 Chemical structures of some conducting polymers.

In the second generation conducting polymers, scientists have focused especially on thiophene based polymers because of their chemical and optical properties. Polythiophene is stable in its conductive state (500 S/cm) [27] at oxidation under ambient conditions. On the other hand, polythiophene has an advantage called "thiophene paradox". It can be explained as the overoxidation of polythiophene chains during monomer oxidation, which is necessary to form electrochemically conducting polythiophene film on the electrode surface. In other words, although the thiophene is polymerized at 2.0 V, polythiophene chain is overoxidized near 1.5 V. Therefore, many scientists in conducting polymers have focused on new derivatives of thiophene based polymers [28, 29]. In order to cope with both overoxidation and insolubility problems, it is needed to modify thiophene ring.

It is well known that the substitution of alkyl chain on 3- or 3,4- positions of thiophene ring can lead to soluble polythiophene derivatives. For example, alkoxy substituted polythiophenes have superior electrical and optical properties over parent polythiophene. The presence of oxygen atom between alkyl chain and thiophene pumps electrons to the ring and alkoxy group behaves as a strong electron-donating group. The related monomer oxidized at lower potential than thiophene and therefore a well-organized and soluble polythiophene can be obtained without overoxidation during polymerization [30, 31]. The presence of substituents on 3,4-positions of

thiophene ring proceeds the polymerization via 2,5 coupling. Therefore, well-defined polymers are obtained without β-β' and α- β' couplings.

Under the lights of this information, the third generation of conducting polymers have been started in 1988 by the invention of alkylenedioxythiophene derivatives and their corresponding polymers such as 3,4-ethylenedioxythiophene (EDOT) and its polymer poly(3,4-ethylenedioxythiophene) (PEDOT) (**Scheme 1.4**) [32].

EDOT PEDOT

Scheme 1.4 Chemical structures of EDOT and its polymer PEDOT.

Unlike polythiophene and its analogues, PEDOT has many advantages over the previously synthesized conducting polymers because of its high electrical stability under ambient conditions, optical transparency in oxidative state and low band gap (1.6-1.7 eV) [26]. PEDOT has an extremely high conductivity up to 600 S/cm when compared to the parent polythiophene [33]. On the other hand, PEDOT is insoluble but its processable suspension form can be obtained during polymerization of EDOT in the presence of poly(styrene sulfonic acid) (PSS). When this processable PEDOT/PSS polymer was applied on a surface, the obtained transparent film has high conductivity and mechanical stability. In addition to its superior features, it has excellent electrochromic properties. PEDOT is a cathodically coloring conducting polymer. It is violet/dark blue color in its neutral state and transmissive sky blue in its oxidized state. It can have thousands of color tones between these two colors and the PEDOT can be switched reversibly between various oxidation states more than thousand times.

By the inspiration of the synthesis of PEDOT, many articles have been published in order to improve its solubility and optical features like optical contrast ratio, coloration efficiency (CE), switching time and so forth. On the other hand, the solubility of PEDOT was tried to enhanced by using substituted EDOT by alkyl

chains on the bridge, but these groups did not give the expected results. Therefore, many scientists focused on the size of alkylene bridge on thiophene ring, especially propylene bridge. Since, it is the fact that the synthesizing of thiophene with propylene bridge is easier than the other analogues. Moreover, the substituted alkyl groups on propylene bridge is highly easy. The attached propylene bridge and alkyl groups on thiophene ring contributes the solubility, low oxidation potential, low band gap and stability under ambient conditions. Alkyl substituted propylenedioxy thiophenes are also violet/dark blue at neutral state and transmissive at oxidized state [34].

1.5.1 Polyselenophenes

While thiophene and its derivatives got the great attention by many scientists, selenophene and its derivatives as thiophene analogues could not get this reputation since selenophene and its derivatives have more difficult synthetic pathway. Nevertheless, polyselenophenes will have superior properties over their thiophene analogues. When compared to S atom, Se atom has

i. larger atomic size,
ii. more metallic character,
iii. more polarizability and
iv. lower electronegativity.

When these properties are transferred to the selenophene ring, a new door will be opened up to new materials based on polyselenophenes. In order to support this assumption, the superior properties of polyselenophenes over polythiophenes obtained from theoretical and experimental studies can be listed as follow:

a) interchain charge transfers because of intermolecular interaction between different Se atoms. Therefore, the obtained polymers have low band gap. Consequently, they will have different optical properties,

b) higher twisting energy than polythiophenes,

c) low aromaticity due to their larger quinoid structures, which leads to lower band gap. It gives rise to the lower band gap for polyselenophenes.

In the literature, polyselenophenes can be synthesized via oxidative polymerization [35, 36], coupling reaction [37, 38] or electrochemical polymerization methods. [35, 39, 40] (**Scheme 1.5**).

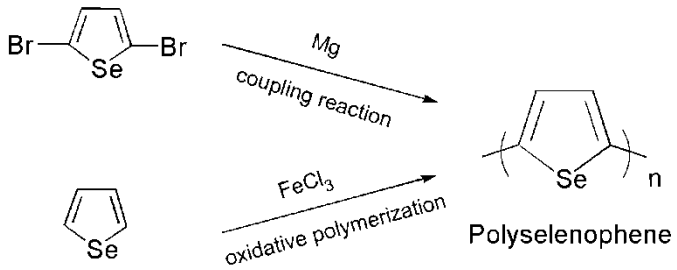

Scheme 1.5 Synthetic route for polyselenophene.

The quality of polyselenophene depends on the chosen polymerization method. This can be explained in terms of an applied oxidation potential to get an electroactive polymer. For example, when the oxidation potential of the selenophene is very high, some unwanted/undesired side products will be obtained and the corresponding polymer will be overoxidized during polymerization. One of the ways for lowering the oxidation potential of selenophene is to substitute 3- or 3,4-positions of the ring by electron-donating groups [41-43]. As mentioned in the previous part, like thiophene, the selenophene has been substituted by various length of alkyl chains. In addition to the efforts for lowering oxidation potential of selenophene, the substituted alkyl chains also affect the solubility of the obtained polymer [44-52].

1.5.2 Poly(3,4-ethylenedioxyselenophene)s (PEDOS)

By the inspiration of EDOT, 3,4-ethylenedioxyselenophene (EDOS) has been synthesized successfully in multi-step by Cava and his colleagues (**Scheme 1.6**) [53].

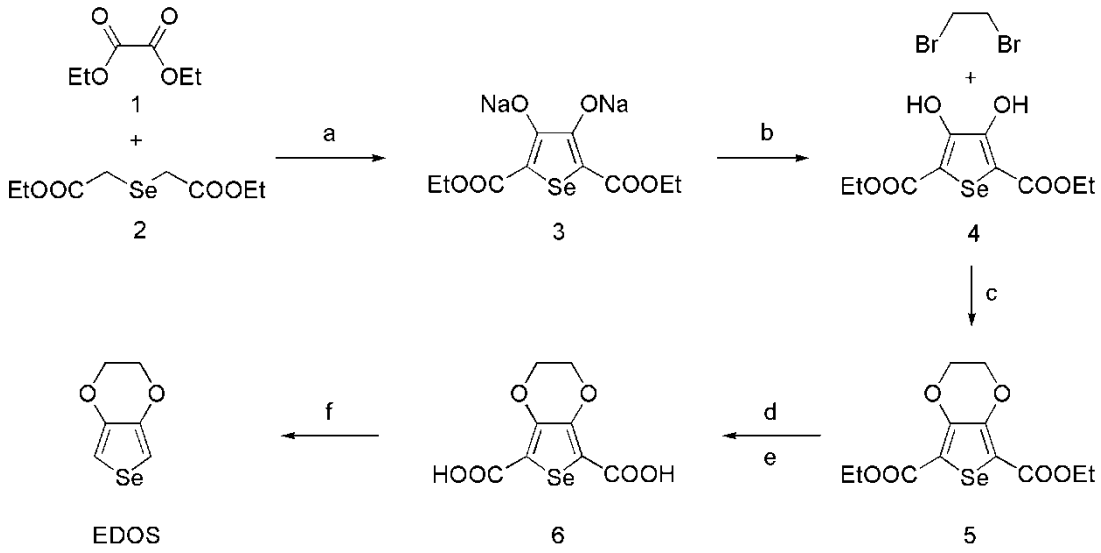

Scheme 1.6 Synthetic pathway of EDOS: (a) C_2H_5ONa/C_2H_5OH, r.t., 15 h (b) 3 N HCl (c) $BrCH_2CH_2Br$, K_2CO_3, DMF, 110 °C (d) KOH/C_2H_5OH, reflux, 5 h (e) 3 N HCl (f) melt.

According to this route, the condensation of diethyl selenodiglycolate (**2**) with diethyl oxalate (**1**) at room temperature gave diethyl-3,4-dihydroxythiophene-2,5-dicarboxylate (**3**) by using the classical Hinsberg synthesis [54]. Acidification of obtained compound (**3**) gave diethyl-3,4-dihydroxythiophene-2,5-dicarboxylic diacid (**4**). The compound **4** and 1,2-dibromoethane gave etherification reaction by the hydrolysis of the ester groups (**5**) and acidification of compound **5** gave a diacid (**6**). Finally, the EDOS was obtained as a colorless liquid by decarboxylation of diacid in the melt.

After synthesizing of EDOS, Cava and his colleagues have reported that EDOS was polymerized succesfully to get poly(3,4-ethylenedioxyselenophene) (PEDOS) via chemical or electrochemical method (**Scheme 1.7**).

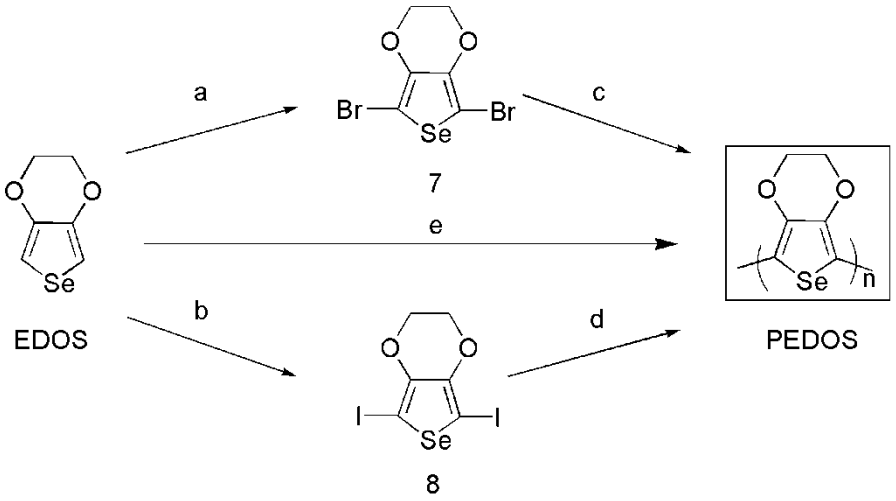

Scheme 1.7 Synthetic pathway for PEDOS (a) N-bromosuccinimid (NBS), $CHCl_3$, 0 ^oC, 1 h, 95% (b) N-iodosuccinimid (NIS), $CHCl_3$, AcOH, 5h, 83% (c) solid state polymerization, 50 ^oC, 1 day (d) solid state polymerization, 80 ^oC, 3 days (e) chemical or electrochemical polymerization.

In cyclic voltammetry study, EDOS showed one irreversible anodic peak at 1. 18 V (vs SCE). When compared to its thiophene analogue EDOT, EDOS has a lower potential by 0.26 V. This difference between two oxidation potential of two materials indicates that EDOS has low aromaticity [55] and more electron-rich compound than EDOT due to the presence of electron-donating features of oxygen atoms in the 3,4 positions of the selenophene unit [56]. Furthermore, EDOS has been polymerized successfully via potentiodynamic electrolysis (repetitive cyclic voltammetry). Like PEDOT, the obtained insoluble PEDOS film has an electrochromic behaviour. It is blue at neutral state (undoped) and transparent sky-blue at oxidized state (doped) on ITO (indium tin oxide).

Although electrochemically obtained PEDOS was insoluble, chemically obtained PEDOS by using of $FeCl_3$ oxidant was soluble in some organic solvents. Bendikov et al. conjectured that chemically obtained Cava's PEDOS had shorter polymer chains than electrochemically obtained polymer chains and therefore they are soluble due to the formation of oligomeric species.

After understanding the importance of PEDOS, many scientists have focused on various synthesis of EDOS [57, 58]. Among them, a straightforward synthetic route was reported by Bendikov and his colleagues. They successfully synthesized

EDOS in only two steps (**Scheme 1.8**). 2,3-dimethoxy-1,3-butadiene (**9**) and freshly prepared $SeCl_2$ gave 3,4-dimethoxyselenophene (**10**) in 42% of yield. Then, a transetherification of obtained compound **10** with ethylene glycol (**11**) gave rise to EDOS in 52% of yield. Furthermore, Bendikov's EDOS is highly stable under the ambient conditions and it was reported that EDOS would be able to keep for few years in refrigerator.

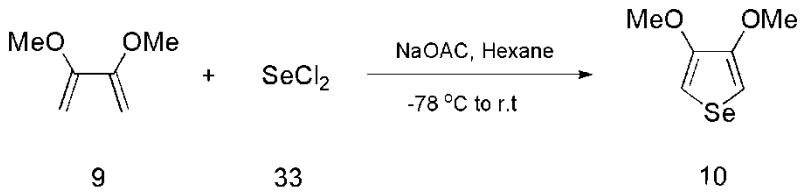

Scheme 1.8 A synthetic pathway for the synthesis of EDOS.

Like Cava's PEDOS, Bendikov et al. reported the insoluble PEDOS films obtained chemically and electrochemically. The optical studies showed that electrochemically obtained film is deep-blue when neutralized and transmissive-gray when oxidized. PEDOS has a band gap of 1.4 eV (876 nm), which is lower than PEDOT (1.7 eV). In addition to this comparison, the twisting energy of oligo- and polyselenophene units is higher than that of the related energy of oligo- and polythiophene units. Therefore, this energy difference causes the shorter C-C distance in selenophene rings. Depending on the bond length of ring, selenophene contributes the quinoid structure [55, 59, 60]. It is well known that the ability of quinoid structure lowers the aromaticity and increases the degree of planarity. Therefore, polyselenophene and its derivatives have low band gaps when compared to their thiophene analogues.

After synthesis EDOS and its polymer PEDOS, spectroelectrochemical studies have showed the formation of polarons and bipolarons at 1050 and 1600 nm, respectively,with a dramatically decreasing in π-π^* transition band at 673 nm during the oxidation (**Figure 1.7**).

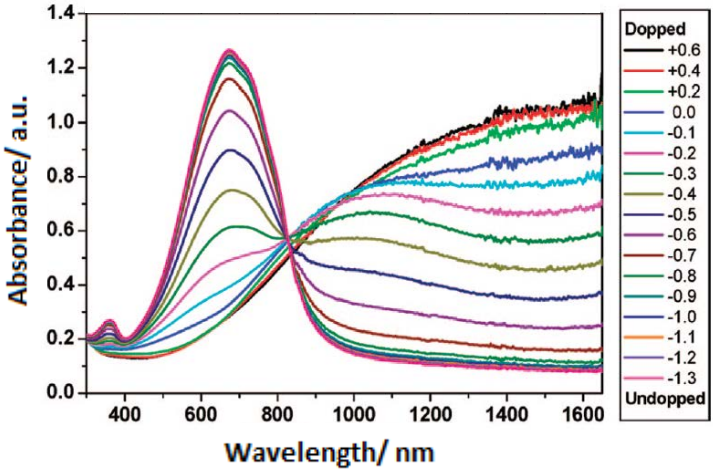

Figure 1.7 Spectroelectrochemical changes of PEDOS coated on ITO depending on applied potential between +0.6 and -1.3 V in 0.1 M tetrabutylammonium perchlorate dissolved in propylene carbonate [58].

While PEDOT exhibits 54% of ΔT% at 585 nm and 137 C/cm^2 of CE at 100 % fully switched [61], PEDOS has higher optical transparency as 55% at 666 nm and CE of 212 cm^2/C at fully switched [62]. Moreover, when focused on PEDOS in tems of electrochemical stability, which is durability after switching many times, PEDOS is electrochemically stable materials since PEDOS retained 83% of its electroactivity after 5,000 cycles when switched between -0.5 V and 0.5 V (vs. Ag/Ag$^+$).

When $FeCl_3$ is used as an oxidant, a highly conducting PEDOS could not been succeeded. On the other hand, solid state polymerization is an appropriate and effective method to obtain a conducting PEDOS, which has a conductivity of 3-30 S/cm in pressed pellet [58].

In order to cope with solubility problem and to enhance the electrochromic properties of PEDOS, Bendikov and his group have published some novel EDOS derivatives by means of substituted alkyl chains on ethylenedioxy bridge, called as PEDOS-C_n (**14**), where n=2, 4, 6, 8 and 12) (**Scheme 1.9**) [62, 63]. These compounds have been synthesized by the transetherification of 3,4-dimethoxythiophene (**10**) and 1,2-alkyldiol (**12**) in a catalytic amount of p-toluenesulfonic acid (p-TSA) to get EDOS-C_n (**13**) derivatives.

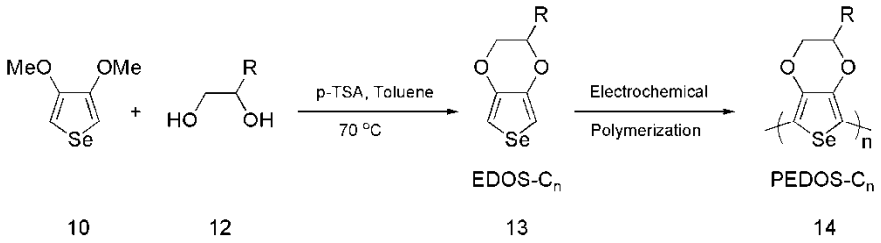

n	R
2	$-C_2H_5$
4	$-C_4H_9$
6	$-C_6H_{13}$
8	$-C_8H_{17}$
12	$-C_{12}H_{25}$

Scheme 1.9 A synthetic pathway for EDOS-C_n and their corresponding polymers.

In this study, Bendikov et al. has reported the effect of the length of the alkyl chains on ethylene bridge on the electrochromic properties of the related PEDOS-C_n derivatives in **Table 1.1**.

Table 1.1 Obtained polymers and their related electrochemical and optical data.

Polymers	**$E^{onset}_{(mon)}$ (V vs SCE)**	**$E^{ox}_{p,1/2}$ (V vs SCE)**	**E_g (eV)**	**λ_{max} (nm)**	**Δ%T**	**CE (cm^2/C)**	**Optical Stability**
PEDOS	-0.95	-0.49	1.40-1.42 [41,58,63]	666 673[41,58] 600[66]	55	212	60% 2,000 cyc.
PEDOS-C_2	-0.75	-0.67	1.46	688, 752	70	243	60% 5,000 cyc.
PEDOS-C_4	-0.52	-0.48	1.54	685, 761	77	369	60% 10,000 cyc.
PEDOS-C_6	-0.55	-0.46	1.54[62,63]	686, 763 692, 763[65]	88-89 [62,63,65]	715 686-773[62]	60% 10,000 cyc. 48%[62] 10,000 cyc.
PEDOS-C_8	-0.33	-0.25	1.55	684, 760	76	400	60% 500 cyc.
PEDOS-C_{14}	-0.37	-0.36	1.55	680, 755	67	219	60% 12,000 cyc.

According to **Table 1.1**, it can be summarized that PEDOS-C_6 has the best electrochromic properties in all PEDOS-C_n derivatives. It changed its color from

dark blue to highly transmissive upon moving from neutral to oxidized states. Among all PEDOS-C_n derivatives, the optical band gap of PEDOS-C_6 was determined as 1.54 eV, which is higher than that of PEDOS. Moreover, for the spectra of PEDOS-C_6 film, two sharp peaks at 686 nm and 763 nm are determined and labelled as the π-π* transitions (**Figure 1.8(a)**). It has a maximum of 88-89% of optical contrast ratio (percent transmittance change) at 763 nm (**Figure 1.8(b)**). This value is the same with another electrochromic polymer, called dibenzyl poly(3,4-propylenedioxythiophene), with highest reported ΔT% (89%) in the literature [64]. Furthermore, it was reported that the obtained PEDOS-C_6 film has a long-term optical stability. It retained 48% of its optical contrast ratio when switched between the reduction and oxidation states after 10,000 cycles under ambient conditions.

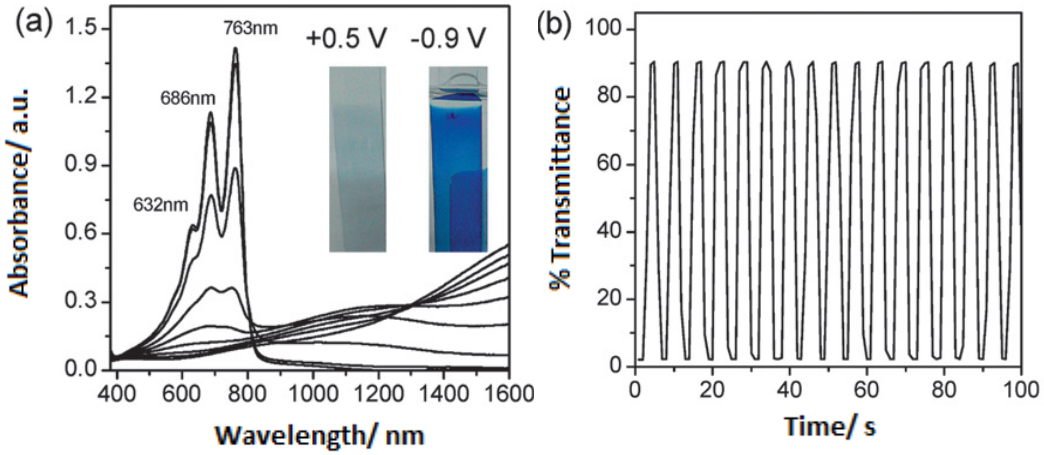

Figure 1.8 (a) Spectroelectrochemical data for PEDOS-C_6 film and (b) its percent transmittance monitored at 763 nm [62].

Also, PEDOS-C_6 film has both photothermal and thermoelectric properties at the same time. Kim et al. reported PEDOS-C_6 film as a promising candidate for near infrared (NIR) sensitive materials [65]. According to this study, it was supported that efficient visible to/from NIR chromism, photon to electric and heat, and heat to electric conversion could be realized in one PEDOS-C_6 film. These features make the PEDOS-C_6 film to amenable for use in displays, invisible NIR sensors, photodynamic therognosis, photothermal, thermoelectric and photo-thermo-electric devices.

Recently, a series of new polyselenophenes derivatives substituted with aromatic moieties in the 3,4-positions of the selenophene ring by alkylenedioxide bridge was reported (**Scheme 1.10**) [66]. Electrochemically formed insoluble polymer films (**17** and **20**) have very similar optical band gaps, which are 1.57 eV and 1.55 eV, respectively. The calculated band gaps are higher than that of PEDOS (1.4 eV). It can be summarized that the additional extension of fused benzene ring has no effect on the band gaps of related polymer.

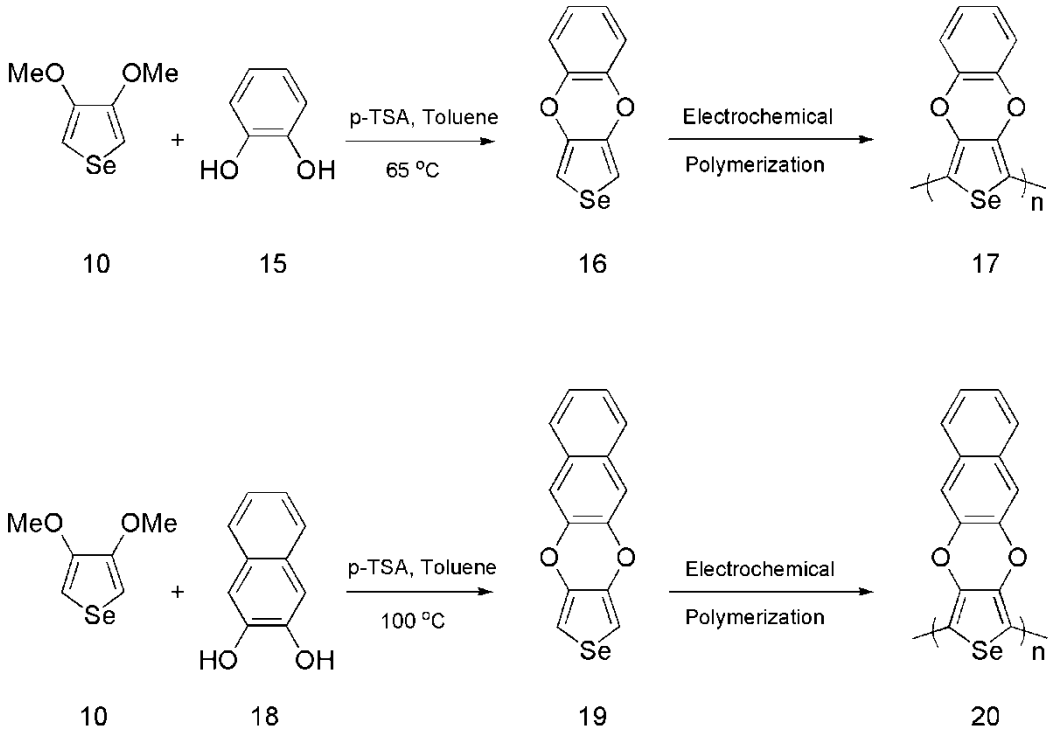

Scheme 1.10 A synthetic pathway for EDOS based monomers and their polymers.

Recently, Poverenov et al. have reported a novel series of electron donor-acceptor-donor trimeric systems containing EDOS and EDOT units. While donor units are EDOS and/or EDOT, 2,1,3-benzothiadiazole and 2,1,3-benzoselenadiazole are used as acceptor units. (**Scheme 1.11**) [67]. The electrochemically obtained polymers (**23** and **24**) are green in their neutral (reduction) states and transparent light blue in their oxidation states. Also, the band gaps were found to be as 1.10 eV for **23** and 1.03 eV for **24**.

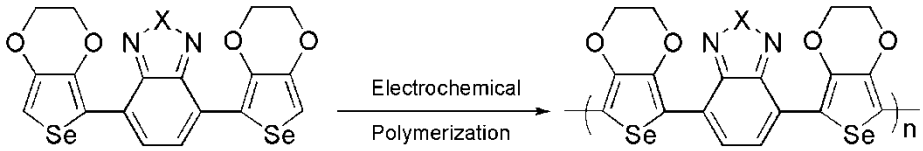

X: S (21)
Se (22)

X: S (23)
Se (24)

Scheme 1.11 Polymerization of donor-acceptor-donor type trimeric systems based on EDOS.

1.5.3 Poly(3,4-propylenedioxyselenophene)s (PProDOS)

Unfortunately, all obtained alkylenedioxyselenophene based polymers (PEDOS-C_n) were insoluble in common organic solvents. In order to overcome the insolubility problem, propylenedioxy bridge bearing alkyl groups with different lengths was used instead of ethylenedioxy bridge on selenophene ring. In this case, like 3,4-propylenedioxythiophene (ProDOT), [68-71, 13], it was expected that the synthesis and polymerization of alkyl chain substituted 3,4-propylenedioxyselenophenes (ProDOS) would give soluble polymers with low oxidation potential, high optical contrast ratio and optical transparency when oxidized.

Recently, Cihaner and his colleagues [72, 73] have focused on dialkyl substituted ProDOS derivatives (ProDOS-C_n; n= 4, 6 and 10) in order to obtain soluble polymers with good electrochemical and optical properties (**Scheme 1.12**).

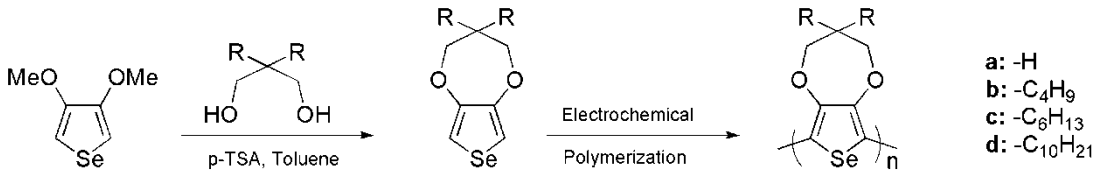

10

ProDOS-C_n
25 (a-d)

PProDOS-C_n
26 (a-d)

Scheme 1.12 A synthetic pathway for ProDOS-C_n derivatives and their polymers, PProDOS-C_n.

Each ProDOS-C_n has one irreversible oxidation peak which is lower than its ProDOT-C_n analogue (**Table 1.2**). As an example, when compared ProDOS-C_6 and its analogue ProDOT-C_6, during the first anodic scan their oxidation peak values are 1.36 and 1.52 V, respectively (**Figure 1.9(A)**). ProDOS-C_6 has a lower oxidation potential of 1.64 V when compared to ProDOT-C_6 (1.88 V). Also, in the case of the corresponding polymers, PProDOS-C_6 has exhibited a well-defined absorption band at longer wavelength.

Table 1.2 Optical and electrochemical stability properties of PProDOS-C_n and PProDOT-C_n [73].

Polymers	**Eg (eV)**	**λmax (nm)**	**Δ%T**	**CE* (cm^2/C)**
PProDOS[77]	1.65	626; 686	51	273
PProDOT[78]	1.7	567; 625	54	-
PProDOS-C_4	1.54	658; 714	55.4; 51.3	864
PProDOT-C_4	1.83	582; 632	68.1; 65.1	850
PProDOS-C_6	1.64	634; 698	59.6; 55.5	857
PProDOT-C_6	1.88	572; 630	64.7; 64.5	514
PProDOS-C_{10}	1.58	636; 697	55.5; 55.0	328
PProDOT-C_{10}	1.82	571; 622	71.5; 73.0	306

*at 95% of the full contrast

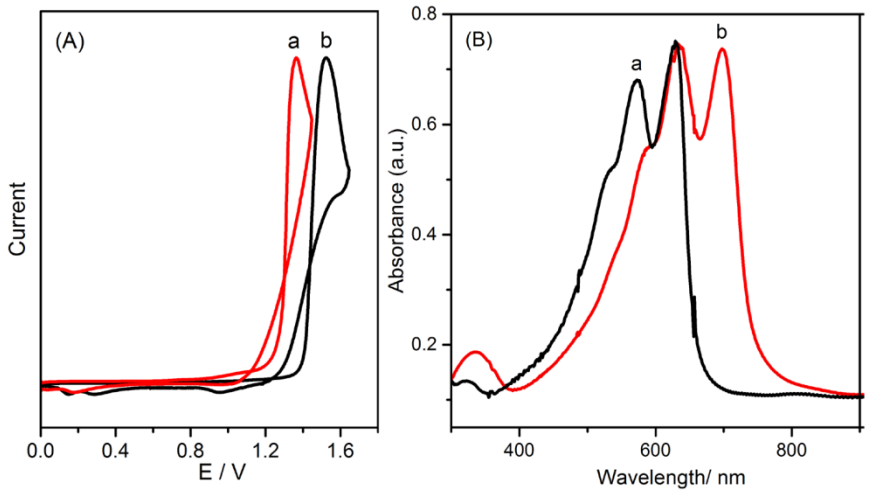

Figure 1.9 (A) Cyclic voltammograms of (a) ProDOS-C_6 (red line) and (b) ProDOT-C_6 (black line) in 0.1 M tetrabutylammonium hexafluorophosphate (TBAH) dissolved in CH_2Cl_2 at 100 mV s^{-1} (vs Ag/AgCl). (B) Optical absorption spectra of the neutral (a) PProDOT-C_6 (black line) and (b) PProDOS-C_6 films (red line) on ITO in CH_3CN.

On the other hand, the oxidation potential of ProDOS-C_n is moderately higher than that of EDOS (1.22 V vs Ag/AgCl) [58] since the increasing alkylenedioxy bridge size decreases the electron donating ability of oxygen atoms on selenophene ring [74].

Electrochemical polymerization of ProDOS-C_n (**26b-d**) gave highly regular polymer chains because of the symmetric alkyl chains on the central carbon atom of the propylene bridge. This regularity with the vibronic coupling exhibited itself as some splittings in the optical spectra of the neutral PProDOS-C_n films. As an example, PProDOS-C_6 film showed two absorption bands at 634 nm and 696 nm with a shoulder at 584 nm in **Figure 1.9(B)**. In a comparison with PProDOT-C_n films, the optical spectra of PProDOS-Cn films were red-shifted between 59 and 82 nm.

About the band gap (E_g) values, which were obtained from the lowest energy end of the π-π^* transitions in optical spectra, 1.65 eV for PProDOS [75], 1.55 eV for PProDOS-C_4, 1.63 eV for PProDOS-C_6, and 1.56 eV for PProDOS-C_{10}. PProDOS-C_n derivatives have smaller band gap values than PProDOT-C_n analogues (see **Table**

1.2). In addition, the optical band gaps of PEDOS-C_n are higher than that of PEDOS (1.40-1.42 eV).

It is well-known that PEDOT and PProDOT derivatives have violet/dark blue colors in their reduced (neutral) state owing to the presence of absorption between 400 and 500 nm. This problem was overcome by PEDOS and PProDOS derivatives since these polymers have no absorbtion between 400 and 500 nm due to the red-shift about 59-82 nm. Thus, the absence of absorption between 400 and 500 nm resulted in pure blue color. Except for PProDOS (**26a**), PProDOS-C_n (**26b-d**) films are pure blue in their neutral states and highly transmissive in their oxidized states (**Figure 1.10(a)**). All PProDOS derivatives have shown visible and NIR electrochromism under applied external potentials. In other words, upon oxidation the π-π^* absorption band in visible region begins to disappear and a new broad absorption band starts to appear in near-infarered (NIR) region, which confirmed that the visible and NIR electrochromism can be easily controlled under applied potential.

Focusing on this property, Kim and his colleagues published the visible and NIR electrochromism properties of PProDOS (**26a**) [75]. They exhibited that under the NIR (near-infrared) laser exposure the polymer film made its temperature of media increase by 10-13 ^oC, which make it a promising material to be amenable. By using of this photothermal property, the obtained polymer film can be used in photoablation and NIR electronics.

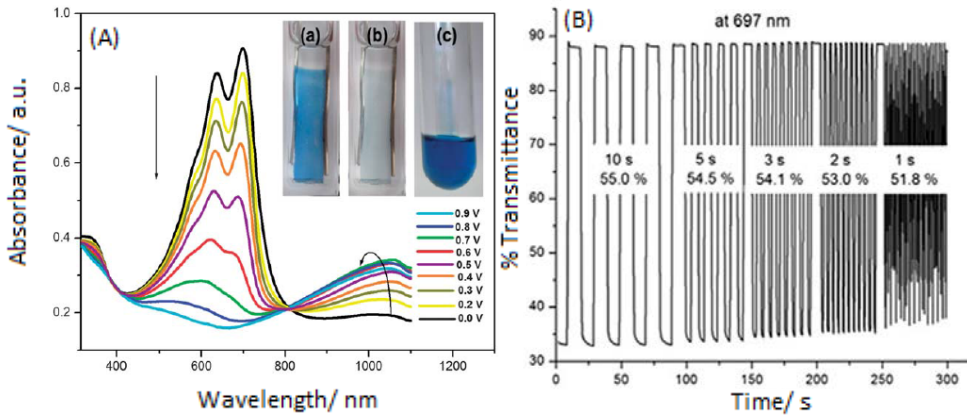

Figure 1.10 (A) Optical absorption spectra of PProDOS-C_{10} (26 mC cm^{-2}) on ITO in 0.1 M TBAH/CH_3CN at various applied potentials between 0.0 and 0.9 V. Inset: colors of PProDOS-C_{10} in (a) a neutral state at 0.0 V, (b) an oxidized state at 0.9 V and (c) dissolved in CH_2Cl_2. (B) Chronoabsoptometry experiments for PProDOS-C_{10} films on ITO in 0.1 M TBAH/CH_3CN while the polymers were switched in different time intervals (10, 5, 3, 2, 1 s) between redox states [73].

The percent transmittance changes (ΔT%) of PProDOS-C_n between the reduced (neutral) and oxidized states were determined between 51 and 60%. It was observed that these values are almost similar to that of PEDOS (55%), and smaller than those of PEDOS-C_n (67–89%) (**Table 1.1**). The response times for the obtained polymer films are about 1 s. As illustrated in **Figure 1.10(B)**, when the switching time was decreased from 10 s to 1 s, no appreciable change was observed in optical contrast ratio. Among obtained PProDOS-C_n films, PProDOS-C_4 and PProDOS-C_6 has shown the highest CE (at 95% of the full contrast) values at about 860 cm^2/C, which is higher than those of PEDOS (212 cm^2/C) and PEDOS-C_n (219-773 cm^2/C) and PProDOS (273 cm^2/C).

In a comparison to PProDOT-C_n and PEDOS, PProDOS-C_n films (**26b-d**) are highly stable and robust since their left electroactivity are between 82–97% even after 5000 cycles in the presence of oxygen **[73]**. Among them, the PProDOS-C_{10} exhibited an excellent stability because its electroactivity is 97% even after 40,000 cycles **[73]**. PProDOS-C_n derivatives (**26b-d**) are soluble and processable polymers and also have both lower band gaps and higher CEs. When focused on these results,

the effects of alkyl chain moieties on the optical features of the electrochromic polymers have been confirmed.

Reynolds and his group [76] have published that electrochromic properties of the polymer can be tuned by changing bridge size and substituents on the thiophene unit. The increasing bridge size and/or rigidity of substituents on the bridge give rise to higher contrast ratio since these two variables depend on the interchain separation and improvement of the charge/discharge ability of the polymer backbone during oxidation (doping) process. Inspired to this approach, Kumar and coworkers [64] have reported a new electrochromic polymer based on dibenzyl substituted poly(3,4-propylenedioxythiophene) (PProDOT-Bz_2). This is the first electrochromic polymer with the highest optical contrast ratio of 89% at 632 nm. Under the light of this approach and result, the advantages of polyselenophenes over polythiophenes (lower band gaps, higher coloration efficiencies, and higher redox stabilities), İçli-Özkut et al. have extended this work to illuminate the substituents and heteroatoms effect on the electrochromic properties in the similar systems. Therefore, they have reported novel ProDOS derivatives bearing benzyl groups (ProDOS-Bz_2) with ProDOT derivatives bearing benzyl (ProDOT-Bz_2) and naphtyl (ProDOT-Np_2) bulky substituents on the propylenedioxy bridge instead of alkyl chains (**Scheme 1.13**) [77].

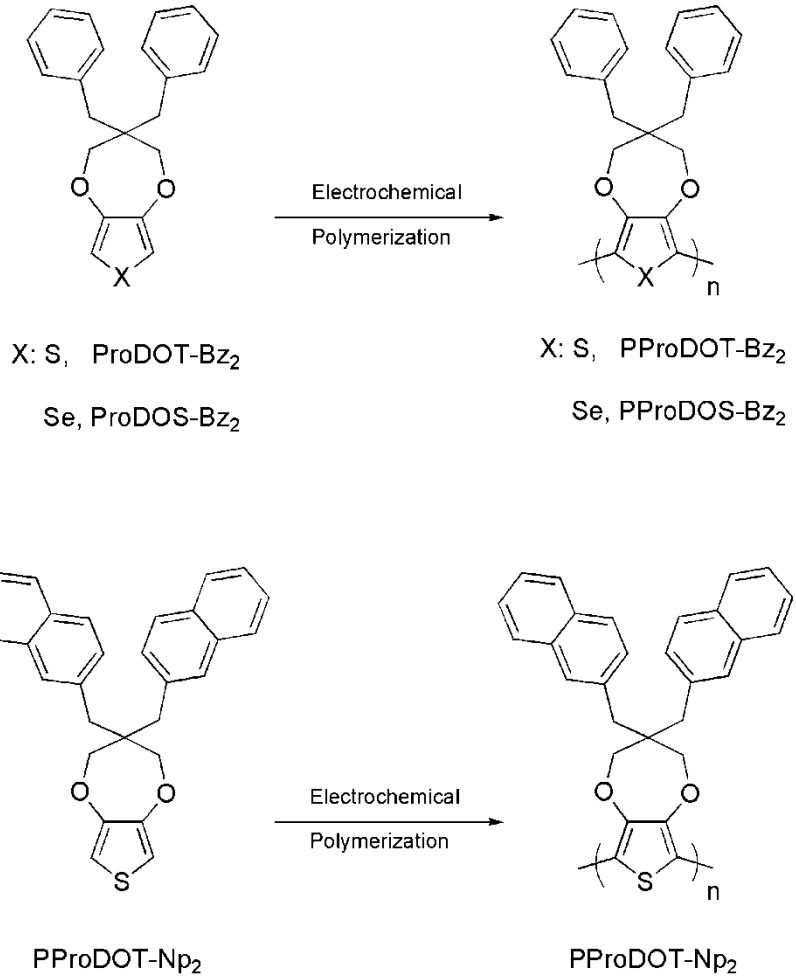

Scheme 1.13 Electrochemical polymerization of ProDOS-Bz_2, ProDOT-Bz_2 and ProDOT-Np_2.

PProDOS-Bz_2 has a band gap of 1.62 eV, which is lower than its analogue PProDOT-Bz_2 (1.85 eV). While PProDOT-Bz_2 is dark blue/violet color in its neutral state, PProDOS-Bz_2 film is pure blue color when neutralized. Both polymers are highly transmissive in their oxidized states. Unfortunately, it is the fact that PProDOT-Bz_2 has 75% of the percent transmittance change, which is not supported the value of 89% at 632 nm reported in the literature [64]. This value was found as 67% for PProDOS-Bz_2 film.

It can be easily concluded that the changing of heteroatom from the S atom to the Se atom in the ring leads to appreciable increase in the optical properties of the corresponding polymers (**Table 1.3**). On the other hand, it was reported that PProDOS-Bz_2 film has a high CE of 992 cm^2/C at 95% of the full contrast, which is the highest reported CE for the polyselenophene derivatives. Also, PProDOS-Bz_2 is

more stable and robust under ambient conditions. It retained 89% of its electroactivity after 5,000 switching, while this value is 67% for PProDOT-Bz_2.

Table 1.3 Optical properties for PProDOS and PProDOT derivatives [77].

Polymers	**Eg (eV)**	**λmax (nm)**	**Δ%T**	**CE (cm^2/C)**	**Color**	
					neutral state	**oxidized state**
PProDOS-Bz_2	1.62	710	67	992	blue	transparent
PProDOT-Bz_2	1.86	630	75	551	violet	transparent
PProDOT-Np_2	1.85	630	64	337	purple	transparent

Inspired by this property, Cihaner and his coworkers have extended their work to replace benzyl groups with naphtyl groups in order to increase the interchain separation more in the polymer chain. Inspite of the changing of bulky substituents, the decreasing in optical contrast was observed for bulky groups substituted PProDOT derivatives. In other words, as the replacement of naphtyl groups instead of benzyl groups in PProDOT ring, it was reported that the optical contrast values for PProDOT-Bz_2 and PProDOT-Np_2 are 75% to 64%, respectively.

Aim of the Study

In this study, the benzyl groups on the propylene bridge of the ProDOS-Bz_2 were replaced with naphtyl groups in order to increase the interchain separation in the PProDOS polymer chain and to achieve a high optical contrast ratio (Δ %T). Therefore, the effect of the heteroatoms and the size of bulky groups on the electrochemical and optical properties of the parent ProDOS and its polythiophene analogue (ProDOT) can be examined systematically. Also, in order to receive this aim, dinaphtyl substituted ProDOS (ProDOS-Np_2) as a new member of polyselenophenes will be synthesized, polymerized electrochemically and compared with its benzyl derivatives and polythiophene analogues (**Scheme 1.14**).

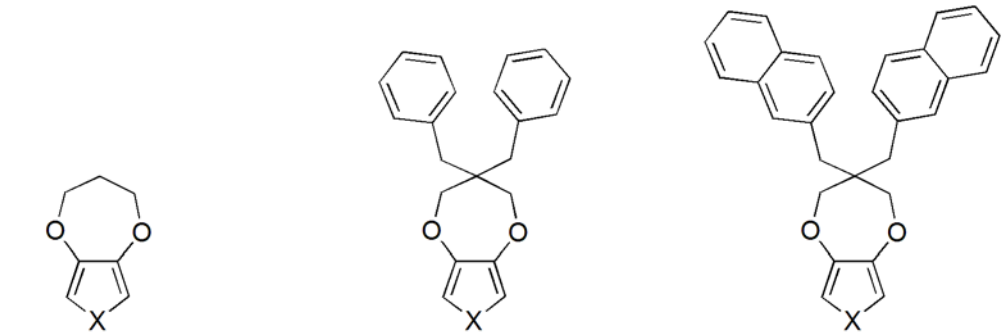

Scheme 1.14 Chemical structures of ProDOT and ProDOS and their benzyl and naphtyl substituted derivatives.

CHAPTER 2

MATERIALS AND METHODS

2.1 Materials

All chemicals were purchased from Sigma-Aldrich Chemical and used as received unless otherwise noted. For electrochemical and chemical experiments, dichloromethane and toluene were freshly distilled over CaH_2 under N_2 atmosphere. Ethyl alcohol was distilled over iodine and magnesium wire under argon atmosphere. The moleculer sieves (4 Å) was activated at high temperature (250 ^oC) for several hours.

2.2 General Methods

^1H and ^{13}C NMR spectra of obtained monomers were recorded on a Bruker Spectrospin Avance DPX-400 Spectrometer with $CDCl_3$ and chemical shifts were given relative to tetramethylsilane as the internal standard. Chemical shifts are reported in terms of ppm and that of $CDCl_3$ is 7.26 ppm. (See Appendix) The spectrum of high resolution mass spectrometry was recorded on A Water, Synapt HRMS (See Appendix). FTIR spectra were recorded by using of Nicolet 510 FTIR with attenuated total reflectance. Photographs of the polymer film were taken using a Canon (PowerShot A75) digital camera. Colorimetric measurements were recorded on Specord S600 (standard illuminator D65, field of width 10^o observer) and color space was given by the International Commission of Illumination with luminance (L), hue (a), and intensity (b). Platinum cobalt DIN ISO 621, iodine DIN EN 1557, and Gardner DIN ISO 6430 are the references of colorimetric measurements.

2.3 Electroanalytical Studies

Cyclic voltammetry and electrolysis experiments were performed by using a Gamry PCI4/300 and Gamry Reference 600 potentiostat–galvanostat. The electro-optical spectra were monitored on a Specord S600 Spectrometer. The

optoelectrochemical spectra of the film were recorded in-situ under applied different potentials. Also, a square wave potential method was used to investigate the ability of switching of the polymer film between its neutral and doped states. Tetrabutylammonium hexafluorophosphate (TBAH) was used as an electrolyte. Redox behaviour and polymerization were performed in an electrolyte solution of 0.1 M TBAH dissolved in dichloromethane. Electrochemical and optical properties of the polymers were also studied in dichloromethane containing 0.1 M TBAH. In three-electrode system, a platinum disc (0.03 cm^2) and a platinum wire electrode were used as working and counter electrodes, respectively. A Ag/AgCl electrode in 3 M NaCl(aq) solution was used as a reference electrode calibrated externally using 0.53 mM solution of ferrocene/ferrocenium couple in 0.1 M TBAH/CH_2Cl_2 solution. The oxidation onset potential of ferrocene was found as 0.54 V vs Ag/AgCl. Electrochemically obtained polymer films were synthesized both by repetitive cycling and constant potential electrolysis. After electropolymerization, polymer coated working electrode was washed with CH_2Cl_2 to remove the unreacted monomers and oligomeric species. Then, the polymer film was switched in several times between its redox states to get repeatable results in electrochemical and optical studies. Optical properties were investigated in situ by using an indium-tin oxide (ITO, Delta. Tech. 8–12 Ω, 0.7 x 5.0 cm^2) electrode as a working electrode in a UV cuvette. A platinum wire and Ag wire electrodes were used as a counter electrode and a pseudo-reference electrode, respectively.

2.4 Synthesis of Chemicals

Compounds 3,4-dimethoxyselenophene [58] and 2,2-bis((naphthalen-2-yl)methyl)propane-1,3-diol [77] were prepared according to literature procedures.

2.4.1 Synthesis of 2-((naphthalen-2-yl)methyl)-2-((naphthalen-3-yl)methyl)propane-1,3-diol (102)

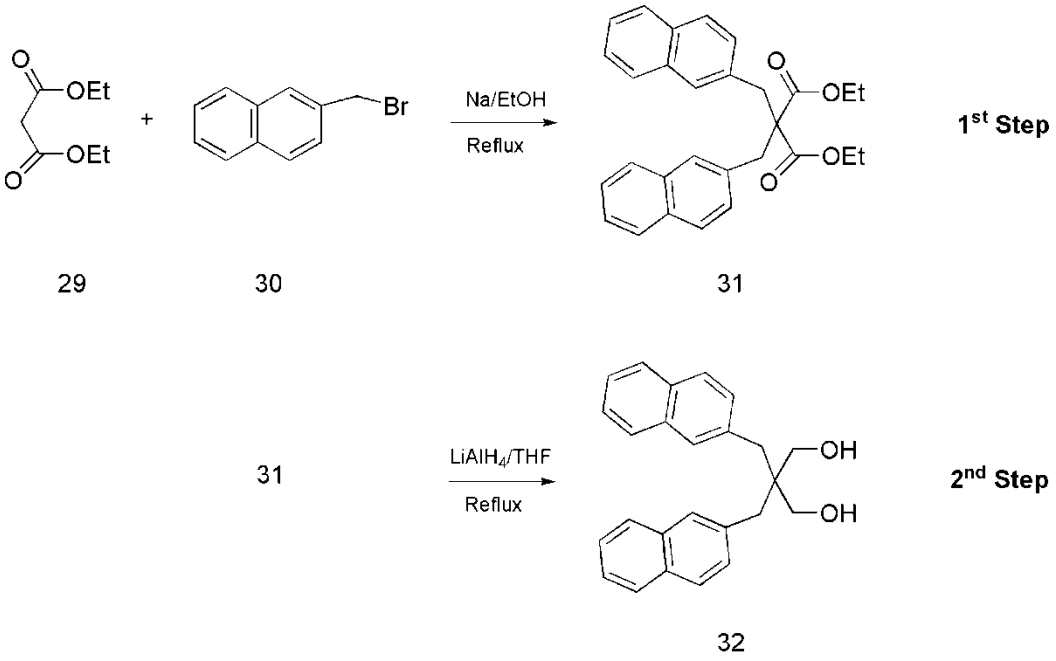

Scheme 2.1 A synthetic route for 2-((naphthalen-2-yl)methyl)-2-((naphthalen-3-yl)methyl)propane-1,3-diol.

Synthesis of diethyl 2,2-bis((naphthalen-2-yl)methyl)malonate (31)

To a 500 mL two-necked reaction flask, 160 mL of freshly distilled dry ethanol and sodium metal (4.67 g, 203 mmol, 3.25 eq.) were taken and stirred to dissolve all sodium at room temperature. After disolving sodium metal (viscous transparent color), diethyl malonate (10 g, 62.4 mmol, 1.0 eq.) was added dropwise to the reaction flask in 1 hour and reaction medium (viscous white color) was heated to reflux (80 ^{o}C). During refluxing, 2-(bromomethyl)-naphthalane (30) (50.4 g, 228 mmol, 3.65 eq) in 100 mL ethanol was added slowly and refluxed for 3 days. After completing the reaction, the solvent was evaporated under the reduced pressure by using a rotary evaporator and the obtained brown slurry mixture was extracted with cold diethyl ether and cold water. Then, the organic phase was dried over anhydrous magnesium sulfate ($MgSO_4$), filtered and the solvent was removed under reduced pressure. The obtained viscous yellow compound (68%, 18.7 g) was purified by using vacuum distillation at 200 ^{o}C. The important point is that it should not be

removed at high temperature because it may be decomposed under open air at high temperature.

Synthesis of diethyl 2,2-bis((naphthalen-2-yl)methyl)malonate (32)

To a 500 mL two-necked reaction flask, 150 mL of freshly distilled dry tetrahydrofuran (THF) and lithium aluminum hydride ($LiAlH_4$) were placed and heated to reflux under Ar atmosphere. Then, synthesized compound **31** (18.7 g, 42.4 mmol, 1 eq.) was added drop by drop in 1 hour. It was stopped after 1 day and the reaction solvent was evaporated under the reduced pressure by using a rotary evaporator and the obtained brown slurry mixture was extracted with cold diethyl ether and cold water. Then, organic phase was dried over anhydrous magnesium sulfate ($MgSO_4$) filtered and the solvent was removed under reduced pressure. The viscous yellow compound (60%, 16.3 g).was obtained without any further purification.

2.4.2 Synthesis of 3,4-dimethoxyselenophene (9)

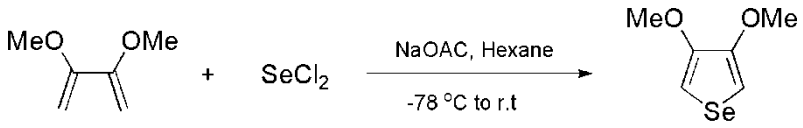

9 33 10

Scheme 2.2 A synthetic pathway for 3,4-dimethoxyselenophene

In order to get selenium dichloride ($SeCl_2$) (**33**), to a 10 mL reaction flask, Se powder (800 mg, 10.1 mmol, 1 eq.) was put under argon gas at 10 ^oC. Then, SO_2Cl_2 (1.36 g, 10.1 mmol, 1eq.) was added to Se powder drop by drop. After 30 min, 3 mL hexane was added to the reaction flask and the resulting mixture was stirred for 3 h at room temperature. During that time, to a 250 mL two-necked reaction flask, 150 mL of freshly distilled dry hexane, 2,3-dimethoxy-1,3-butadiene (1.0 g, 8.76 mmol, 1 eq.) and sodium acetate (NaOAc) (2.05 g, 25 mmol, 2,85 eq.) were taken and stirred under Ar atmosphere at room temperature for 30 minutes and then at -78 ^oC for 1 h. After getting thermal balance, the obtained fresh $SeCl_2$ was added as drop wise to the

main reaction flask at -78 ^{o}C. The obtained yellow mixture was further stirred for 1 h at the same temperature and then brought to room temperature over a period of 2 h. Finally, this mixture was further stirred for 4 h. The reaction mixture was filtered through neutral silica gel. The obtained yellow mixture was concantrated under reduced pressure. The formed crystalline yellow compound was stored for the next step at -20 ^{o}C and characterized by NMR (see Appendix A) and FTIR (see Appendix C) spectroscopic techniques as follow; ^{1}H NMR (400 MHz, $CDCl_3$) δ 6.48 (s, 1H), 3.78 (s, 3H) ^{13}C NMR (100 MHz, $CDCl_3$) δ 149.05, 96.04, 57.04

2.4.3 Synthesis of 3,4-dihydro-3,3-bis((naphthalen-2-yl)methyl)-2H-thieno[3,4-b][1,4]dioxepine (ProDOT-Np_2)

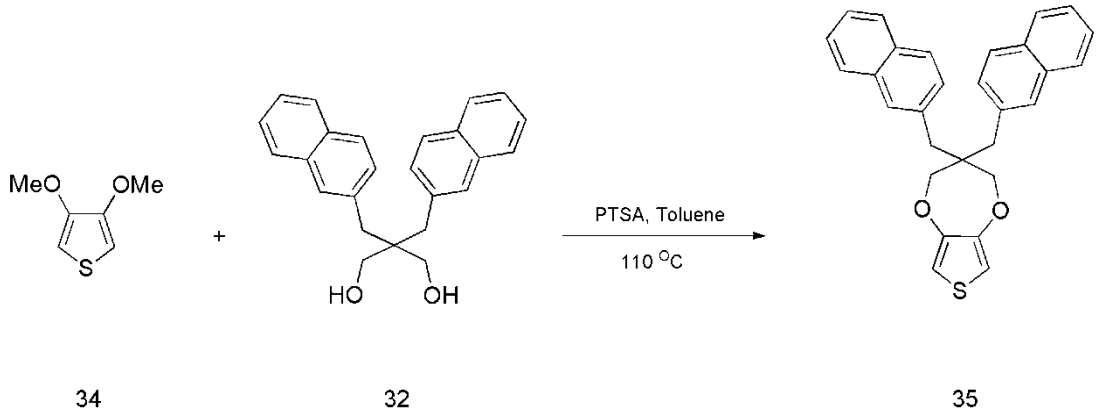

Scheme 2.3 A synthetic pathway for ProDOT-Np_2.

To a 50 mL two-necked reaction flask, 3,4-dimethoxythiophene (100 mg, 0.694 mmol, 1 eq.) and the synthesized diol compound (32) (495 mg, 1.39 mmol, 2.0 eq.) in freshly distilled toluene (30 mL) were taken and stirred under Ar atmosphere. Then, a catalytic amount of para-tolunesulfonic acid (p-TSA) (12 mg, 0.0694 mmol, 0.1 eq.) was added to this mixture and refluxed via a soxhelet apparatus containing 4 A^{o} molecular sieves for 2 days. After the reaction was stopped, the black reaction mixture was poured onto the distilled water to wash the organic phase by using a seperatory funnel. The obtained organic phase was dried over anhydrous magnesium sulfate ($MgSO_4$) and filtered. The resulting yellowish mixture was concantrated under reduced pressure. Finally, the obtained yellowish-brown slurry compound was

further purified via silica gel column chromatography in a mixture of hexane and CH_2Cl_2 (10:1) and characterized by NMR (see Appendix A) and FTIR (see Appendix C) spectroscopic techniques as follow; ^{1}H NMR (400 MHz, $CDCl_3$) δ 7.69 (m, 6H), 7.53 (s, 2H), 7.35 (m, 4 H), 7.22 (dd, *J* = 8.4, 2H), 6.40 (s, 2H), 3.85 (s, 4H), 2.96 (s, 4H). ^{13}C NMR (100 MHz, $CDCl_3$) δ 150.26, 134.23, 133.35, 132.26, 129.33, 129.14, 127.79, 127.65, 126.19, 125.71, 106.55, 77.63, 77.30, 45.85, 40.12. HRMS: 437.193 g.mol^{-1} (calculated: 436.565 g.mol^{-1}) in +80 ppm

2.4.4 Synthesis of 3,4-dihydro-3,3-bis((naphthalen-2-yl)methyl)-2H-selenopheno[3,4-b][1,4]dioxepine (ProDOS-Np$_2$)

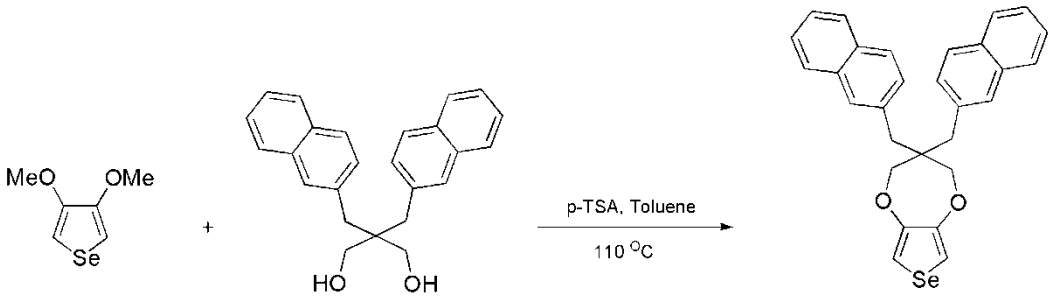

Scheme 2.4 A synthetic pathway for ProDOS-Np$_2$.

To a 50 mL two-necked reaction flask, 3,4-dimethoxyselenophene (100 mg, 0.523 mmol, 1 eq.) and the diol compound (32) (374 mg, 1.05 mmol, 2.0 eq.) in freshly distilled toluene (30 mL) were taken and stirred under Ar atmosphere. Then, a catalytic amount of p-TSA (8.9 mg, 0.0523 mmol, 0.1 eq.) was added to this mixture and refluxed via a soxhelet apparatus containing 4 A^o molecular sieves for 2 days. The black colored mixture was poured onto the distilled and extracted with water to wash the organic phase by using of seperatory funnel. The obtained organic phase was dried over anhydrous magnesium sulfate ($MgSO_4$) and filtered. The resulting yellowish-brown mixture was concantrated under reduced pressure. Finally, the obtained brown slurry compound was further purified via neutral silica gel column chromatography in a mixture of hexane and CH_2Cl_2 (5:1) and characterized by NMR (see Appendix A) and FTIR (see Appendix C) spectroscopic techniques as

follow; ^{1}H NMR (400 MHz, $CDCl_3$) δ 7.80 (m, 6H), 7.64 (s, 2H), 7.46 (m, 4H), 7.33 (dd, *J* = 8.4, 2H), 7.01 (s, 2H), 3.93 (s, 4H), 3.07 (s, 4H). ^{13}C NMR (100 MHz, $CDCl_3$) δ 151.40, 134.24, 133.29, 132.19, 129.28, 129.11, 127.73, 127.59, 126.12, 125.64, 109.36, 77.22, 60.41, 45.79, 40.03. HRMS: 483.460 g.mol^{-1} (calculated: 485.101 g.mol^{-1}) in -1.9 ppm

CHAPTER 3

RESULTS AND DISCUSSION

3.1 Electrochemical Polymerization

The redox behavior of ProDOS-Np_2 was investigated via cyclic voltammetry in an electrolyte solution of 0.1 M TBAH dissolved in CH_2Cl_2. As expected, ProDOS-Np_2 has a lower oxidation potential of 1.82 V than its thiophene analogue ProDOT-Np_2 (2.02 V) (**Figure 3.1**). This lower oxidation potential indicates the lower aromaticity of the selenophene ring [55].

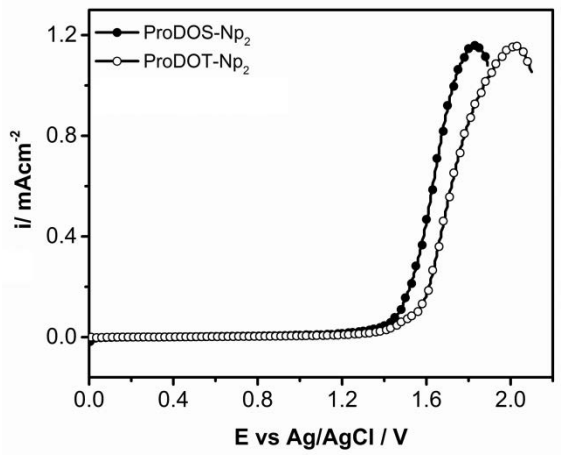

Figure 3.1 Cyclic voltammograms of $8x10^{-3}$ M of ProDOS-Np_2 and ProDOT-Np_2 in an electrolyte solution of 0.1 M TBAH/CH_2Cl_2 at a scan rate of 100 mV/s.

As shown in **Figure 3.2**, the polymerization was performed between -0.3 V and 1.5 V vs Ag/AgCl. During the first reverse scan, a nucleation loop was observed, which confirmed the formation of highly reactive species resulting in polymerization formed on the electrode surface, and one reduction peak at 0.18 V was appeared due to the oligomeric species coated on the electrode. These species are oxidized at 0.28 V and during the second scan and after each successfull repetitive cycle, the intensities of the peak currents started to increase. After a certain number of cycles,

two well-defined reversible redox couples were observed at 0.43 V/0.06 V and 1.02 V/0.75 V, which could be attributed to the formation of polaron and bipolaron charge carriers in the obtained polymer film called PProDOS-Np_2 (**Scheme 3.1**).

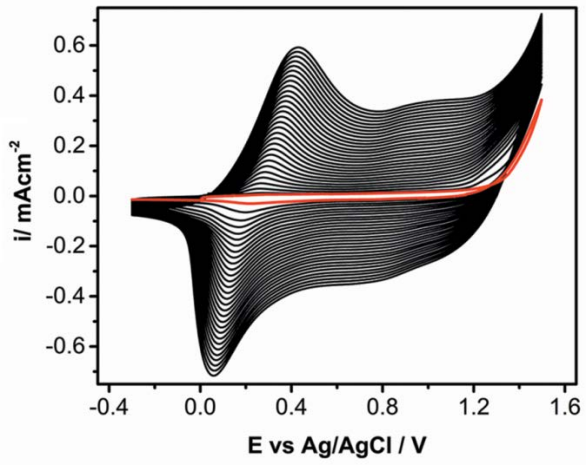

Figure 3.2 Repetitive cyclic voltammogram of ProDOS-Np_2 (0.05 M) in order to form PProDOS-Np_2 on Pt electrode in an electrolyte solution of 0.1 M TBAH/CH_2Cl_2 at a scan rate of 100 mV/s between -0.3 V and 1.5 V.

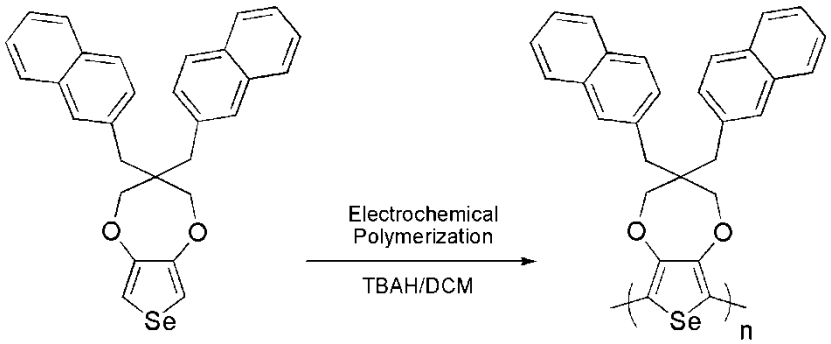

Scheme 3.1 Electrochemical polymerization of ProDOS-Np_2 to form PProDOS-Np_2 polymer.

The polymer film was washed with CH_2Cl_2 to remove unreacted monomers and oligomeric species from the coated electrode surface. The polymer film was insoluble in common organic solvents. PProDOS-Np_2 film has a well-defined

reversible redox couple at a half wave potential of 0.24 V (**Figure 3.3(a)**), which is lower than PProDOT-Np_2

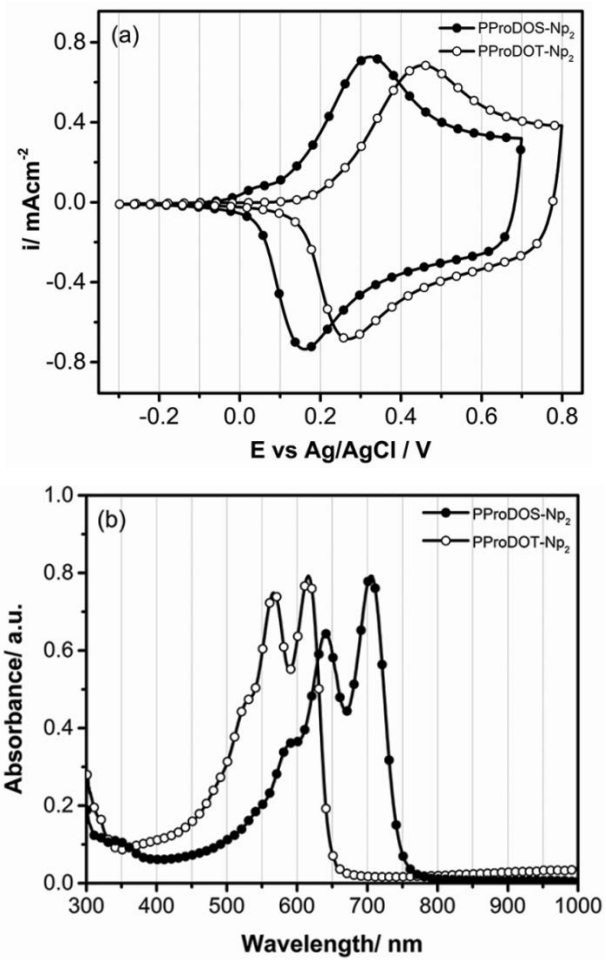

Figure 3.3 (a) Cyclic voltammograms of PProDOS-Np_2 and PProDOT-Np_2 films on the Pt electrode in 0.1 M TBAH/CH_2Cl_2 solution at a scan rate of 100 mV/s vs Ag/AgCl. (b) Absorption spectra of PProDOS-Np_2 and PProDOT-Np_2 films on ITO in CH_2Cl_2.

As shown in **Figure 3.4(a)**, redox couple currents of PProDOS-Np_2 film intensified with an increase in the scan rate when switched between -0.3 V and 0.7 V. Both anodic and cathodic peak currents changed linearly as a function of scan rate, which confirmed that the redox process is non-diffusional and the polymer film was well adhered to the electrode surface (**Figure 3.4(b)**). Also, the amount of charge and discharge was constant with an increase in scan rate, which showed that

this polymer film can be charged and discharged (doping/dedoping) even at high scan rates (**Figure 3.4(c)**).

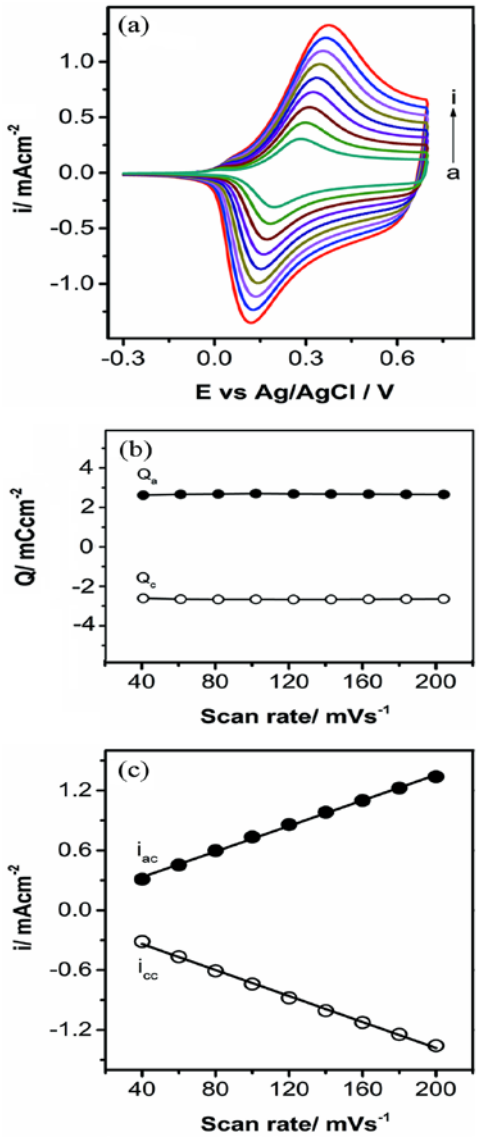

Figure 3.4 (a) Scan rate dependence of PProDOS-Np_2 film on the Pt disk electrode in 0.1 M TBAH/CH_2Cl_2 at different scan rates between 40 mV/s and 200 mV/s with 20 mV/s increments: (mV/s) (a) 40; (b) 60; (c) 80; (d) 100; (e) 120; (f) 140; (g) 160; (h) 180; and (i) 200, (b) the amount of charge (Q_a) and discharge (Q_c) as a function of scan rate for neutralized and oxidized film and (c) the relationship of anodic (i_{ac}) and cathodic (i_{cc}) current peaks with scan rates in 0.1 M TBAH/CH_2Cl_2 solution.

It is well known that superior p-doping process of the film can make it a promising candidate for battery and capacitor applications. For example, a conjugated polymer film with a nearly rectangle shape of cyclic voltammogram with a wide potantial window can be amenable for use in electrochemical capacitors. In order to show the utulity of PProDOS-Np_2 film as a capacitor, flat current responses as a fingerprint of the capacitors were observed when the film was cycled between 0.45 V and 1.2 V (**Figure 3.5(a)**). The polymer film preserved its rectangle shape in cyclic voltammogram even at high scan rates with no appreciable change in voltammogram and also the amount of charge (Q_a) and discharge (Q_c) did not change as a function of scan rate, indicating a fast charge process (doping/dedoping) (**Figure 3.5(b)** and **(c)**). This intriguing feature makes the polymer film a good candidate for use in supercapacitors as an electrode with a broad potential window.

The stability of PProDOS-Np_2 was tested under ambient condition in the presence of air (without purging with an inert gas). It exhibited highly stable and robust behavior after thousands of switching between -0.2 V and 0.9 V via a square wave potential method. For example, it retained 84% of its electroactivity even after 5000 cycles (**Figure 3.6**). Also, PProDOS-Np_2 has higher stability than its thiophene analogue PProDOT-Np_2 (63% after 5000 cycles) [77]. Without breaking traditions, the polymer films based on ProDOS units are exceptionally more stable than their ProDOT analogs [72, 73, 77].

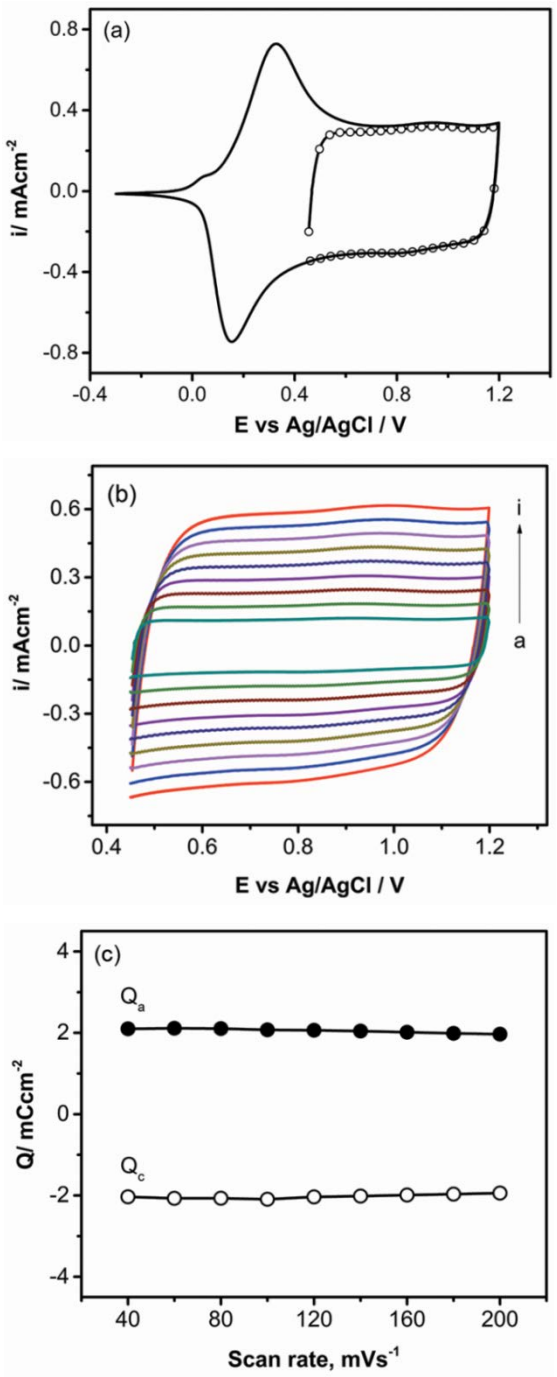

Figure 3.5 (a) Cyclic voltammogram of PProDOS-Np_2 film on the Pt electrode in 0.1 M TBAH/CH_2Cl_2 solution between -0.3 V and 1.2 V and then between 0.45 V and 1.2 V at a scan rate of 100 mV/s vs Ag/AgCl. (b) Cyclic capacitance effect of PProDOS-Np_2 film on the Pt disk electrode in 0.1 M TBAH/CH_2Cl_2 at different scan rates between 40 mV/s and 200 mV/s with 20 mV/s increments: (mV/s) (a) 20; (b) 40; (c) 60; (d) 80; (e) 100; (f) 120; (g) 140; (h) 160; (i) 180; and (j) 200 and (c) the amount of charge (Q_a) and discharge (Q_c) as a function of scan rate for oxidized and then neutralized film in 0.1 M TBAH/CH_2Cl_2 solution.

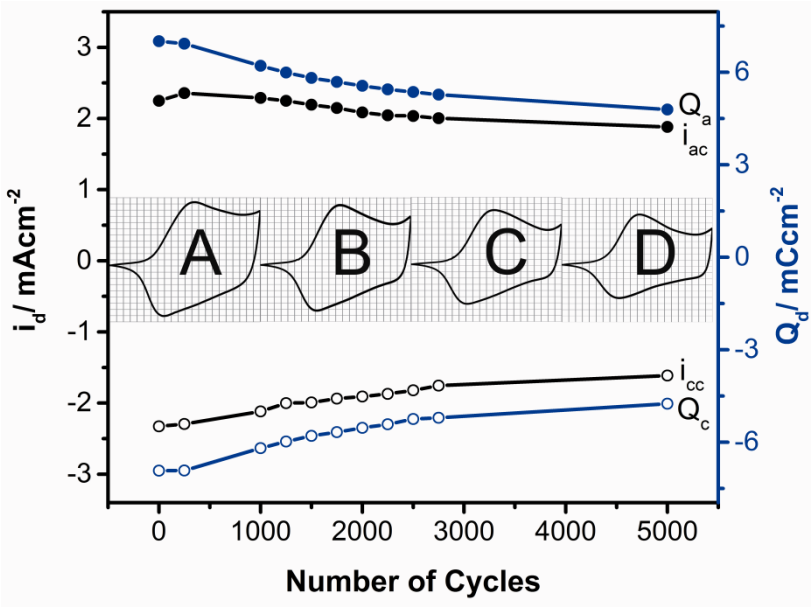

Figure 3.6 Stability test for the PProDOS-Np_2 (159 mC/cm^2) film in 0.1 M TBAH/CH_2Cl_2 by using a square wave potential method between -0.2 V and 0.9 V for 3 s under ambient conditions. The voltamograms of the PProDOS-Np_2 (159 mC/cm^2) film at a scan rate of 100 mV/s by cyclic voltammetry as a function of the number of cycles: A: 1, B: 1000, C: 2500, D: 5000 cycles; (a) Q_a (anodic charge stored), (b) i_{pa} (anodic peak current), (c) i_{pc} (cathodic peak current).

3.2 Spectroelectrochemistry

Unlike PProDOT-Np_2 films, the optical spectrum of the neutral PProDOS-Np_2 film showed vibronic couplings at 595, 641 and 705 nm in its π-π* transition band (**Figure 3.3(b)**). These splittings in the optical spectrum indicated well-organized (regioregular) and more rigid structure like PProDOT-Np_2 (529, 566 and 616 nm). Also, the optical spectrum of PProDOS-Np_2 films was red shifted between 66 and 89 nm. The band gap (E_g) value was determined from the lowest energy end of the π-π* transition and found as 1.67 eV, which is 0.24 eV smaller than PProDOT-Np_2 film (1.91 eV) and somewhat higher than PProDOS (1.65 eV) (see **Table 3.1**) [75].

Table 3.1 Optical properties of PProDOS and PProDOT derivatives.

Polymers	E_g (eV)	λ_{max} (nm)	Δ% T	CE* (cm^2/C)	Color at	
					neutral state	oxidized state
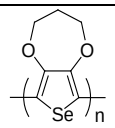 PProDOS[75]	1.65	626, 686	51	273	blue	transparent
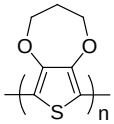 PProDOT[78]	1.7	567, 625	54	255	violet	transparent
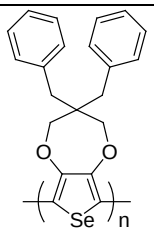 PProDOS-Bz_2[77]	1.62	645, 710	67	992	blue	transparent
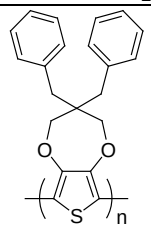 PProDOT-Bz_2[77]	1.86	575, 630	75	551	violet	transparent
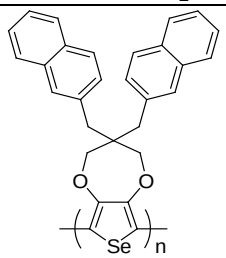 PProDOS-Np_2	1.67	641, 705	84	755	blue	transparent
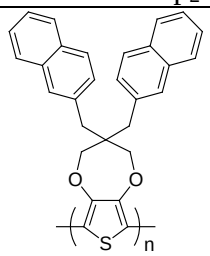 PProDOT-Np_2[77]	1.91	566, 630	64	337	purple	transparent

* at 95% of the full contrast

PProDOT-Np_2 film was purple at the neutral state (L=61.86, a=10.35, b=-36.98), whereas PProDOS-Np_2 film was pure blue (L=75.14, a=-27.85, b=-35.34) when neutralized due to the absence of absorbance between 400 and 500 nm. Both polymer films are highly transmissive at their oxidized states: L=92.70, a=-2.84, b=2.93 for PProDOS-Np_2 and L=93.88, a=-1.43, b=0.84 for PProDOT-Np_2. Upon moving from neutral state to oxidized state under various applied external potentials, PProDOS-Np_2 exhibited 84% of the percent transmittance change, to our best knowledge (**Figure 3.7**) , which is the second highest reported optical contrast ratio as a member of polyselenophenes [62, 63], which can make it one of the most attractive electrochromic materials. Unfortunately, this value decreased to 64% at 630 nm for PProDOT-Np_2 film.

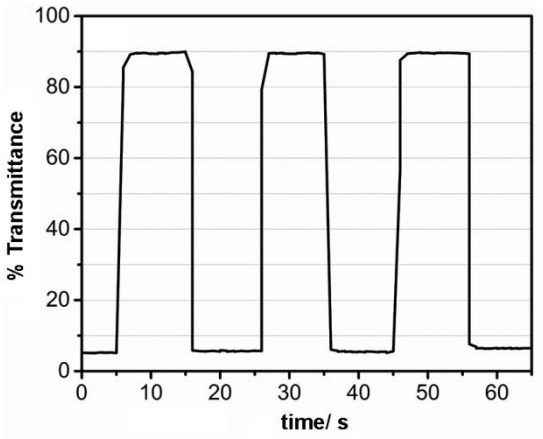

Figure 3.7 Chronoabsoptometry experiment for PProDOS-Np_2 film on ITO in 0.1 M TBAH/CH_2Cl_2 while the polymer film was switched in 10 s time intervals between -0.3 V and 0.7 V.

Unlike polythiophene analogues, the results of optical experiments indicated that an increase in the size of the substituent on the bridge gave rise to an increase in the optical contrast of the related ProDOS based polymers. While the parent PProDOS film has 51% optical contrast, dibenzyl substituted PProDOS-Bz_2 has 65% and dinaphtyl substituted PProDOS-Np_2 has 84% optical contrast (**Table 3.1**).

On the other hand, response time (or switching time), which is the time necessary to change the color of the polymer film, is a key parameter for electrochromic materials to be found an application in optical devices and displays. In order to find the response time, the percent transmittance changes were recorded

in-situ via a square-wave potential method. The polymer film on ITO was switched between its redox states under external potentials of -0.3 V and 0.7 V with a switching time of 10 s and the response time was found as about 1 s.

The transmissivity of the PProDOS-Np_2 film was also confirmed by using the relative luminance measurement (Δ%Y). The polymer film exhibited high luminance over 90% during oxidation, and Δ%Y was calculated to be as 19% between the colored and bleached states (**Figure 3.8**).

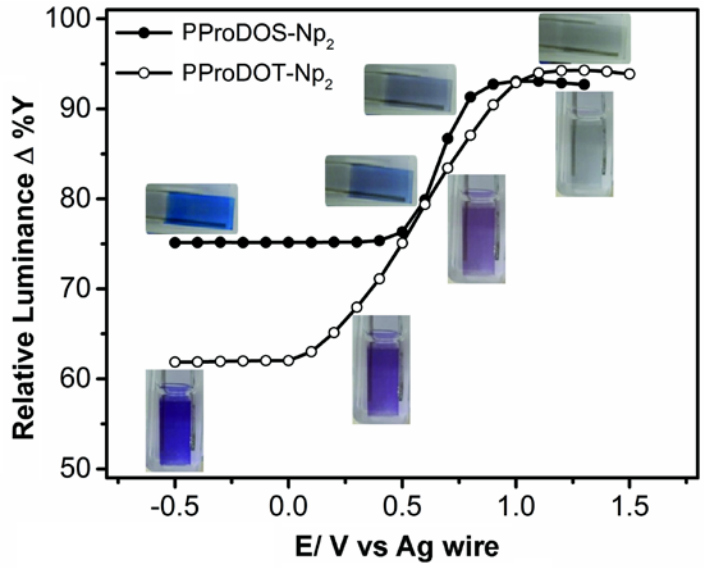

Figure 3.8 Relative luminances of PProDOS-Np_2 (a.u. 1.1 at 705 nm) and PProDOT-Np_2 films (a.u. 1.9 at 630 nm) on ITO in 0.1 M TBAH/CH_2Cl_2 at various applied potentials.

As shown in **Figure 3.9(a)**, during oxidation of PProDOS-Np_2 film on ITO π-π* transition band started to decrease with a concomitant increase after 750 nm attributed the formation of charge carriers. Upon further oxidation, the color of the polymer film changed from pure blue to transmissive state/colorless and the π-π* transition band disappeared completely. The absorption band intensified after 750 nm received a maximum level and then decreased, which is the conversion of polaron to bipolaron charge carriers as a signature of a doped conjugated polymer during oxidation. The low-absorption intensity beyond 750 nm for oxidized PProDOS-Np_2 indicated a weak interaction between polymer chains [62]. This interaction is

stronger for PProDOT-Np_2 chains as shown in **Figure 3.9(b)**. Also, the similar changes in optical spectrum were observed for PProDOT-Np_2 film, which is purple when neutralized and transmissive when oxidized.

The PProDOS-Np_2 film changed its color reversibly many times. Its stability, robustness, neutral state pure blue color and transparency in the oxidized state make it a promising candidate for electrochromic displays and devices.

The coloration efficiency (CE) is an important parameter for optical and display applications. The CE measures the power efficiency of the electrochromic materials and can be calculated by the following equation:

$$CE = \Delta OD/Q_d \text{ and } \Delta OD = \log(T_{colored}/T_{bleached}) \qquad \text{Equation 3.1}$$

Where ΔOD is the optical density, Q_d is the injected/ejected charge during a redox step; $T_{colored}$ and $T_{bleached}$ are the percent transmittance in the neutral and oxidized states, respectively. The CE of PProDOS-Np_2 was calculated as 755 cm^2/C, which is one of the highest reported CE for polyselenophene derivatives.

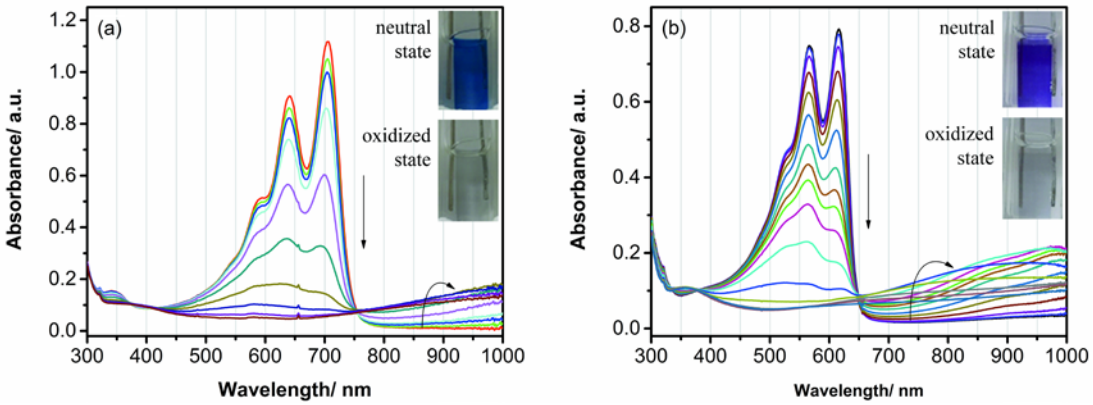

Figure 3.9 Optical absorption spectra of (a) PProDOS-Np_2 film and (b) PProDOT-Np_2 film on ITO in 0.1 M TBAH/CH_2Cl_2 at various applied potentials. Insets: Colors of the polymers at their neutral and oxidized states.

CHAPTER 4

CONCLUSION

A new derivative of 3,4-propylenedioxyselenophene (ProDOS) bearing naphtyl appeandages on the center of the propylenedioxy bridge was sysnthesized and polymerized electrochemically. The corresponding polymer film exhibited one of the highest optical contrast ratios among the polythiophene and polyselenophene derivatives. Electrochemically obtained insoluble polymer film is pure blue at the neutral state and highly transmissive in the oxidized state. Unlike the polythiophene analogue, the results of optical experiments indicated that an increase in the size of the substituent on the bridge gave rise to an increase in the optical contrast of the related ProDOS based polymers. For example, while the parent PProDOS film has 51% optical contrast, dibenzyl substituted PProDOS-Bz_2 has 65% and dinaphtyl substituted PProDOS-Np_2 has 84% optical contrast. Also, PProDOS-Np_2 film is highly stable and robust under ambient conditions. The polymer film preserved 84% of its electroactivity when switched for 5000 cycles between its neutral and oxidized states under ambient conditions. In addition, the film reversibly repeated its electrochemical and optical properties even after thousands cycles.

When compared to polythiophene analogue, the obtained polyselenophene based polymer PProDOS-Np_2 has lower oxidation potential, lower band gap, higher optical contrast, coloration efficiency and stability.

REFERENCES

[1] Dai, L. 2004. Intelligent Macromolecules for Smart Devices, Springer-Verlag: Berlin.

[2] Kumar, D., Sharma, R.C. 1998. Advances in Conductive Polymers. Eur. Polym. J., 34, 8, 1053-1060.

[3] Street, B.G., Clarke, T.C., Krounbi, M., Kanazawa, K., Lee, V., Pfluger, P., Scott, J.C., Weiser, G. 1982. Preparation and Characterization of Neutral and Oxidized Polypyrrole Films. Mol. Cryst. Liq. Cyrst., 83, 1, 253-264.

[4] Shimidzu, T., Ohtani, A., Iyoda, T., Honda, K. 1986. Effective Adsorption Desorption of Cations on a Polypyrrole Polymer Anion Composite Electrode. J. Chem. Soc., Chem. Commun., 18, 1415-1417.

[5] Chiang, C K., Fincher, C.R., Park, Y.W., Heeger, A.J., Shirakawa, H., Louis, E.J., Gau, S.C., MacDiarmid, A.G. 1977. Electrical Conductivity in Doped Polyacetylene. Phys. Rev. Lett., 39, 17, 1098-1101.

[6] Rieger, P.H. 1994. Electrochemistry, 2nd ed., Chapman&Hall Inc., USA.

[7] Mann, C.K. 1969. Elektroanalytical Chemistry, (ed. A.J. Bard), Marcel Dekker, New York, 3, 57-134.

[8] Baizer, M.M., Lund, H. 1983. Organic Electrochemistry, Marcel Dekker, New York.

[9] Noel, M., Vasu, K.I. 1990. Cyclic Voltammetry and the Frontiers of Electrochemistry. Oxford & IBH Publishing Co. Pvt. Ltd., New Delhi.

[10] Algı, F., Cihaner, A. 2009. An ambipolar neutral state green polymeric electrochromic. Org. Electron., 10, 4, 704-710.

[11] www.linocolor.com

[12] Dyer, A.L., Thompson, E.J., Reynolds, J.R. 2011. Completing the Color Palette With Spray-Processable Polymer Electrochromics. Appl. Mater. Interfaces, 3, 6, 1787-1795.

[13] Beaujige, P.M., Reynolds, J.R. 2010. Color Control in pi-Conjugated Organic Polymers for Use in Electrochromic Devices. Chem. Rev., 110, 1, 268-320.

[14] http://www.nobelprize.org/nobel_prizes/chemistry/laureates/2000.html

[15] Sariciftci, N.S., Smilowitz, L., Heeger, A.J., Wudl, F. 1992. Photoinduced Electron Transfer From A Conducting Polymer To Buckminsterfullerene. Science, 258, 5087, 1474-1476.

[16] Hoppe, H., Sariciftci, N.S. 2004. Organic Solar Cells: An Overview. J. Mater. Res., 19, 7, 1924-1945.

[17] Ho, P.K.H., Kim, J.S., Burroughes, J.H. , Becker, H., Li, S.F.Y., Brown, T.M., Cacialli, F., Friend, R.H. 2000. Molecular-Scale Interface Engineering for Polymer Light-Emitting Diodes. Nature, 404, 6777, 481-484.

[18] Perepichka, I.F., Perepichka, D.F., Meng, H., Wudl, F. 2005. Light-Emitting Polythiophenes. Adv. Mater., 17, 19, 2281-2305.

[19] Katz, H.E. 2004. Recent Advances in Semiconductor Performance and Printing Processes for Organic Transistor-Based Electronics. Chem. Mater., 16, 23, 4748-4756.

[20] Schwendeman, I., Hickman, R., Sonmez, G., Schottland, P., Zong, K., Welsh, D., Reynolds, J.R. 2002. Enhanced Contrast Dual Polymer Electrochromic Devices. Chem. Mater., 14, 7, 3118-3122.

[21] Meng, H., Tucker, D., Chaffins, S., Chen, Y., Helgeson, R., Dunn, B., Wudl, F. 2003. An Unusual Electrochromic Device Based on A New Low-Bandgap Conjugated Polymer. Adv. Mater., 15, 2, 146-149.

[22] Pennisi, A., Simone, F., Barletta, G., Di Marco, G., Lanza, L. 1999. Preliminary Test of a Large Electrochromic Window. Electrochim. Acta, 44, 18, 3237-3243.

[23] Rauh, R. 1999. Electrochromic Windows: An Overview. Elemctrochim. Acta, 44, 18, 3165-3176.

[24] Hermans, E.C.M. 1984. CO, CO_2, CH_4 and H_2O Sensing by Polymer Covered Interdigitated Electrode Structures. Sensors and Actuators, 5, 3, 181-186.

[25] Shoa, T.N., Shoa, T., Madden, J.D.W., Mirfakhrai, T., Alici, G., Spinks, G.M., Wallace, G.G. 2010. Electromechanical Coupling in Polypyrrole. Sensors and Actuators, 161, 1-2, 127-133.

[26] Skotheim, T.A., Reynolds, J.R. 2007. Conjugated Polymers: Theory, Synthesis, Properties and Characterization. Handbook of Conducting Polymers, CRC Press, Boca Raton.

[27] Kaneto, K., Yoshino, K., Inuishi, Y. 1983. Electrical and Optical Properties of Polythiophene Prepared By Electrochemical Polymerization. Solid State Commun., 46, 5, 389-391.

[28] Jen, K.Y., Miller, G.G., Elsenbaumer, R.L. 1986. Highly Conducting, Soluble, and Environmentally-Stable Poly(3-alkylthiophenes). J. Chem. Soc., Chem. Commun., 17, 1346-1347.

[29] Rughooputh, S.D.D.V., Nowak, M., Hotta, S., Heeger, A.J., Wudl, F. 1987. Soluble Conducting Polymers: The Poly(3-Alkylthienylenes). Synth. Met., 21, 41-50.

[30] Chen, S.A., Tsai, C.C. 1993. Structure Properties of Conjugated Conductive Polymers. 2-3-Ether-Substituted Polythiophenes and Poly(4-methylthiophene)s. Macromolecules, 26, 2234-2239.

[31] Chayer, M., Faid, K., Leclerc. M. 1997. Highly Conducting Water-Soluble Polythiophene Derivatives. Chem. Mater., 9, 12, 2902-2905.

[32] Heywang, G., Jonas, F. 1994. Electrochemical and Spectroscopic Characterization of Polyalkylenedioxythiophenes. J. Electroanal. Chem., 369, 1-2, 87-92.

[33] Hokazono, M., Anno, H., Toshima N. 2014. Thermoelectric Properties and Thermal Stability of PEDOT:PSS Films on A Polyimide Substrate and Application in Flexible Energy Conversion Devices. J. Electron. Mater., 43, 6, 2196-2201.

[34] Groenendaal, L.B., Jonas, F., Freitag, D., Pielartzik, H., Reynolds, J.R. 2000. Poly(3,4-ethylenedioxythiophene) and Its Derivatives: Past, Present, and Future. Adv. Mater., 12, 7, 481-494.

[35] Ong, T.T, Ng, S.C., Chan, H.S.O. 2003. Synthesis, Characterization and Electrochemical Properties of Polybiselenophene. Polymer, 44, 19, 5597-5603.

[36] Sugimoto, R., Yoshino, K., Inoue, S., Tsukagoshi, K. 1985. Preparation and Properties of Polytellurophene and Polyselenophene. Jpn. J. Appl. Phys., 24, 6, L425-L427.

[37] Bezoari, M.D, Kovacic, P., Gronowitz, S., Hörnfedt, A.B. 1981. Polymerization of Aromatic Nuclei. XXVIII. Synthesis and Properties of Poly(2,5-selenienylene). J. Polym. Sci., Polym. Lett. Ed. 19, 347-353.

[38] Montheard, J.P, Pascal, T., Seytre, G., Steffan-Boiteux, G., Douillard, A. 1984. New Semiconducting Polymers From Aromatic and Heterocyclic Nuclei and Their Doping With Iodine. Synth. Met., 9, 389-396.

[39] Pu, S., Hou, J., Xu, J., Nie, G., Zhang, S., Shen, L., Xiao, Q. 2005. Electrosyntheses of Freestanding and Conducting Polyselenophene Films. Mater. Lett., 59, 1061-1065.

[40] Dong, B., Xing, Y., Xu, J., Zheng, L., Hou, J., Zhao, F. 2008. Electrosyntheses of Free-Standing and Highly Conducting Polyselenophene Films in An Ionic Liquid. Electrochim. Acta, 53, 5745-5751.

[41] Wijsboom, Y.H., Patra, A., Zade, S.S., Sheynin, Y., Li, M., Shimon, L.J.W., Bendikov, M. 2009. Controlling Rigidity and Planarity in Conjugated Polymers: Poly(3,4-ethylenedithioselenophene). Angew. Chem. Int. Ed., 48, 30, 5443-5447.

[42] Patra, A., Wijsboom, Y.H., Leitus, G., Bendikov, M. 2011. Tuning the Band Gap of Low-Band-Gap Polyselenophenes and Polythiophenes: The Effect of the Heteroatom . Chem. Mater., 23, 3, 896-906.

[43] Weijsboom, Y.H., Sheynin, Y., Patra, A., Zamoshchik, N., Vardimon, R., Leitus, G., Bendikov, M. 2011. Tuning of Electronic Properties and Rigidity in PEDOT Analogs. J. Mater. Chem., 21, 5, 1368-1372.

[44] Dian, G., Barbey, G., Decroix, B. 1986. Electrochemical Synthesis of Polythiophenes and Polyselenophenes. Synth. Met., 13, 4, 281-289.

[45] Dian, G., Merlet, N., Barbey, G. 1987. Electrochemical Polymerization of β-substituted and β,β'-disubstituted Selenophenes. J. Electroanal. Chem., 238, 1-2, 225-237.

[46] Merlet, N., Dian, G., Barbey, G., Outurquin, F., Paulmier, C. 1988. Electrochemical Study of Poly(3-methylselenophene). Synth. Met., 24, 1-2, 77-80.

[47] Yoshino, K., Onoda, M., Manda, Y., Sawada, K., Sugimoto, R.I., Inoue, S. 1989. Fusible Poly(3-alkylselenophene) and Its Properties. Jpn. J. Appl. Phys., 28, L138.

[48] Tourillon, G., Dartyge, E., Guay, D., Mahatsekake, C.,. Andrieu, C.G., Bernstorff, S., Braun, W. 1990. Electronic Properties and Orientation Studies of Poly-3-alkylselenophene Electrochemically Deposited on Pt as Observed by NEXAFS. J. Electrochem. Soc., 137, 6, 1827-1832.

[49] Bourahla. A., Saiter, J.M., Vautier, C. 2001. Electrical Conductivity of Polymethyl-3-Selenophene. Mater. Chem. Phys, 69, 1, 163-165.

[50] Heeney, M., Zhang, W., Crouch, D.J., Chabinyc, M.L., Gordeyev, S., Hamilton, R., Higgins, S.J., McCulloch, I., Skabara, P.J., Sparrowe, D., Tierney, S. 2007. Regioregular poly(3-hexyl)selenophene: A Low Band Gap Organic Hole Transporting Polymer. Chem. Commun., 21, 47, 5061-5063.

[51] Patra, A., Wijsboom, Y.H., Leitus, G., Bendikov, M. 2009. Synthesis, Structure, and Electropolymerization of 3,4-dimethoxytellurophene: Comparison with Selenium Analogue. Org. Lett., 11, 7, 1487-1490.

[52] Das, S., Zade, S.S. 2010. Poly(cyclopenta[c]selenophene): A New Polyselenophene. Chem. Commun., 46, 7, 1168-1170.

[53] Aqad, E., Lakshmikantham, M.V., Cava, M.P. 2001. Synthesis of 3,4-ethylenedioxyselenophene (EDOS): A Novel Building Block for Electron-Rich pi-Conjugated Polymers. Org. Lett., 3, 26, 4283-4285.

[54] Hinsberg, O. 1910. Synthetische Versuche mit Thiodiglykolsäureester. Ber. Dtsch. Chem. Ges., 43, 1, 901-906.

[55] Zade, S.S., Bendikov, M. 2006. From Oligomers to Polymer: Convergence in the HOMO-LUMO Gaps of Conjugated Oligomers. Org. Lett., 8, 23, 5243-5246.

[56] Leclerc, M., Faid,K. 1997. Electrical and Optical Properties of Processable Polythiophene Derivatives: Structure-Property Relationships. Adv. Mater., 9, 14, 1087-1094.

[57] Das, S., Dutta, P.K., Panda, S., Zade, S.S. 2010. 3,4-ethylenedioxythiophene and 3,4-ethylenedioxyselenophene: Synthesis and Reactivity of C(alpha)-Si Bond. J. Org. Chem., 75, 14, 4868-4871.

[58] Patra, A., Wijsboom, Y.H., Zade, S.S., Li, M., Sheynin, Y., Leitus, G., Bendikov, M. 2008. Poly(3,4-ethylenedioxyselenophene). J. Am. Chem. Soc., 130, 21, 6734-6736.

[59] Salzner, U., Lagowski, J.B., Pickup, P.G., Poirier, R.A. 1998. Comparison of Electronic Structures of Polycylopentadiene, Polypyrrole, Polyfuran, Polysilole, Polyphosphole, Polythiophene, Polyselenophene, and Polytellurophene. Synth. Met., 96, 177-189.

[60] Zade, S.S., Zamoshchik, Bendikov, M. 2009. Oligo- and Polyselenophenes: A Theoretical Study. Chem. Eur. J., 15, 34, 8613-8624.

[61] Gaupp, C.L., Welsh, R.D., Rauh, R.D., Reynolds, J.R. 2002. Composite Coloration Efficiency Measurements of Electrochromic Polymers Based on 3,4-Alkylenedioxythiophene. Chem. Mater., 14, 9, 3964-3970.

[62] Li, M., Patra, A., Sheynin, Y., Bendikov, M. 2009. Hexyl-Derivatized Poly(3,4-ethylenedioxyselenophene): Novel Highly Stable Organic Electrochromic Material with High Contrast Ratio, High Coloration Efficiency, and Low-Switching Voltage. Adv. Mater., 21, 17, 1707-1711.

[63] Li, M., Sheynin, Y., Patra, A., Bendikov, M. 2009. Tuning the Electrochromic Properties of Poly(alkyl-3,4-ethylenedioxyselenophenes) Having High Contrast Ratio and Coloration Efficiency. Chem. Mater., 21, 12, 2482-2488.

[64] Krishnamoorthy, K., Ambade, A.V., Kanungo, M., Contractor, A.Q, Kumar, A. J. 2001. Rational Design of Electrochromic Polymer With High Contrast In the Visible Region: Dibenzyl Substituted Poly(3,4-Propylenedioxythiophene). J. Mater. Chem., 11, 12, 2909-912.

[65] Kim, B., Shin, H., Park, T., Lim, H., Kim, E. 2013. NIR-Sensitive Poly(3,4-ethylenedioxyselenophene) Derivatives for Transparent Photo-Thermo-Electric Converters. Adv. Mater., 25, 38, 5483-5489.

[66] Poverenov, E., Sheynin, Y., Zamoshchik, N., Patra, A., Leitus, G., Perepichka, I.F., Bendikov, M. 2012. Flat Conjugated Polymers Combining a Relatively Low HOMO Energy Level and Band Gap: Polyselenophenes Versus Polythiophenes. J. Mater. Chem., 22, 29, 14645-4655.

[67] Poverenov, E., Zamoshchik, N., Patra, A., Ridelman, Y., Bendikov, M. 2014. Unusual Doping of Donor-Acceptor-Type Conjugated Polymers Using Lewis Acids. J. Am. Chem. Soc., 136, 13, 5138-5149.

[68] Patra, A., Bendikov, M., Chand, S. 2014. Poly(3,4-ethylenedioxyselenophene) and Its Derivatives: Novel Organic Electronic Materials. Acc. Chem. Res., 47, 5, 1465-1474.

[69] Groenendaal, L., Zotti, G., Aubert, P.H., Waybrigth, S.M., Reynolds, J.R. 2003. Electrochemistry of Poly (3, 4-alkylenedioxythiophene) Derivatives. Adv. Mater., 15, 11, 855-879.

[70] Cirpan, A., Argun, A.A., Grenier, C.R.G., Reeves, B.D., Reynolds, J.R. 2003. Electrochromic Devices Based on Soluble and Processable Dioxythiophene Polymers. J. Mater. Chem., 13, 10, 2422-2428.

[71] Reeves, B.D., Grenier, C.R.G, Argun, A.A., Cirpan, A., McCarley, T.D., Reynolds, J.R. 2004. Spray Coatable Electrochromic Dioxythiophene Polymers with High Coloration Efficiencies. Macromolecules, 37, 20, 7559-7569.

[72] Icli-Ozkut, M., Atak, S., Onal, A.M., Cihaner, A. 2011. Blue to Highly Transmissive Soluble Electrochromic Based on Poly(3,4-propylenedioxyselenophene) with High Stability and Coloration Efficiency. J. Mater. Chem., 21, 14, 5268-5272.

[73] Atak, S., Icli-Ozkut, M., Onal, A.M., Cihaner, A. 2011. Soluble Alkyl Substituted Poly(3,4-Propylenedioxyselenophene)s: A New Platform for Optoelectronic Materials. J. Polym. Sci. Part A: Polym. Chem., 49, 20, 4398-4405.

[74] Welsh, D. M., Kumar, A., Meijer, E.W., Reynolds, J.R. 1999. Enhanced Contrast Ratios and Rapid Switching in Electrochromics Based on Poly(3,4-propylenedioxythiophene) Derivatives. Adv. Mater.,11, 16, 1379-1382.

[75] Kim, B., Kim, J., Kim, E. 2011.Visible to Near-IR Electrochromism and Photothermal Effect of Poly(3,4- propylenedioxyselenophene)s. Macromolecules, 44, 22, 8791-8797.

[76] Groenendaal, L.B., Jonas, F., Freitag, D., Pielartzik, H., Reynolds, J.R. 2000. Poly(3,4-ethylenedioxythiophene) and Its Derivatives: Pat, Present and Future. Adv. Mater., 12, 7, 481-494.

[77] Icli-Ozkut, M., Mersini, J., Onal, A.M., Cihaner, A. 2012. Substituent and Heteroatom Effects on the Electrochromic Properties of Similar Systems. J. Polym. Sci. Part A: Polym. Chem., 50, 4, 615-621.

[78] Bu HB, Gotz G, Reinold E, Vogt A, Schmid S, Blanco R, Segura JL, Bauerle P. Chem. Commun. 2008. Click-functionalization of conducting poly(3,4-ethylendioxythiophene) (PEDOT). Chem Comm. 21, 11, 1320-1322.

APPENDIX A

NMR SPECTRA OF MONOMERS

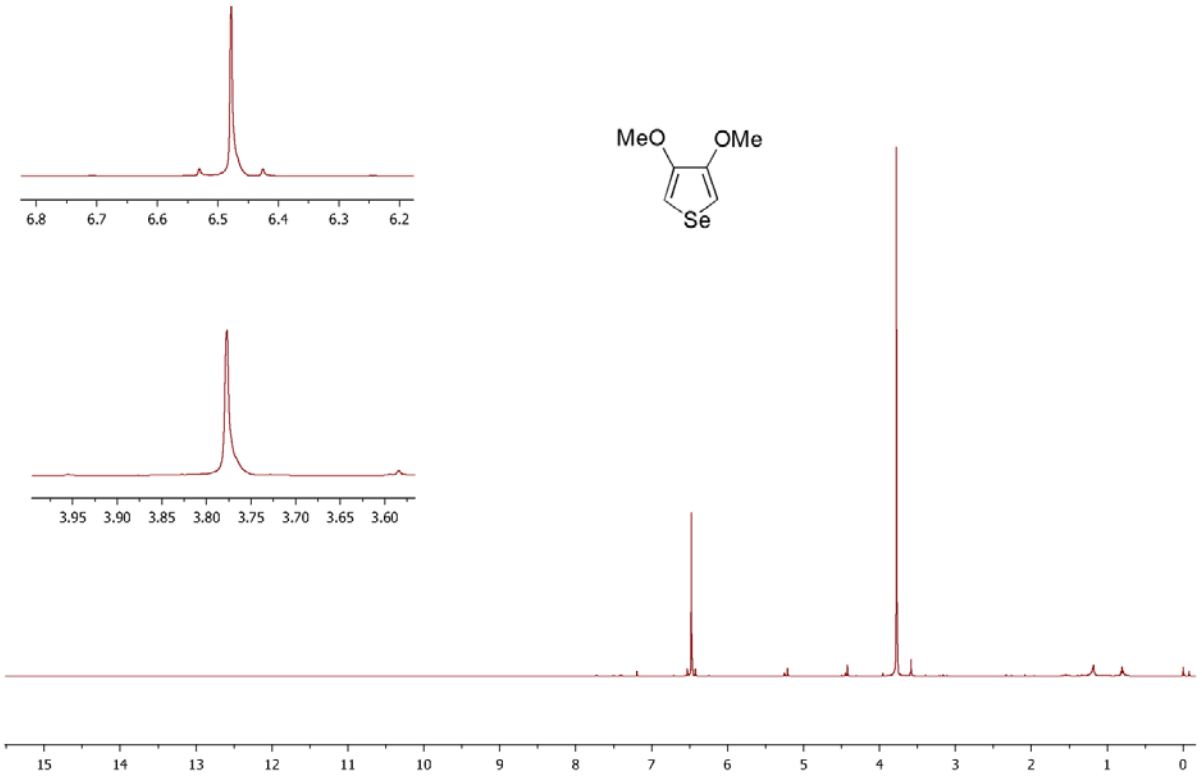

Figure A1 ^{1}H NMR spectrum of DMS in $CDCl_3$

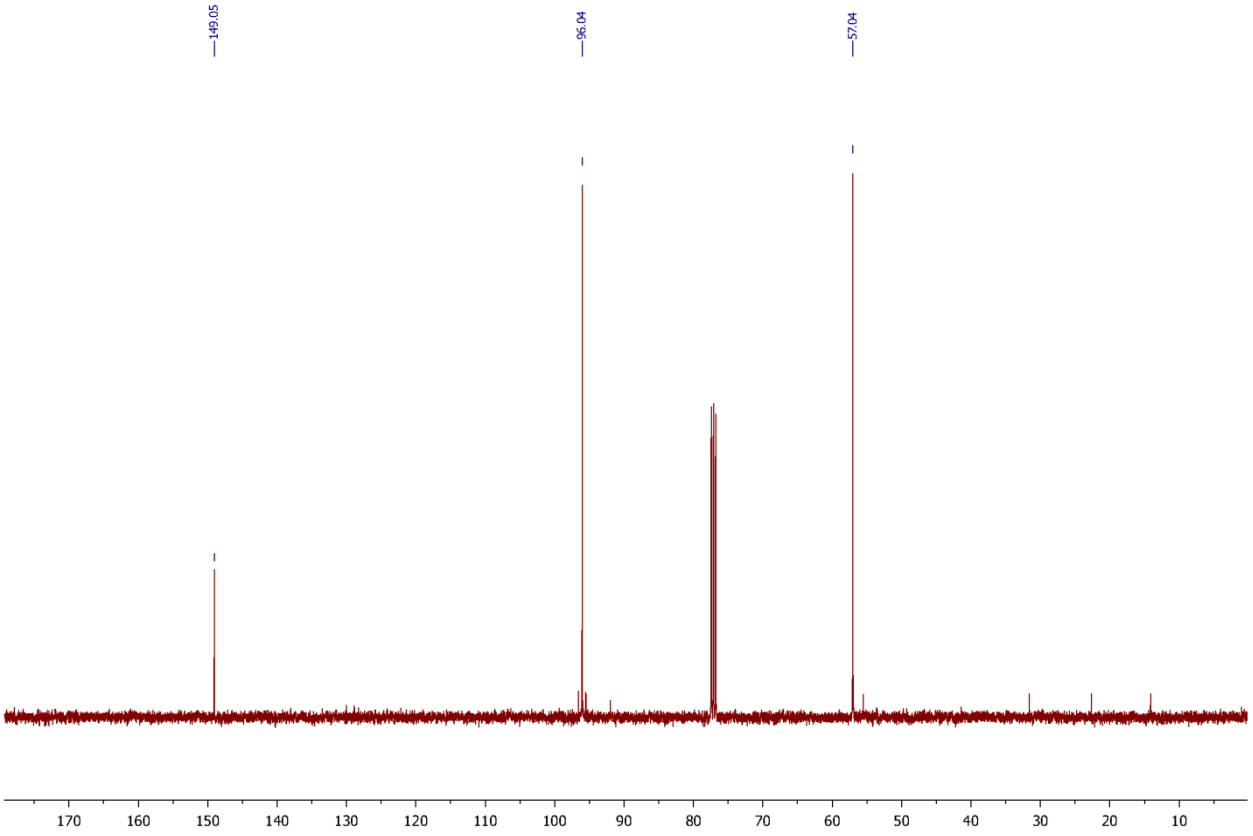

Figure A2 ^{13}C NMR spectrum of DMS in $CDCl_3$

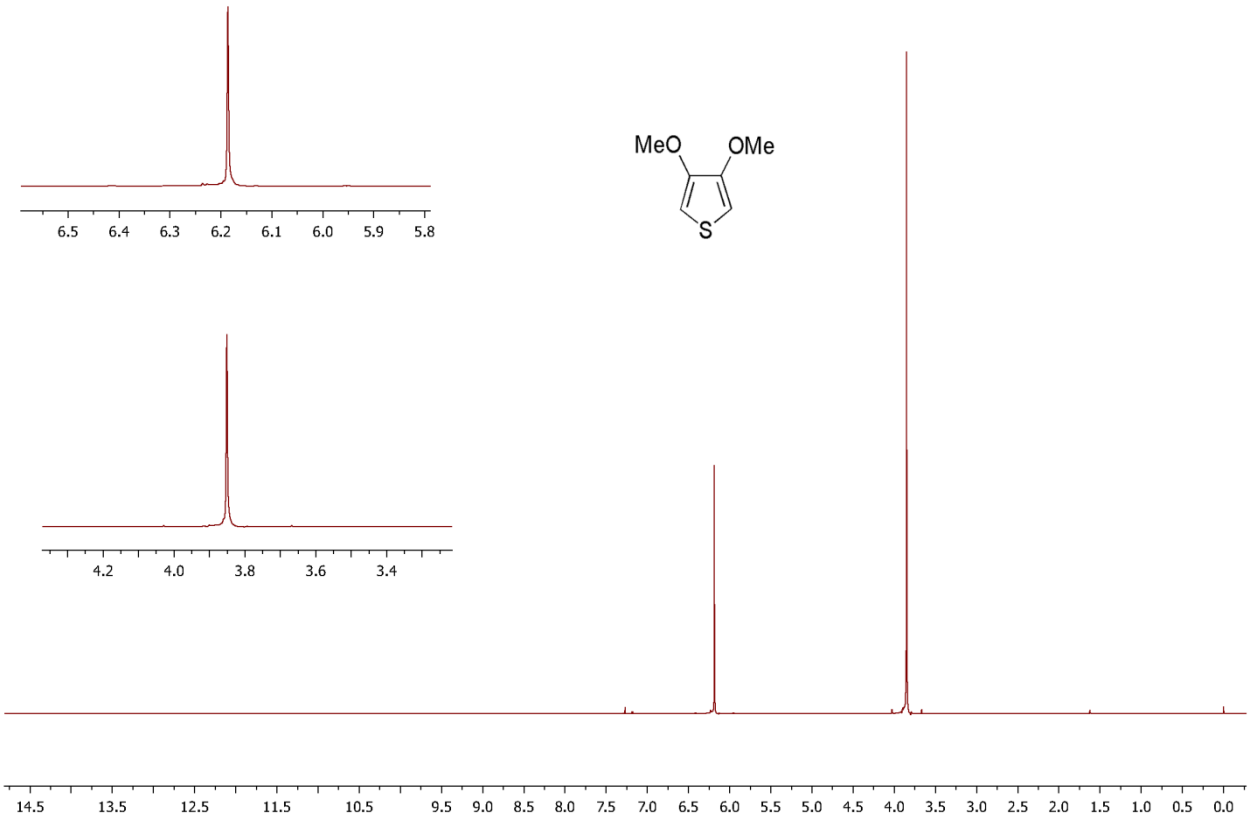

Figure A3 ^{1}H NMR spectrum of DMT in $CDCl_3$

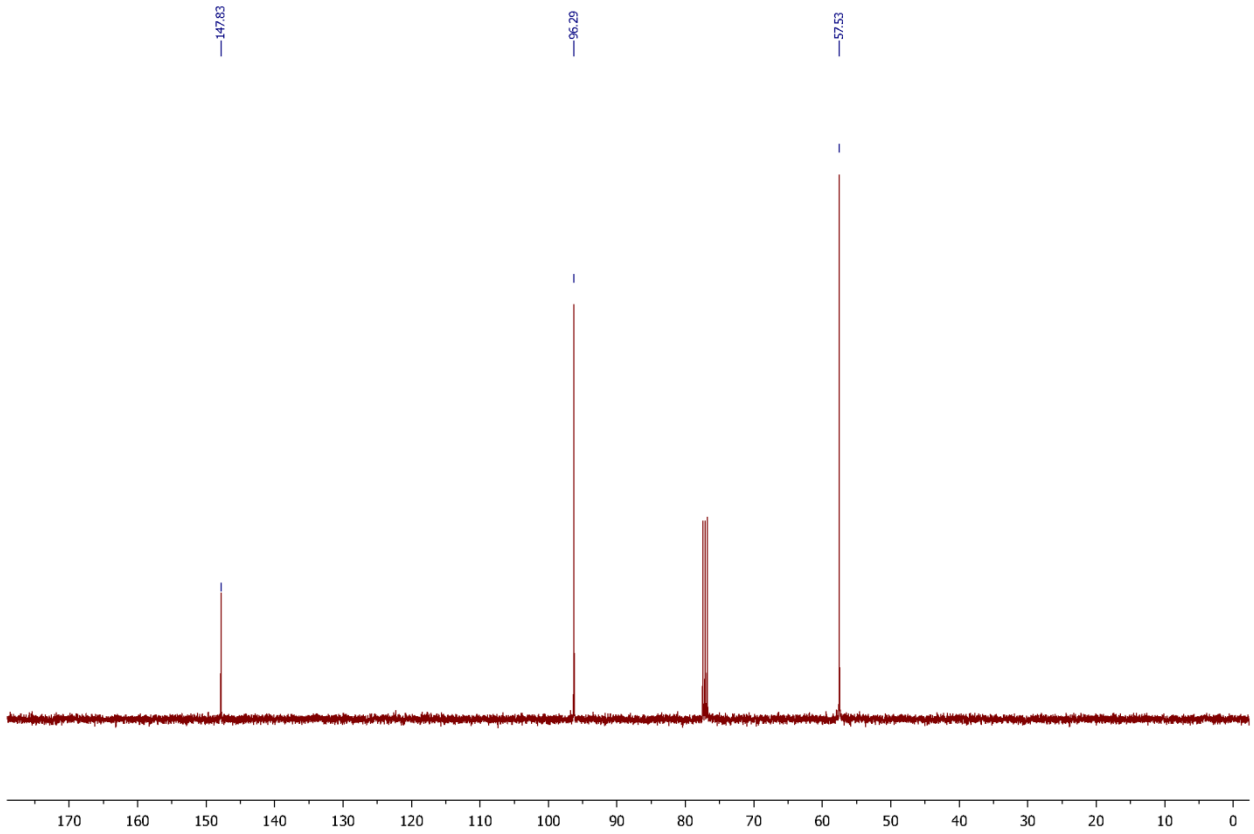

Figure A4 ^{13}C NMR spectrum of DMT in $CDCl_3$

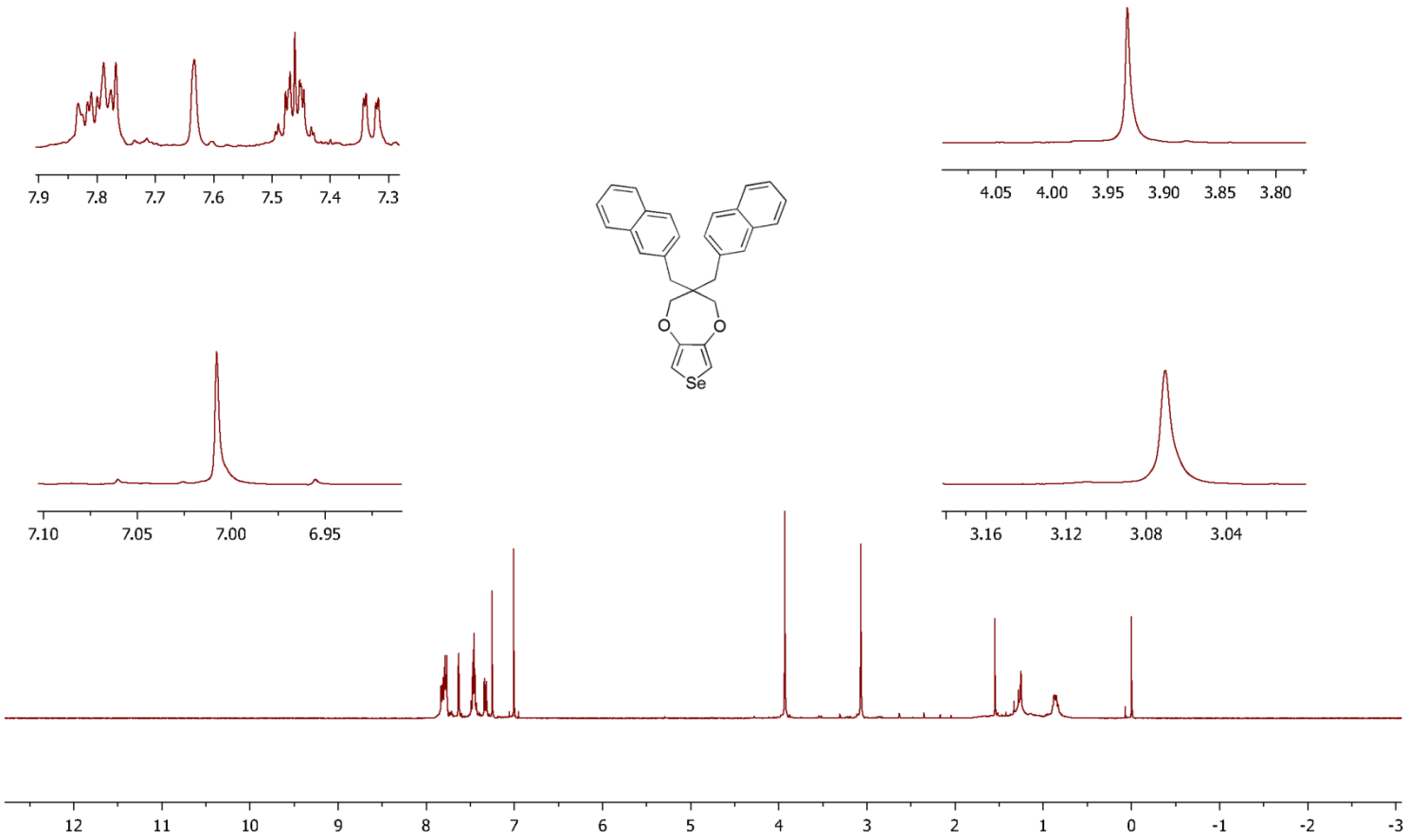

Figure A5 ^{1}H NMR spectrum of ProDOS-Np_2 in $CDCl_3$

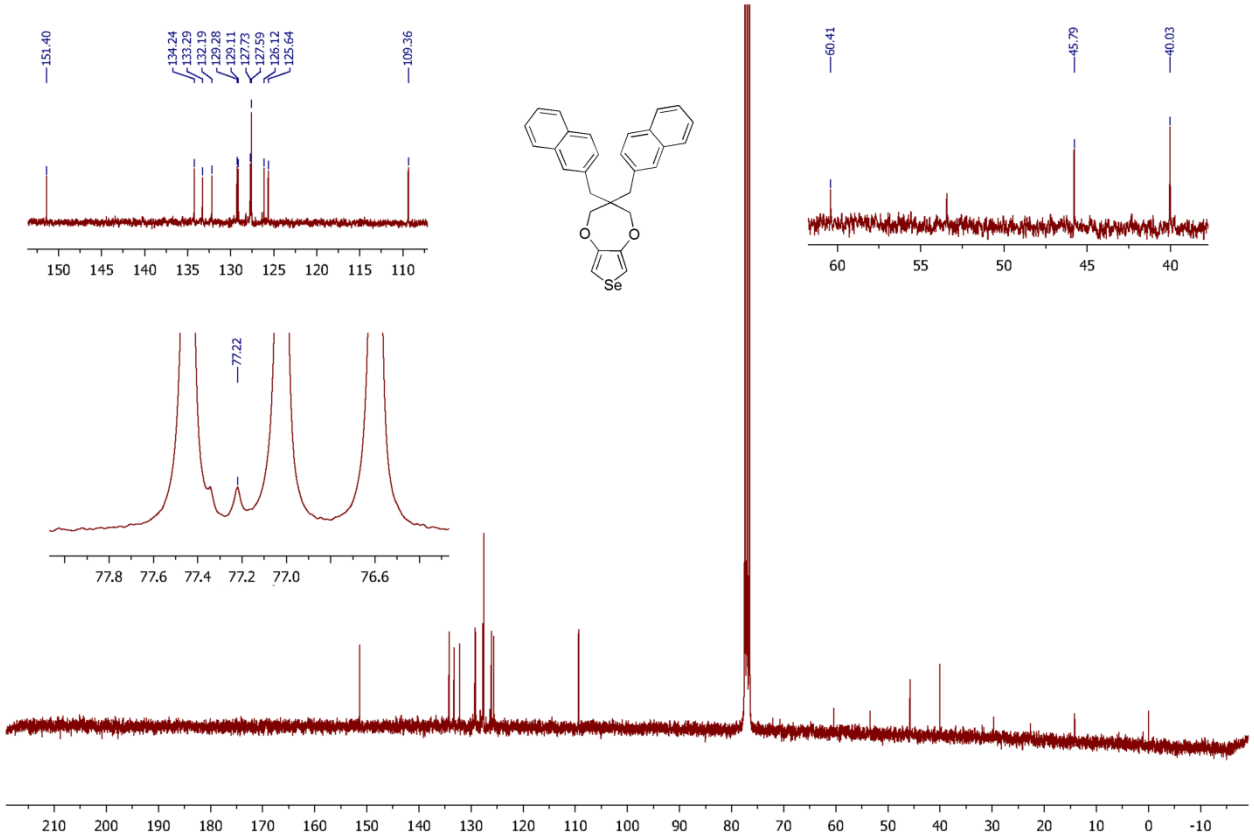

Figure A6 ^{13}C NMR spectrum of ProDOS-Np_2 in $CDCl_3$

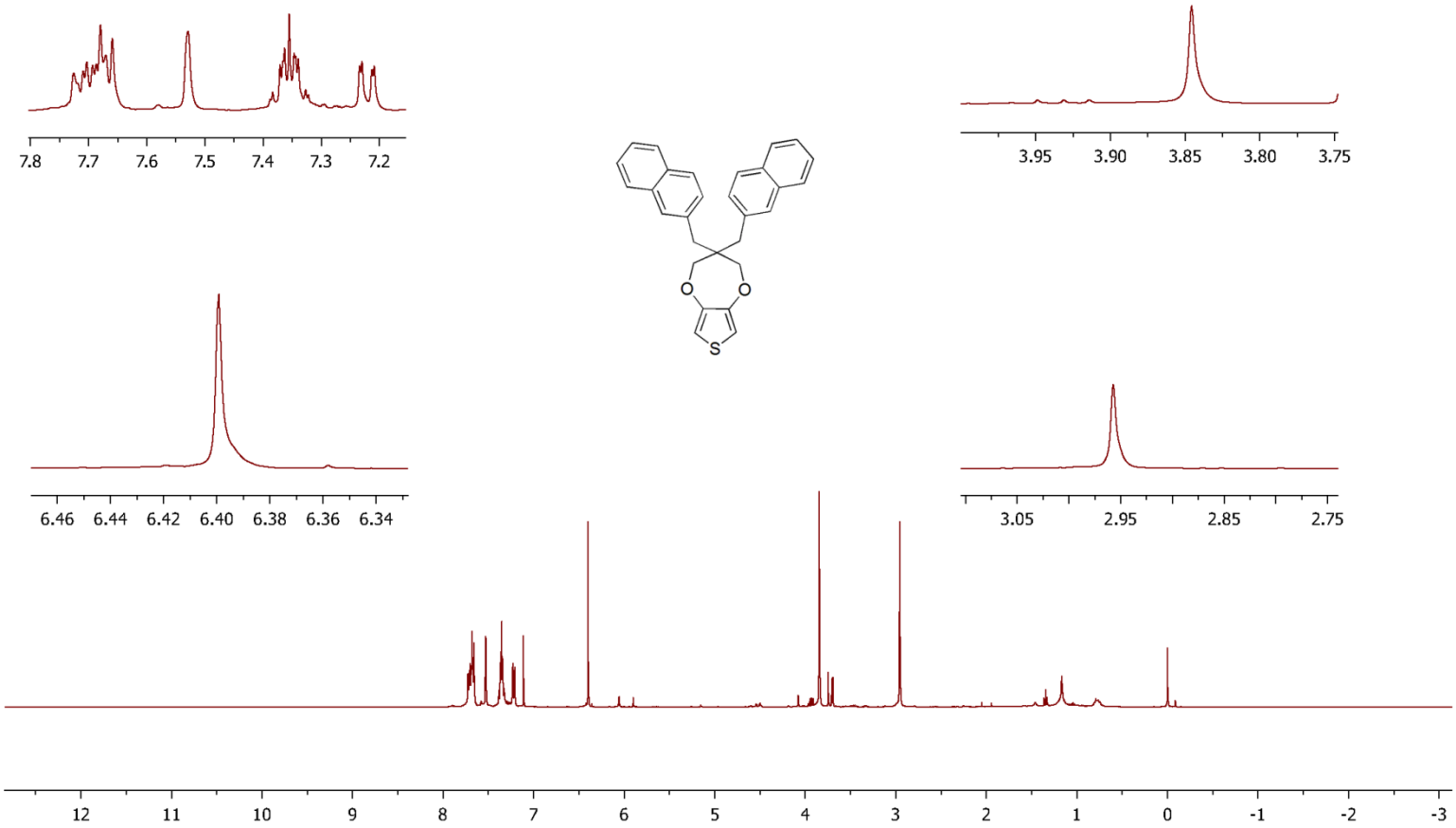

Figure A7 ^{1}H NMR spectrum of ProDOT-Np_2 in $CDCl_3$

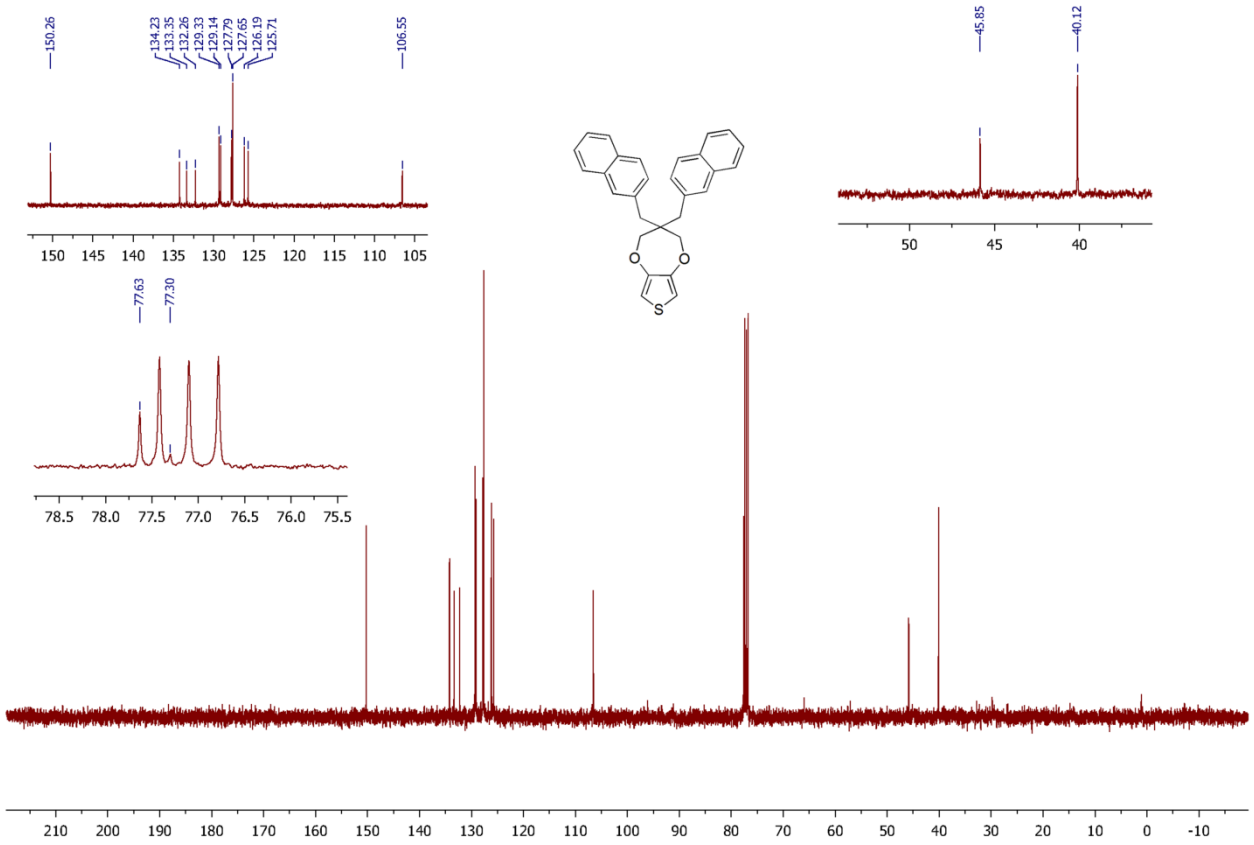

Figure A8 ^{13}C NMR spectrum of ProDOT-Np_2 in $CDCl_3$

APPENDIX B

ELEMENTAL COMPOSITION REPORT OF MONOMERS

Single Mass Analysis
Tolerance = 1000.0 PPM / DBE: min = -1.5, max = 1000.0
Element prediction: Off
Number of isotope peaks used for i-FIT = 3
Monoisotopic Mass, Odd and Even Electron Ions
3 formula(e) evaluated with 1 results within limits (up to 50 closest results for each mass)
Elements Used:
C: 29-29 H: 24-25 O: 2-2 Se: 0-2

Minimum:				-1.5			
Maximum:		5.0	1000.0		1000.0		
Mass	Calc. Mass	mDa	PPM	DBE	i-FIT	i-FIT (Norm)	Formula
485.1010	485.1020	-1.0	-2.1	18.5	294.5	0.0	$C_{29}H_{25}O_2Se$

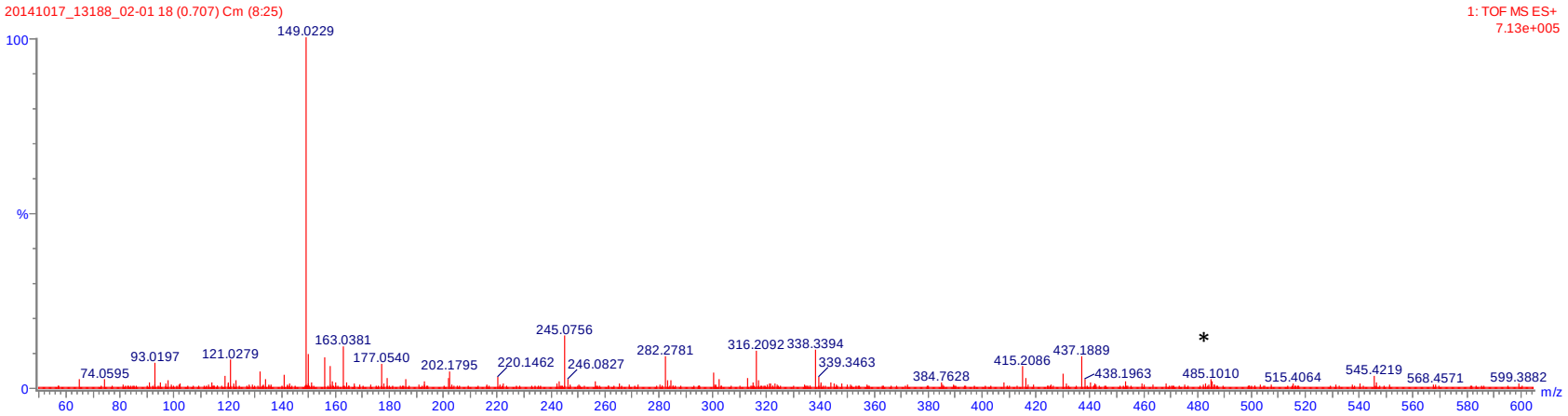

Figure B1 Elemental composition report of ProDOS-Np_2.

Single Mass Analysis
Tolerance = 1000.0 PPM / DBE: min = -1.5, max = 1000.0
Element prediction: Off
Number of isotope peaks used for i-FIT = 3
Monoisotopic Mass, Even Electron Ions
1 formula(e) evaluated with 1 results within limits (up to 50 closest results for each mass)
Elements Used:
C: 29-29 H: 24-25 O: 2-2 S: 1-1

Minimum:				-1.5				
Maximum:		5.0	1000.0		1000.0			
Mass	Calc. Mass	mDa		PPM	DBE	i-FIT	i-FIT (Norm)	Formula
437.1927	437.1575	35.2		80.5	17.5	239.6	0.0	$C_{29}H_{25}O_2S$

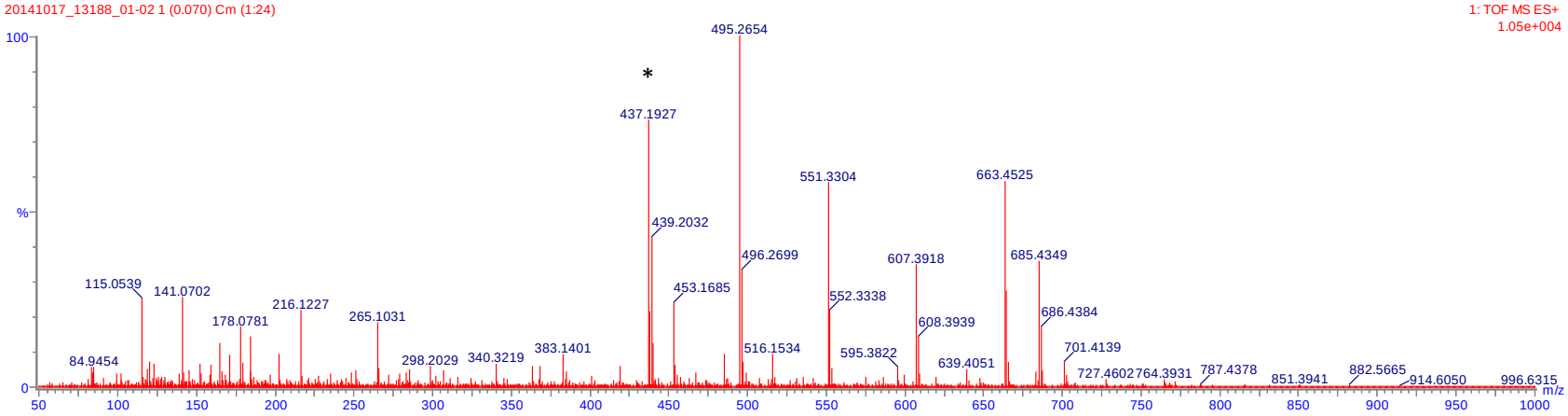

Figure B2 Elemental composition report of ProDOT-Np_2.

APPENDIX C

FTIR SPECTRA OF MONOMERS

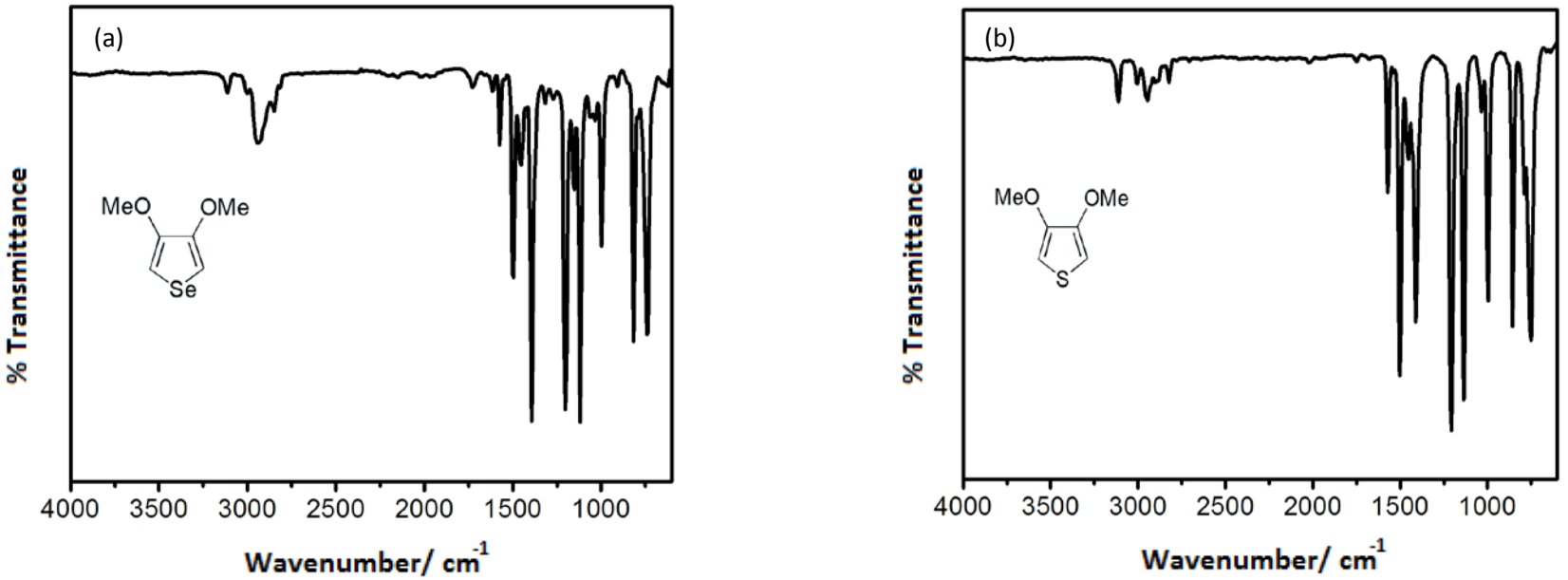

Figure C1 FTIR spectrum of **a)** DMS and **b)** DMT.

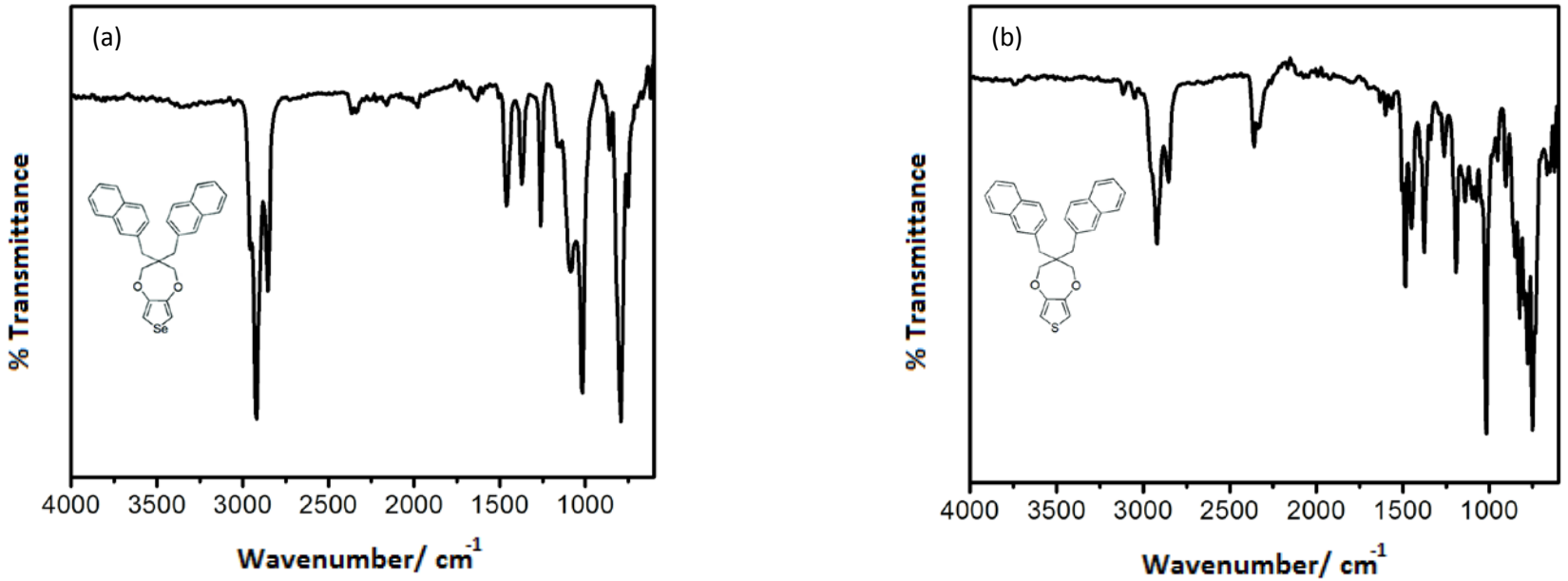

Figure C2 FTIR spectrum of **a)**ProDOS-Np_2 and **b)** ProDOT-Np_2

APPENDIX D
ELECTRICAL AND OPTICAL STUDIES OF MONOMERS AND POLYMERS

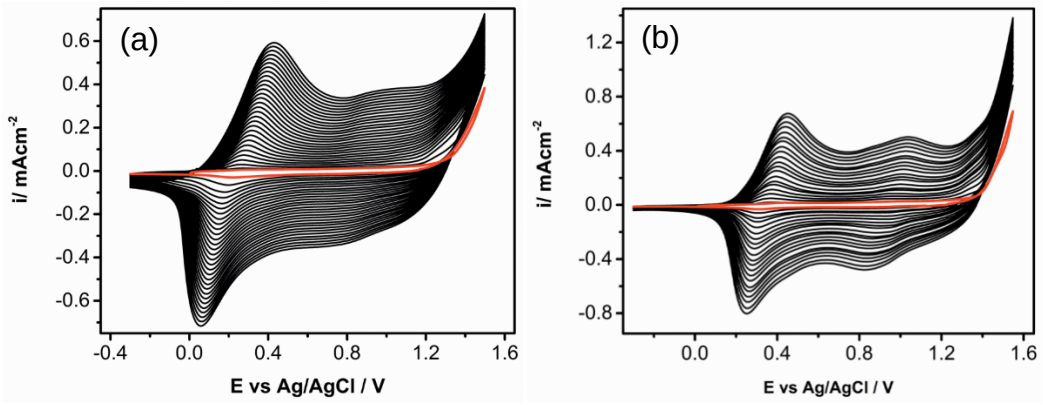

Figure D1 Repetitive cyclic voltammogram of (a) ProDOS-Np_2 and (b) ProDOT-Np_2 in order to get PProDOS-Np_2 and PProDOT-Np_2 films on Pt electrode in an electrolyte solution of 0.1 M TBAH/CH_2Cl_2 at a scan rate of 100 mV/s between -0.3 V and 1.5 V.

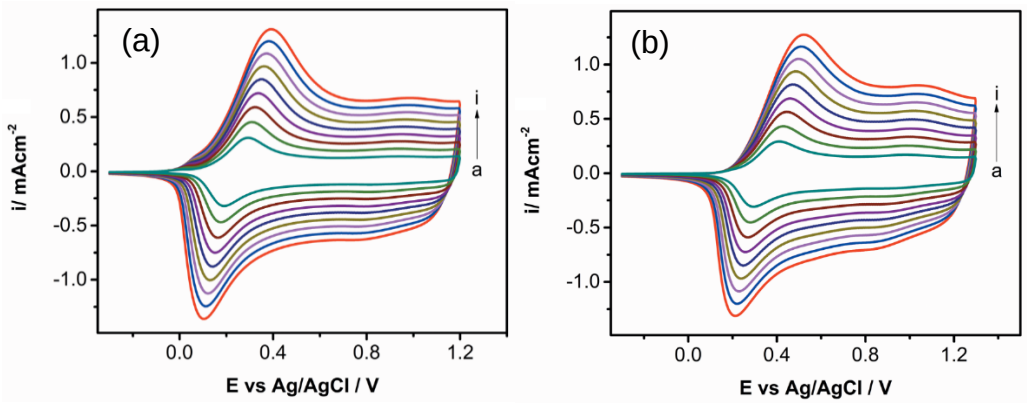

Figure D2 Scan rate dependence of (a) PProDOS-Np_2 and (b) PProDOT-Np_2 films on a Pt disk electrode in 0.1 M TBAH/CH_2Cl_2 at different scan rates between 40 mV/s and 200 mV/s with 20 mV/s increments: (mV/s) (a) 40; (b) 60; (c) 80; (d) 100; (e) 120; (f) 140; (g) 160; (h) 180; and (i) 200.

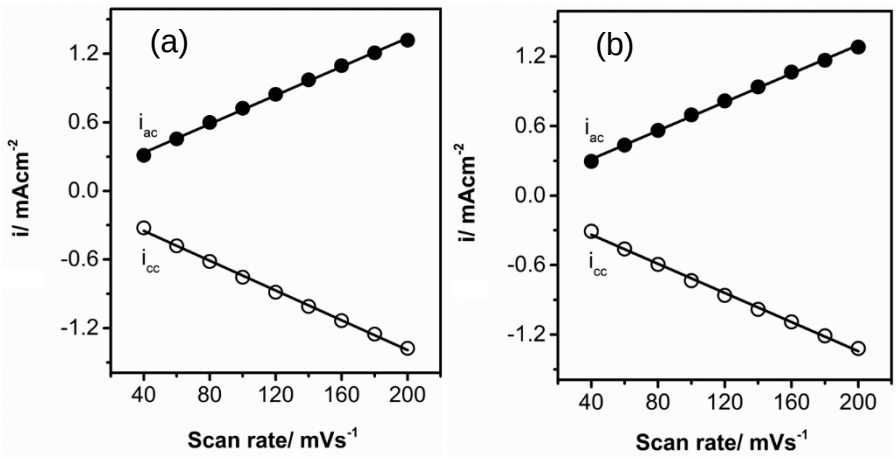

Figure D3 Relationship of anodic (i_{ac}) and cathodic (i_{cc}) current peaks as a function of scan rate for neutralized and oxidized (a) PProDOS-Np_2 and (b) PProDOT-Np_2 films in 0.1 M TBAH/CH_2Cl_2 solution.

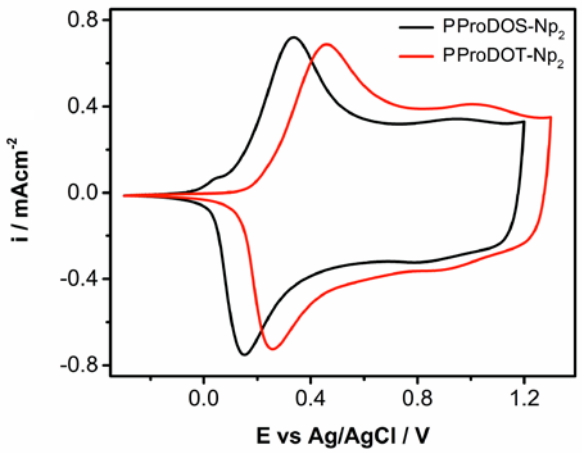

Figure D4 Cyclic voltammograms of PProDOS-Np_2 and PProDOT-Np_2 films on Pt electrode in 0.1 M TBAH/CH_2Cl_2 solution at a scan rate of 100 mV/s.

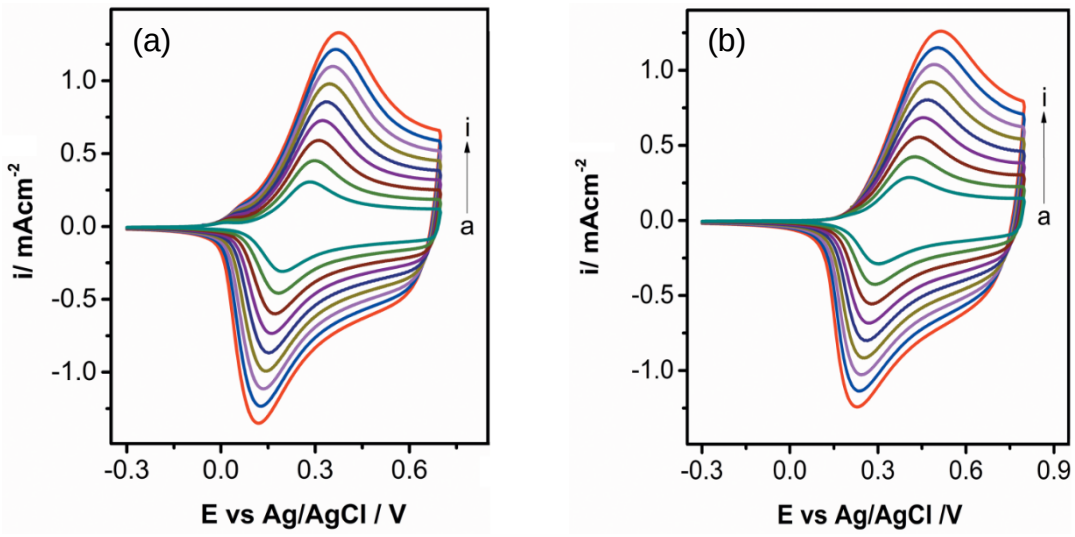

Figure D5 Scan rate dependence of (a) PProDOS-Np_2 and (b) PProDOT-Np_2 films on a Pt disk electrode in 0.1 M TBAH/CH_2Cl_2 at different scan rates between 40 mV/s and 200 mV/s with 20 mV/s increments: (mV/s) (a) 40; (b) 60; (c) 80; (d) 100; (e) 120; (f) 140; (g) 160; (h) 180; and (i) 200.

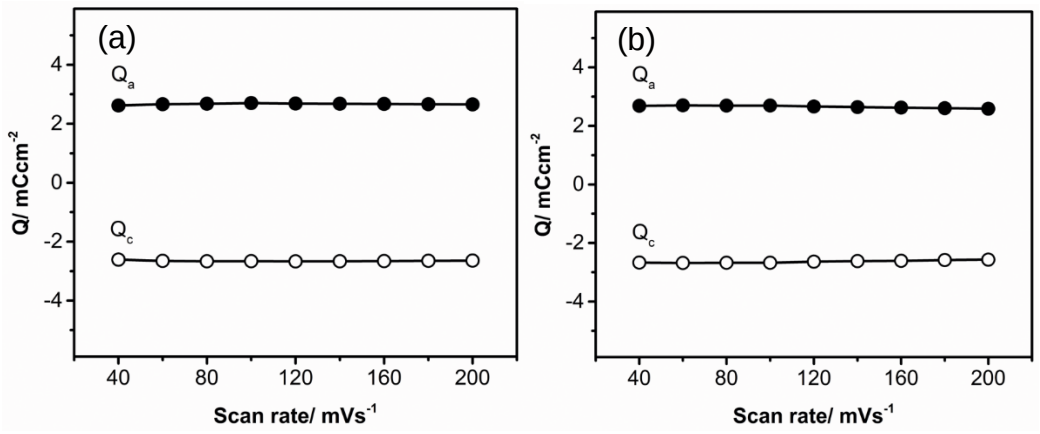

Figure D6 The amount of charge (Q_a) and discharge (Q_c) as a function of scan rate for (a) PProDOS-Np_2 film when switched between -0.3 V and 1.2 V and (b) PProDOT-Np_2 film when switched between -0.3 V and 1.3 V in 0.1 M TBAH/CH_2Cl_2 solution.

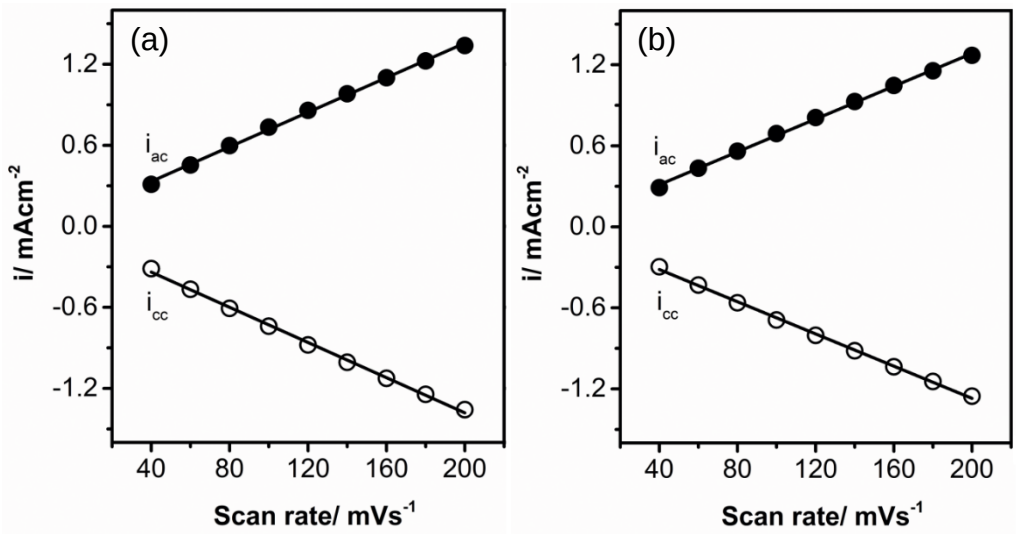

Figure D7 Relationship of anodic (i_{ac}) and cathodic (i_{cc}) current peaks as a function of scan rate for (a) PProDOS-Np_2 and (b) PProDOT-Np_2 films when switched between -0.3 V and 0.7 V in 0.1 M TBAH/CH_2Cl_2 solution.

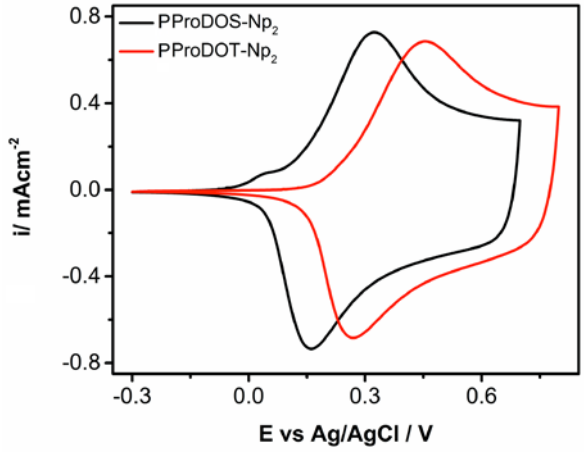

Figure D8 Cyclic voltammograms of PProDOS-Np_2 and PProDOT-Np_2 films on Pt electrode in 0.1 M TBAH/CH_2Cl_2 solution at a scan rate of 100 mV/s.

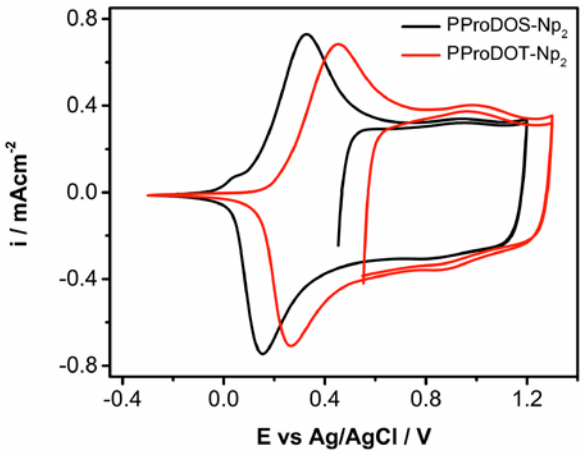

Figure D9 Cyclic voltammogram of PProDOS-Np_2 film on the Pt electrode in 0.1 M TBAH/CH_2Cl_2 solution between -0.3 V and 1.2 V and then between 0.45 V and 1.2 V at a scan rate of 100 mV/s vs. Ag/AgCl (black line), and cyclic voltammogram of PProDOT-Np_2 film on Pt electrode in 0.1 M TBAH/CH_2Cl_2 solution between -0.3 V and 1.3 V and then between 0.55 V and 1.3 V at a scan rate of 100 mV/s (red line).

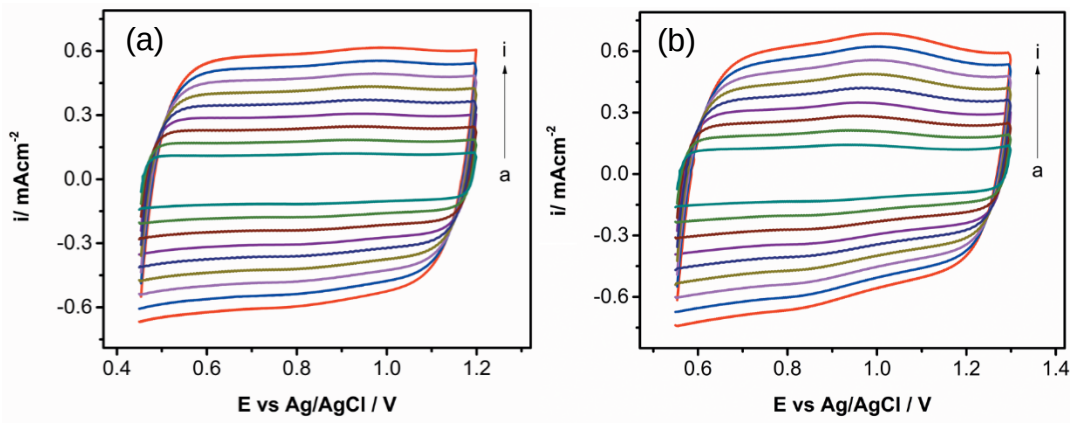

Figure D10 Cyclic capacitance effect of (a) PProDOS-Np_2 and (b) PProDOT-Np_2 films on the Pt disk electrode in 0.1 M TBAH/CH_2Cl_2 at different scan rates between 40 mV/s and 200 mV/s with 20 mV/s increments: (mV/s) (a) 20; (b) 40; (c) 60; (d) 80; (e) 100; (f) 120; (g) 140; (h) 160; (i) 180; and (j) 200.

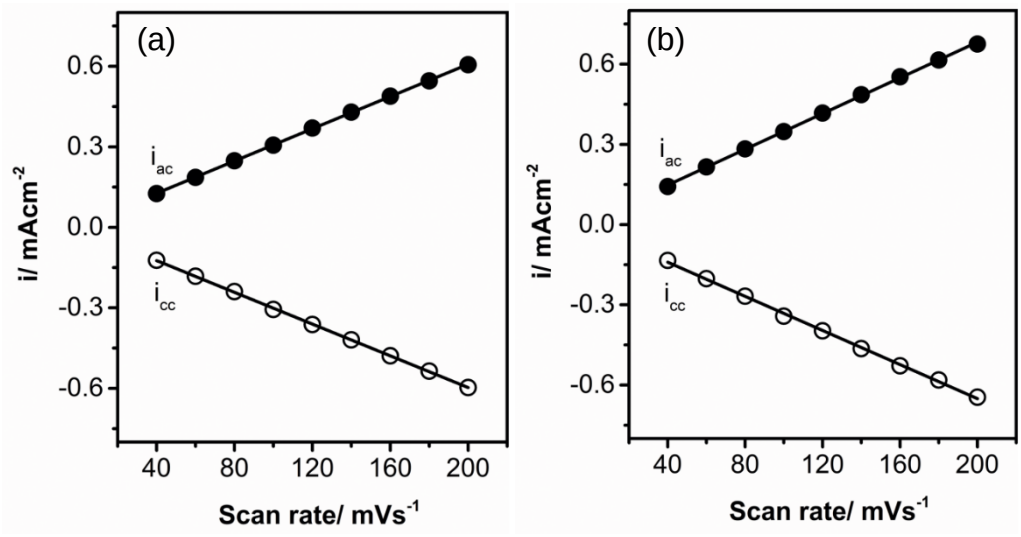

Figure D11 Relationship of anodic (i_{ac}) and cathodic (i_{cc}) current peaks as a function of scan rate for (a) PProDOS-Np_2 film when switched between 0.45 V and 1.2 V and (b) PProDOT-Np_2 film when switched between 0.55 V and 1.3 V in 0.1 M TBAH/CH_2Cl_2 solution.

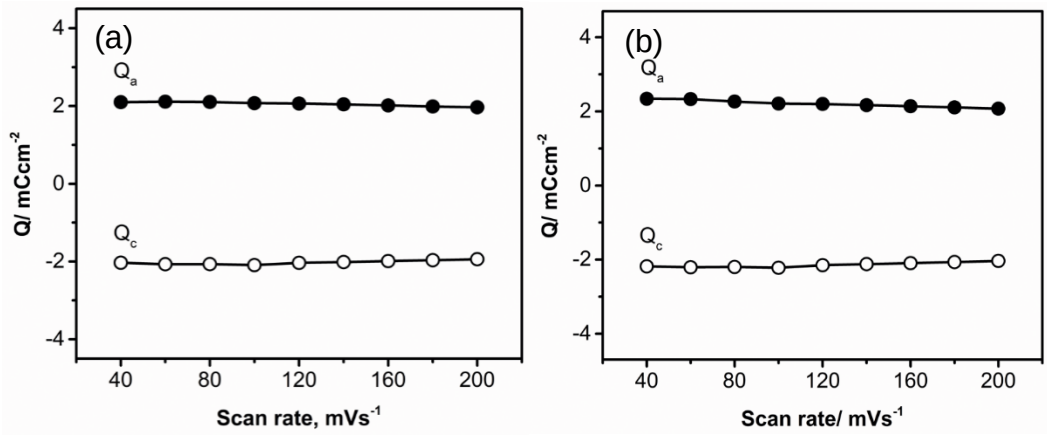

Figure D12 The amount of charge (Q_a) and discharge (Q_c) as a function of scan rate for (a) PProDOS-Np_2 film when switched between 0.45 V and 1.2 V and (b) PProDOT-Np_2 film when switched between 0.55 V and 1.3 V in 0.1 M TBAH/CH_2Cl_2 solution.

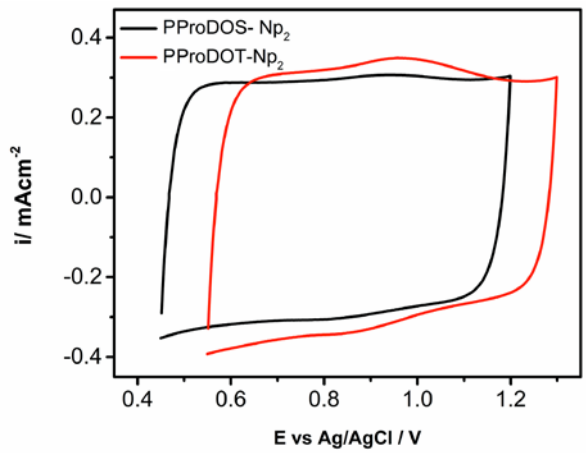

Figure D13 Cyclic voltammograms of PProDOS-Np_2 and PProDOT-Np_2 films on Pt electrode in 0.1 M TBAH/CH_2Cl_2 solution at a scan rate of 100 mV/s.

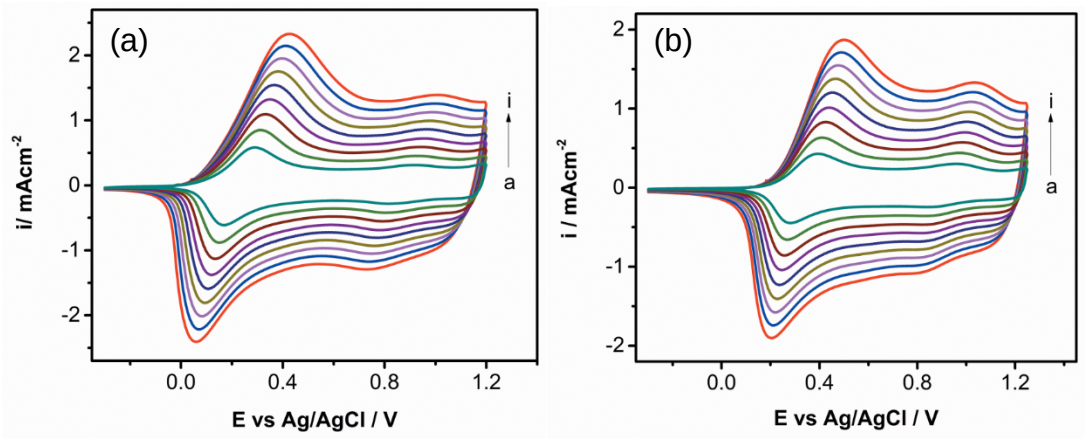

Figure D14 Scan rate dependence of (a) PProDOS-Np_2 (67 mC/cm^2) and (b) PProDOT-Np_2 (67 mC/cm^2) films obtained via contant potential electrolysis on a Pt disk electrode in 0.1 M TBAH/CH_2Cl_2 at different scan rates between 40 mV/s and 200 mV/s with 20 mV/s increments: (mV/s) (a) 40; (b) 60; (c) 80; (d) 100; (e) 120; (f) 140; (g) 160; (h) 180; and (i) 200.

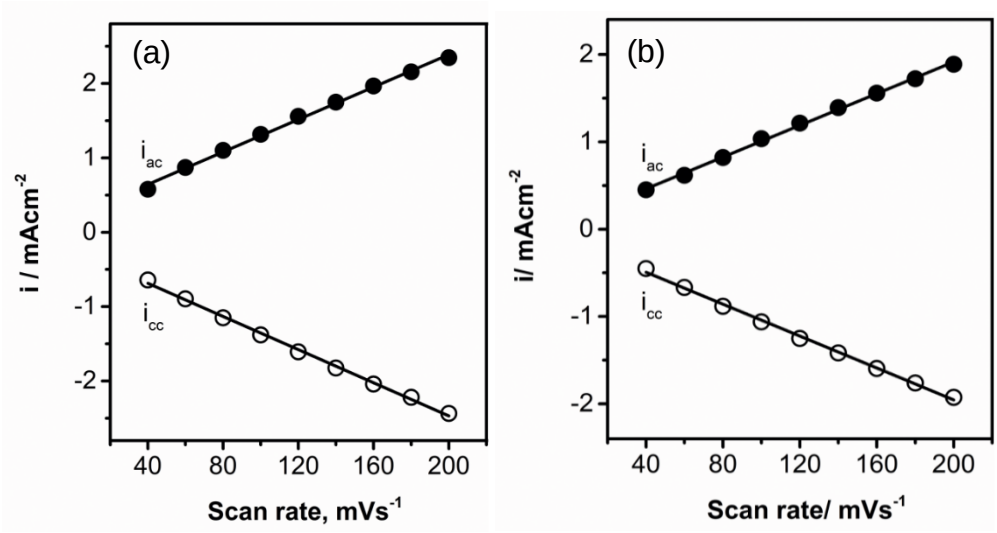

Figure D15 Relationship of anodic (i_{ac}) and cathodic (i_{cc}) current peaks as a function of scan rate for (a) PProDOS-Np_2 film when switched between -0.3 V and 1.2 V and (b) PProDOT-Np_2 film when switched between -0.3 V and 1.3 V in 0.1 M TBAH/CH_2Cl_2 solution.

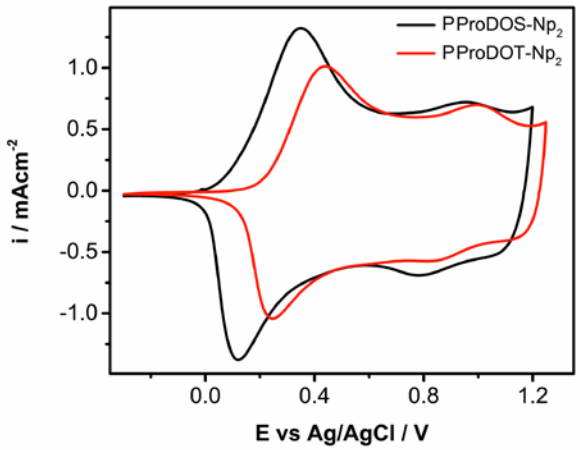

Figure D16 Cyclic voltammograms of PProDOS-Np_2 (67 mC/cm^2) and PProDOT-Np_2 (67 mC/cm^2) films on Pt electrode in 0.1 M TBAH/CH_2Cl_2 solution at a scan rate of 100 mV/s.

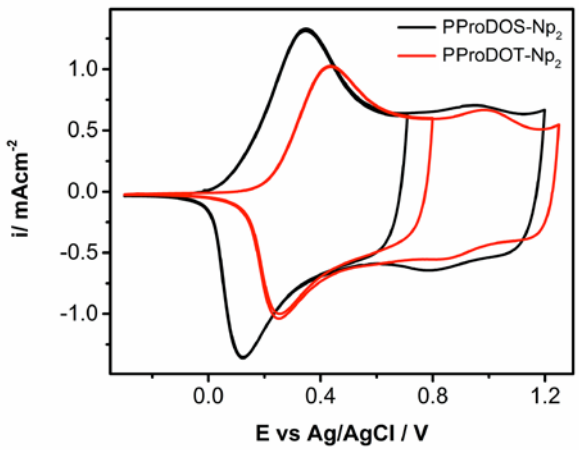

Figure D17 Cyclic voltammogram of PProDOS-Np_2 film (67 mC/cm^2) on Pt electrode in 0.1 M TBAH/CH_2Cl_2 solution between -0.3 V and 1.2 V and then between -0.3 V and 0.7 V at a scan rate of 100 mV/s vs. Ag/AgCl (black line), cyclic voltammogram of PProDOT-Np_2 film (67 mC/cm^2) on Pt electrode in 0.1 M TBAH/CH_2Cl_2 solution between -0.3 V and 1.3 V and then between -0.3 V and 0.8 V at a scan rate of 100 mV/s (red line).

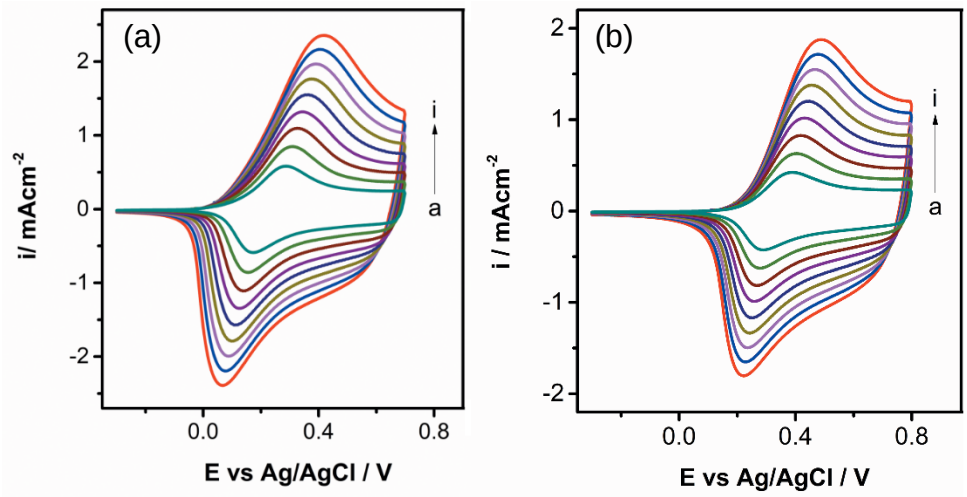

Figure D18 Scan rate dependence of (a) PProDOS-Np_2 (67 mC/cm^2) and (b) PProDOT-Np_2 (67 mC/cm^2) films on a Pt disk electrode in 0.1 M TBAH/CH_2Cl_2 at different scan rates between 40 mV/s and 200 mV/s with 20 mV/s increments: (mV/s) (a) 40; (b) 60; (c) 80; (d) 100; (e) 120; (f) 140; (g) 160; (h) 180; and (i) 200.

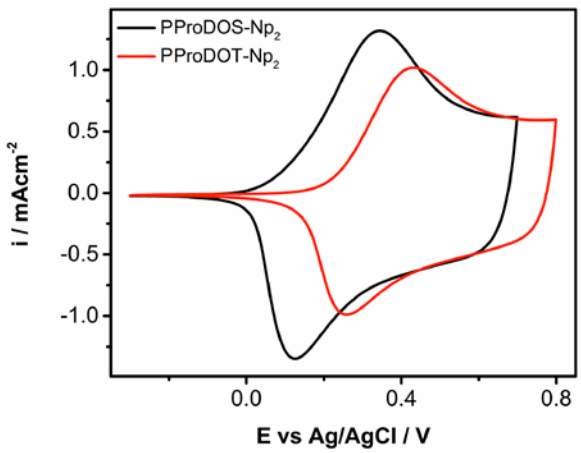

Figure D19 Cyclic voltammograms of PProDOS-Np_2 (67 mC/cm^2) and PProDOT-Np_2 (67 mC/cm^2) films on Pt electrode in 0.1 M TBAH/CH_2Cl_2 solution a scan rate of 100 mV/s.

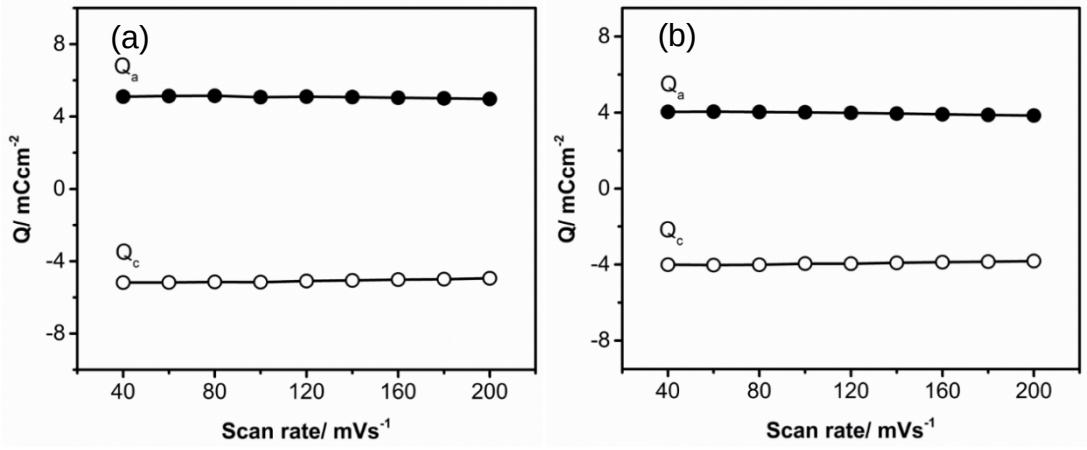

Figure D20 The amount of charge (Q_a) and discharge (Q_c) as a function of scan rate for (a) PProDOS-Np_2 film (67 mC/cm^2) when switched between -0.3 V and 0.7 V and (b) PProDOT-Np_2 film (67 mC/cm^2) when switched between between -0.3 V and 0.8 V in 0.1 M TBAH/CH_2Cl_2 solution.

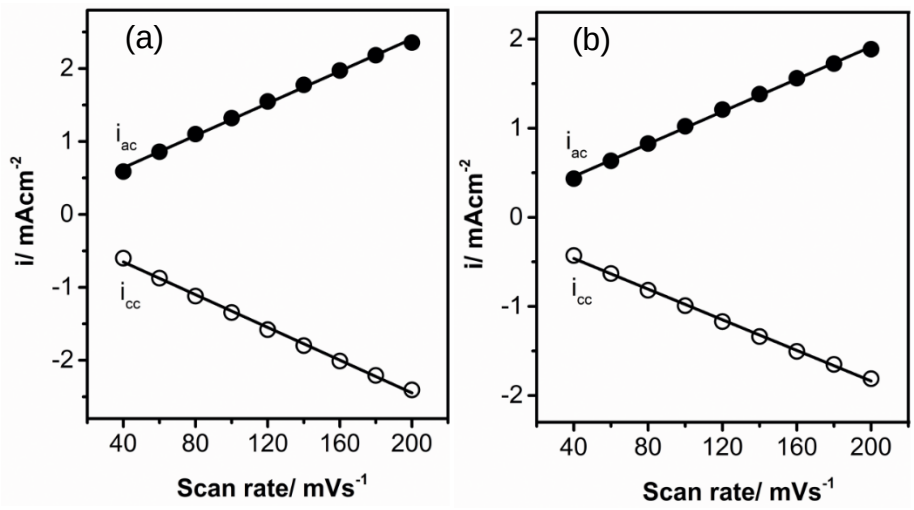

Figure D21 Relationship of anodic (i_{ac}) and cathodic (i_{cc}) current peaks as a function of scan rate for (a) PProDOS-Np_2 film (67 mC/cm^2) when switched between -0.3 V and 0.7 V and (b) PProDOT-Np_2 film (67 mC/cm^2) when switched between between -0.3 V and 0.8 V in 0.1 M TBAH/CH_2Cl_2 solution.

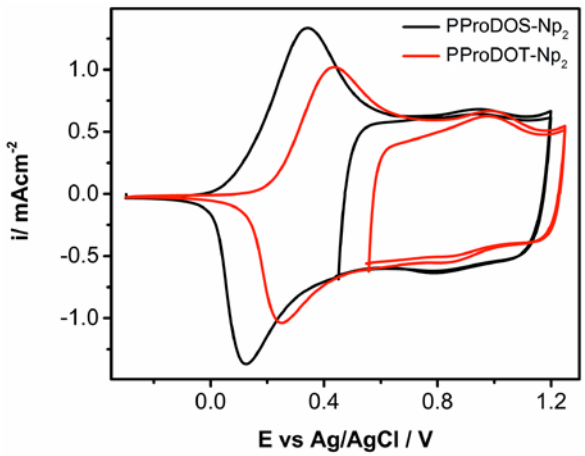

Figure D22 Cyclic voltammogram of PProDOS-Np_2 film (67 mC/cm^2) on the Pt electrode in 0.1 M TBAH/CH_2Cl_2 solution between -0.3 V and 1.2 V and then between 0.45 V and 1.2 V at a scan rate of 100 mV/s vs. Ag/AgCl (black line), and cyclic voltammogram of PProDOT-Np_2 film (67 mC/cm^2) on Pt electrode in 0.1 M TBAH/CH_2Cl_2 solution between -0.3 V and 1.3 V and then between 0.55 V and 1.3 V at a scan rate of 100 mV/s (red line).

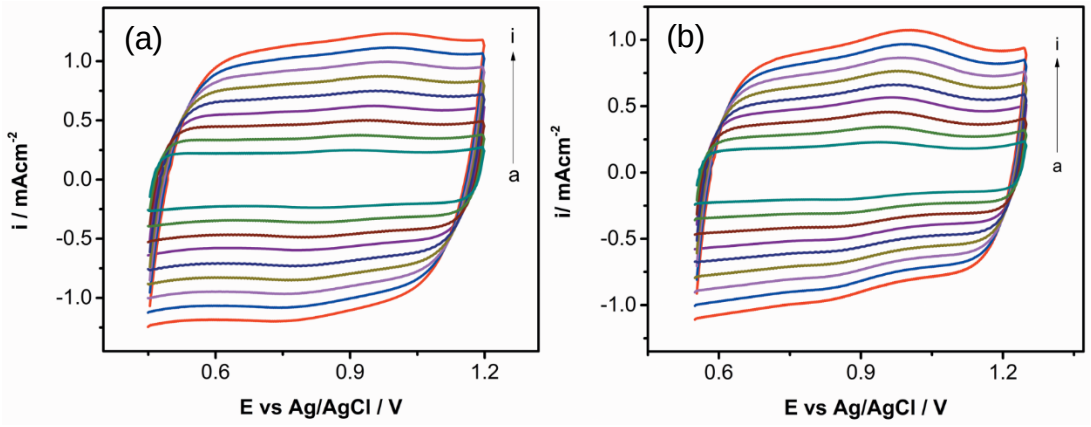

Figure D23 Cyclic capacitance effect of (a) PProDOS-Np_2 (67 mC/cm^2) and (b) PProDOT-Np_2 (67 mC/cm^2) films on a Pt disk electrode in 0.1 M TBAH/CH_2Cl_2 at different scan rates between 40 mV/s and 200 mV/s with 20 mV/s increments: (mV/s) (a) 20; (b) 40; (c) 60; (d) 80; (e) 100; (f) 120; (g) 140; (h) 160; (i) 180; and (j) 200.

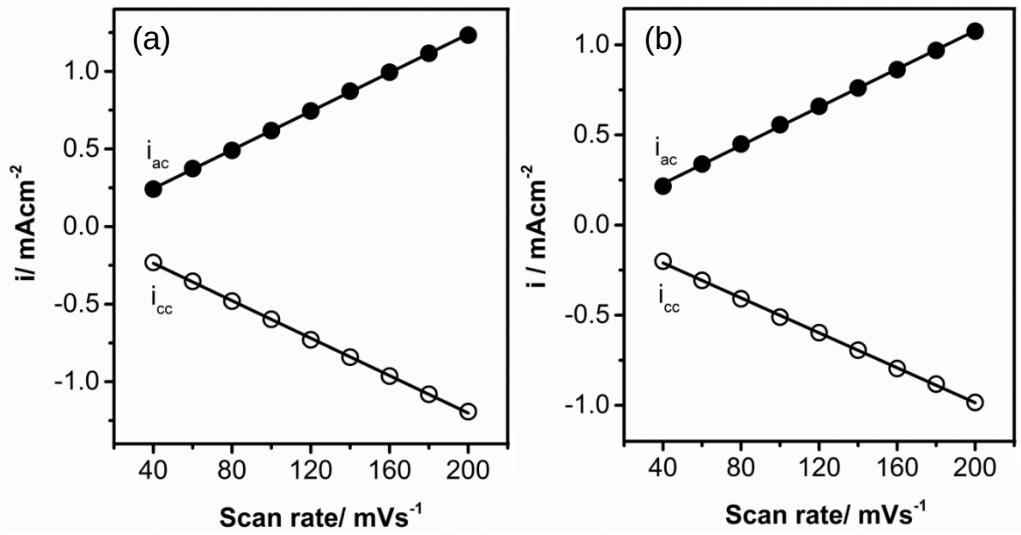

Figure D24 Relationship of anodic (i_{ac}) and cathodic (i_{cc}) current peaks as a function of scan rate for (a) PProDOS-Np_2 film (67 mC/cm^2) when switched between 0.45 V and 1.2 V and (b) PProDOT-Np_2 film (67 mC/cm^2) when switched between 0.55 V and 1.3 V in 0.1 M TBAH/CH_2Cl_2 solution.

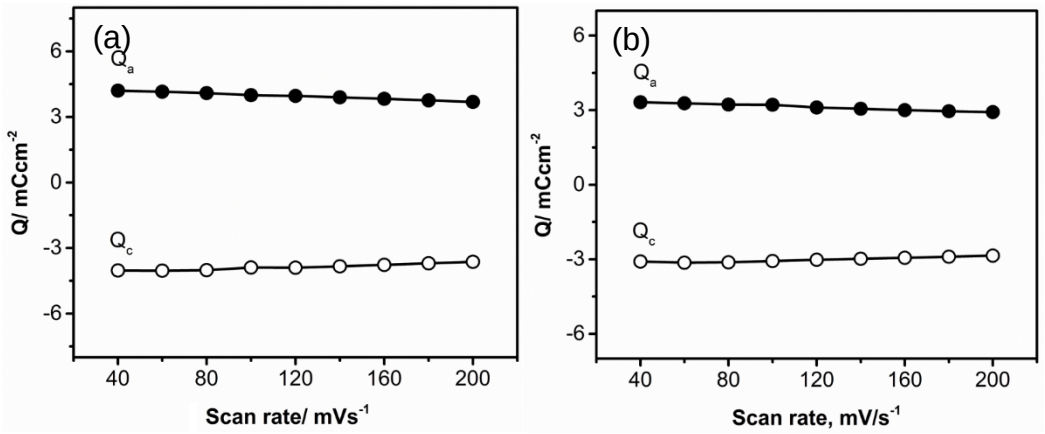

Figure D25 The amount of charge (Q_a) and discharge (Q_c) as a function of scan rate for (a) PProDOS-Np_2 film (67 mC/cm^2) when switched between 0.45 V and 1.2 V and (b) PProDOT-Np_2 film (67 mC/cm^2) when switched between 0.55 V and 1.3 V in 0.1 M TBAH/CH_2Cl_2 solution.

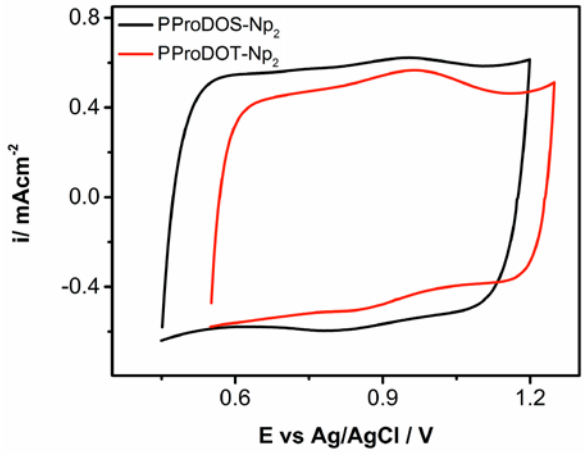

Figure D26 Cyclic voltammograms of PProDOS-Np_2 (67 mC/cm^2) and PProDOT-Np_2 (67 mC/cm^2) films on the Pt electrode in 0.1 M TBAH/CH_2Cl_2 solution a scan rate of 100 mV/s.

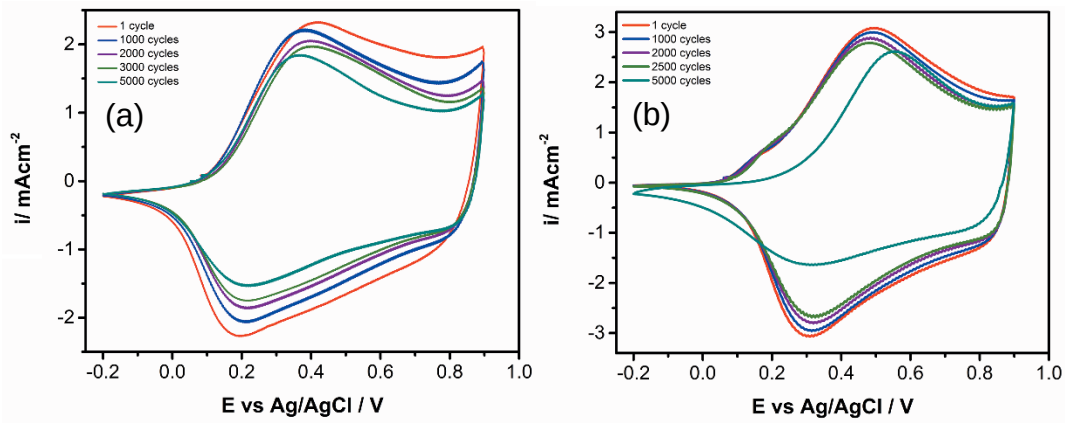

Figure D27 Stability test for the (a) PProDOS-Np_2 film (67 mC/cm^2) in 0.1 M TBAH/CH_2Cl_2 by using a square wave potential method between -0.2 V and 0.9 V for 3 s under ambient conditions. The voltamograms of the PProDOS-Np_2 filmat a scan rate of 100 mV/s by cyclic voltammetry. (b) PProDOT-Np_2 film (67 mC/cm^2) in 0.1 M TBAH/CH_2Cl_2 by using a square wave potential method between -0.2 V and 0.9 V for 3 s under ambient conditions. The voltamograms of the PProDOT-Np_2 film at a scan rate of 100 mV/s by cyclic voltammetry.

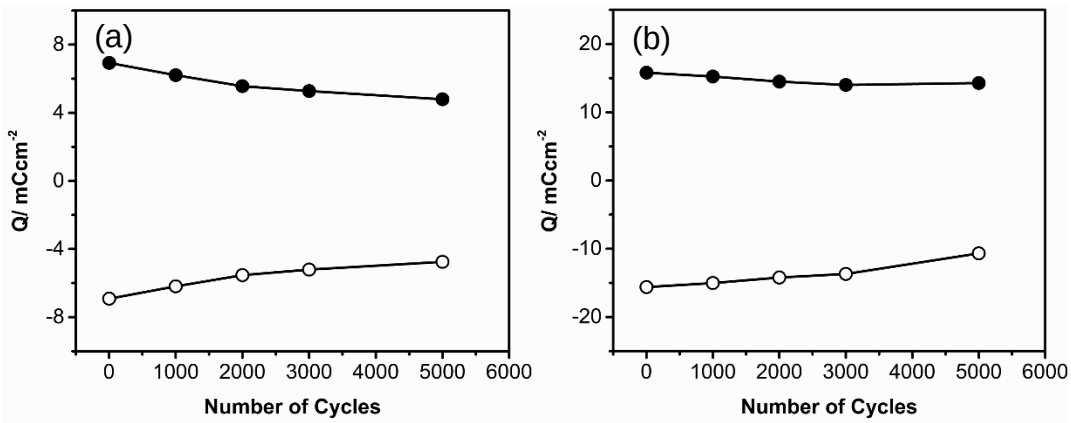

Figure D28 Stability test for the PProDOS-Np_2 (67 mC/cm^2) film in 0.1 M TBAH/CH_2Cl_2 by using a square wave potential method between -0.2 V and 0.9 V for 3 s under ambient conditions. The change in the amount of charge/discharge at a scan rate of 100 mV/s by cyclic voltammetry as a function of the number of cycles.

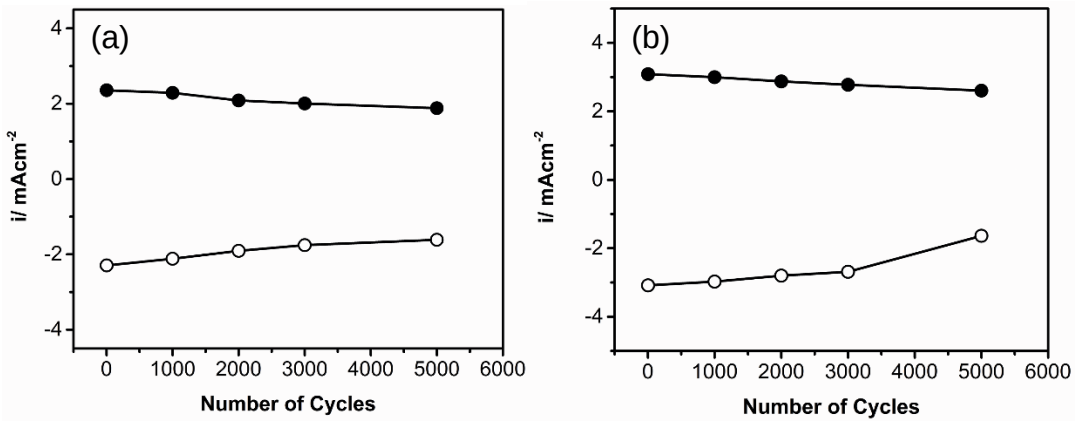

Figure D29 Stability test for the PProDOS-Np_2 (67 mC/cm^2) film in 0.1 M TBAH/CH_2Cl_2 by using a square wave potential method between -0.2 V and 0.9 V for 3 s under ambient conditions. The change in the current intensity of redox couple at a scan rate of 100 mV/s by cyclic voltammetry as a function of the number of cycles.